Green Business Cycles*

Diego R. Känzig
Northwestern University

Maximilian Konradt
Imperial College Business School

Lixing Wang
University of Bonn

Donghai Zhang
National University of Singapore

June, 2025

Abstract

This paper examines the relationship between green innovation and the business cycle, revealing that while non-green innovation is procyclical, green innovation is countercyclical. This pattern holds unconditionally over the business cycle and conditional on economic shocks. Motivated by these findings, we develop a business cycle model with endogenous green and non-green innovation to explain their distinct cyclical behavior. The key mechanism operates through a 'green is in the future' channel: green patents are expected to generate higher profits in the future, making green patenting less sensitive to short-term economic fluctuations. In general equilibrium, this channel is reinforced, making green and non-green innovation effective substitutes. We provide direct evidence supporting the model mechanism using data on market-implied values of green and non-green patents.

JEL classification: E32, O31, Q55, Q58

Keywords: Green innovation, patenting, business cycles, medium-run impacts

*Känzig: Northwestern University, CEPR and NBER (email: dkaenzig@northwestern.edu); Konradt: Imperial College Business School (email: mkonradt@ic.ac.uk); Wang: University of Bonn (email: wang.lixing@uni-bonn.de); Zhang: National University of Singapore (email: donghai.d.zhang@gmail.com). We thank Adrien Auclert, Marios Angeletos, Patrick Bolton, Gadi Barlevy, Gideon Bornstein, Maarten De Ridder, Nida Çakır Melek, Bard Harstad, David Hémous, Ben Jones, Marcin Kacperczyk, Pete Klenow, Yueran Ma, Marti Mestieri, Dimitris Papanikolaou, Monika Piazzesi, Marcel Peruffo, Giorgio Primiceri, Felipe Saffie, and Martin Schneider as well as participants at the Chicago Fed, the KC Fed, Kellogg, Stanford, HKUST, Tinbergen, NUS, Cambridge University, Imperial College Business School for helpful comments and suggestions. Konradt acknowledges financial support from the Swiss National Science Foundation (grant 222367). Wang acknowledges financial support from the Bonn Graduate School of Economics. Zhang thanks the Singapore Ministry of Education for financial support under the SSRTG grant SSRC2023-SSRTG-026.

1. Introduction

Climate change is the defining challenge of our time, posing severe threats to lives, livelihoods, ecosystems, and the global economy. Carbon pricing remains a central tool for mitigation, but its distributional impacts have sparked public resistance, as higher energy costs weigh disproportionately on low-income households and carbon-intensive industries. Against this backdrop, green innovation is key for a successful transition, enabling emissions reductions while sustaining economic growth. Yet recent global shocks, such as the COVID-19 pandemic and subsequent recession, have raised concerns that economic downturns may stall the green transition by tightening financial constraints or shifting firms' innovation priorities. Understanding how green innovation responds to the business cycle is therefore critical.

This paper provides an anatomy of the cyclicality of innovation, with a focus on green and non-green technologies. We define green innovation as the development of clean technologies that replace or reduce reliance on existing carbon-intensive ones. Based on the universe of patents filed in the United States, we document a striking pattern: while overall patenting activity tends to be procyclical, green and non-green innovation follow markedly different cyclical patterns. Specifically, while non-green patenting moves in tandem with the business cycle, decreasing during economic downturns, green patenting is *countercyclical*: it actually increases during economic contractions. As a result, the share of green patents rises during recessions—but notably, we also find evidence that the absolute number of green patents increases.

To establish these patterns, we examine the dynamics of patent applications—both unconditionally over the business cycle and conditional on macroeconomic shocks. For the former, we analyze the dynamic correlations of the number of patent applications with business cycle shocks, measured as innovations to output that cannot be forecasted using past macroeconomic variables. For the latter, we estimate the dynamic causal effects of monetary policy shocks on patenting. We think of monetary policy shocks as a stand-in for a well-identified demand shock. Additionally, these shocks have the appealing feature that they induce a negative co-movement between real interest rates and output, which allows us to shed light on the underlying transmission channels.

The patenting responses to business cycle and monetary policy shocks are remarkably similar: the green patent share increases after a contractionary shock, driven by a rise in the number of green patents and a decline in non-green patenting. The procyclicality of non-green innovation aligns with the common notion that tighter credit conditions, lower revenues, and reduced profits during economic downturns result in cuts to R&D budgets and a decrease in patenting intensity. This raises the question of what can explain the different cyclicality of green innovation.

A key difference between green and non-green patents lies in their duration. As the economy transitions away from carbon-intensive technologies, green patents generate profits that are heavily backloaded. This payoff structure makes the value of green patents and thus green patenting less sensitive to business cycle shocks, which operate at much shorter frequencies. There are two channels that could be driving this result. The first works through cash flows: as profits are backloaded, they are less affected by transitory shocks. The second works through discounting: economic contractions are typically associated with a fall in discount rates. Thus, future profits are discounted by less, which helps stabilize patent values. The fact that we find comparable results for general business cycle and monetary policy shocks suggests that the cash flow channel dominates—since monetary policy shocks imply a negative co-movement between output and discount rates, the discount rate channel would predict more cyclical green innovation.

The contrasting cyclical patterns of green and non-green patenting are robust across multiple dimensions. First, we show that these cyclical patterns extend beyond national borders. While our primary focus is on the United States, we document similar divergent cyclicality between green and non-green patenting in OECD countries and globally. Second, we show that the cyclicality is comparable for patenting among listed and private firms. Third, the result holds true not only in the aggregate but also at the firm level. By linking patent data with balance sheet information for U.S. public firms, we find comparable firm-level patenting responses to monetary policy shocks, even when controlling for firm characteristics such as leverage, size, or firm age. Importantly, we also document a reallocation from non-green to green patenting *within* firms. Finally, we show that firms with longer duration, as proxied by a low book-to-market value or a high green patent share, display a more pronounced green patenting increase following a contractionary shock. Beyond this, we find little heterogeneity based on observed firm characteristics.

To explain the different cyclicality of green and non-green innovation, we develop a business cycle model with directed technical change. The model features endogenous innovation in green and non-green technologies. We first study a simple production economy, taking the aggregate level of innovation and labor as given. The production block consists of a final good producer that assembles the final good using materials and energy. The energy input is a composite of fossil fuels and green energy. Intermediate input producers produce non-green materials and green energy varieties.

We show that in this economy, the equilibrium market share of the green energy composite increases along the green transition, and green patents generate higher profits in the future. We label this phenomenon *green is in the future*. The intuition for this result goes as follows. In our model, the number of green varieties reflects the productivity of green inputs. As the green share increases along the transition, the productivity of green inputs rises, leading to lower prices and higher demand for green inputs. Consequently, the profits from producing green inputs are higher in the future. This implies that the value of a green patent, which is proportional to the discounted sum of future profits, is more heavily influenced by future profits relative to that of non-green patents.

The backloaded profit structure of green patents combined with the transitory nature of business cycle shocks implies that their value responds less to such shocks than the value of non-green patents. This in turn generates an incentive to change the green patenting intensity by less when faced with macroeconomic shocks. We keep discount rates fixed in this partial equilibrium setting, but provide a decomposition between the cash flow and discount rate channel in general equilibrium.

We close the model by introducing innovators that engage in R&D to create new green and non-green varieties, and a standard household block. The model features a positive externality from the aggregate technological level, assuming that each successful innovation creates new varieties of green energy and materials.

The green is in the future channel—as distilled in partial equilibrium—is able to generate the countercyclicality of the share of green varieties, also in general equilibrium. Even though we allow for the discount rate channel which could work against the countercyclicality, we find that the cash flow channel generally dominates.

While the green is in the future channel can account for the relative cyclicality, it cannot generate the countercyclicality of the number of green patents. In general equilibrium, however, there is an additional effect driven by the inelastic supply of skilled labor. When the labor supply curve is positively sloped, a recessionary shock reduces non-green innovation, which in turn lowers aggregate demand for skilled labor and thus wages. The lower wage then decreases the cost of green R&D, incentivizing firms to undertake more green innovation and offsetting the partial-equilibrium effect. When this effect is sufficiently strong, the model is able to generate the differential cyclicality of the number of green and non-green patents observed in the data.

Finally, we provide direct evidence on the key mechanisms of the model. At the core of the green is in the future channel lies the weaker cyclicality of green patent values. We confront this model prediction with the data, leveraging the Kogan et al. (2017) dataset on market-implied values of patents filed in the United States. In line with our model, green patent values move less with the business cycle and macroeconomic shocks such as monetary policy shocks. This holds true at the patent level and for green and non-green value indices at the firm level.

To shed light on the general equilibrium effects via skilled labor, we construct a firm-level dataset on inventors based on information extracted from the patent data. We find that both the share and the number of green inventors in firms increases significantly following a contractionary shock—consistent with the higher demand for green skilled workers that our model predicts in general equilibrium.

Related literature. This paper contributes to several strands of literature. First, it relates to the extensive body of research on the cyclicality of innovation. A large literature documents that aggregate innovation, as measured by R&D expenditures and patent filings, is procyclical (e.g. Aghion et al., 2010; Aghion et al., 2012; Barlevy, 2007). Related research shows that business cycle shocks can have long-lasting effects on economic activity through their impact on investment, innovation and productivity (Antolin-Diaz and Surico, 2022; Jordà, Singh, and Taylor, 2024; Ilzetzki, 2024; Furlanetto et al., 2025). In recent work, Ma and Zimmermann (2023) focus on monetary policy and show that contractionary monetary shocks decrease aggregate innovation. The procyclicality of innovation is typically explained by the fact that economic contractions reduce firms' cash flows and tighten financial constraints, leading to lower R&D investment and innovation output. Our findings confirm this broad pattern for overall patenting but reveal an important distinction between green and non-green innovation.

Second, our paper relates to the literature on green innovation and its determinants. Given recent estimates of the social cost of carbon (Burke et al., 2023; Bilal and Känzig, 2024), understanding the drivers of green innovation is of utmost importance. Prior studies have examined how environmental policies, such as carbon pricing and subsidies, influence green technological development (Calel and Dechezleprêtre, 2016; Colmer et al., 2024; Aghion et al., 2016; Känzig, 2023). Popp (2002) provides early evidence that higher energy prices induce clean innovation by directing inventive activity. Acemoglu et al. (2012) emphasize the central role played by market size and price effects on the direction of technical change. Acemoglu et al. (2023) examine the shale gas revolution, showing that the natural gas boom discourages green innovation.

In an important and closely related paper, Aghion et al. (2024) study the role of financial barriers to green innovation. They show that young, financially constrained firms substantially curb their green innovation when faced with credit shocks. Our analysis complements theirs by studying different aspects of the relationship between macroeconomic conditions and green innovation. First, while their focus is on how the global financial crisis contributed to the recent slowdown in the green transition, we examine cyclical fluctuations in green and non-green innovation more broadly. Second, we study more mature firms in the United States, which are less likely to be financially constrained, whereas their analysis centers on younger, smaller firms in Germany and across Europe.

Our paper contributes to this literature by documenting the cyclicality of green patenting and providing a theoretical explanation for its countercyclicality. Unlike Fornaro, Guerrieri, and Reichlin (2025), we document reallocative effects between green and non-green innovation across and *within* firms. The countercyclicality of green innovation is consistent with the Schumpeterian view (Aghion and Saint-Paul, 1998): economic downturns and the associated fall in wages reduce the opportunity cost of innovative activity and induce more green innovation, at the expense of non-green innovation.

Our general equilibrium model with both green and non-green innovation also contributes to the literature on medium-run fluctuations, which emphasizes the interplay between technological progress, capital accumulation, and business cycle dynamics (Comin and Gertler, 2006; Anzoategui et al., 2019; Wang and Zhang, 2025, among others). A number of influential studies focus on understanding the historically slow recoveries from recessions (Benigno and Fornaro, 2018; Bianchi, Kung, and Morales, 2019; Queralto, 2020). Other research examines the implications for asset prices and exchange rates (Kung and Schmid, 2015; Gornemann, Guerrón-Quintana, and Saffie, 2021). While existing models typically focus on aggregate technical change, our framework incorporates the dynamics of directed green and non-green innovation during the green transition.

Outline. The paper proceeds as follows. Section 2 presents stylized facts on the cyclicality of green and non-green innovation: in the aggregate and at the firm-level, unconditional and conditional on macroeconomic shocks. Section 3 introduces our business cycle model with green and non-green innovation. In Section 4, we confront key model predictions with the data. Section 5 concludes.

2. Green Innovation Over the Business Cycle

How does innovation activity vary with the business cycle? Does green innovation display a different sensitivity to economic downturns and upswings than other types of innovation? Answering these questions presents two key challenges. First, how to accurately measure different types of innovation. Second, how to best represent the business cycle. For the former, we will rely on patent data—a widely used proxy for innovation (see e.g. Nagaoka, Motohashi, and Goto, 2010). For the latter, we start by documenting the unconditional dynamic co-movements of patenting with the business cycle before studying the relationship conditional on structural economic shocks.

2.1. Measuring Green Innovation

Measuring innovation presents a fundamental challenge in understanding how technological change responds to economic fluctuations. Patent data offer a well-established proxy for innovation, providing a consistent and detailed record of inventive activity across industries and time. Importantly, patents capture both the scale and nature of innovation: a detailed classification system enables researchers to distinguish between green and non-green technological advances.

The ability to classify patents is a key advantage over R&D expenditure data, another widely used measure of innovation. Unlike patents, R&D expenditure data are typically reported at the aggregate level and lack detailed breakdowns by type of research activity. This poses a challenge because firms engage in many types of research simultaneously. These activities do not necessarily correlate with observable characteristics, making it difficult to disentangle targeted investments in specific technologies from broader innovation efforts. For instance, many firms in carbon-intensive industries display substantial engagement in green R&D. Patents, by contrast, provide a direct and observable measure of directed innovation, which is why we focus on patent data in our analysis.

We rely on the Worldwide Patent Statistical Database (PATSTAT), which encompasses bibliographic information for close to the universe of patents globally. The data allow us to identify patent families—patents representing the same innovation filed at different patent offices. To avoid double counting, we treat all patents in a patent family as a single innovation (Hémous et al., 2025). For each patent family, we use the original application date to capture the time of innovation and assign nationality based on the respective filing office. See Appendix Table A.2 for an example of a patent family.

Our key goal is to measure green innovation. To that end, we use the International Patent Classification (IPC) and Cooperative Patent Classification (CPC) codes associated with patent filings. The OECD has developed specific categories for climate change mitigation technologies (Y02) and smart grids (Y04S), allowing us to systematically identify and track relevant technological advancements (see Migotto and Haščič, 2015). Our definition of green patents follows Acemoglu et al. (2023) and is a subset of the patents in Y02, excluding innovations that do not directly compete with fossil-fuel technologies.[1] Including all Y02E subclasses or adding smart grid technologies (Y04S) as in Calel and

[1]Specifically, we exclude patents aimed at reducing pollution from fossil-fuel electricity generation (Y02E20), improving grid efficiency (Y02E40) or storage (Y02E60).

Figure 1: Green innovation in the U.S. and OECD countries, 1986–2019

(a) United States (b) OECD countries

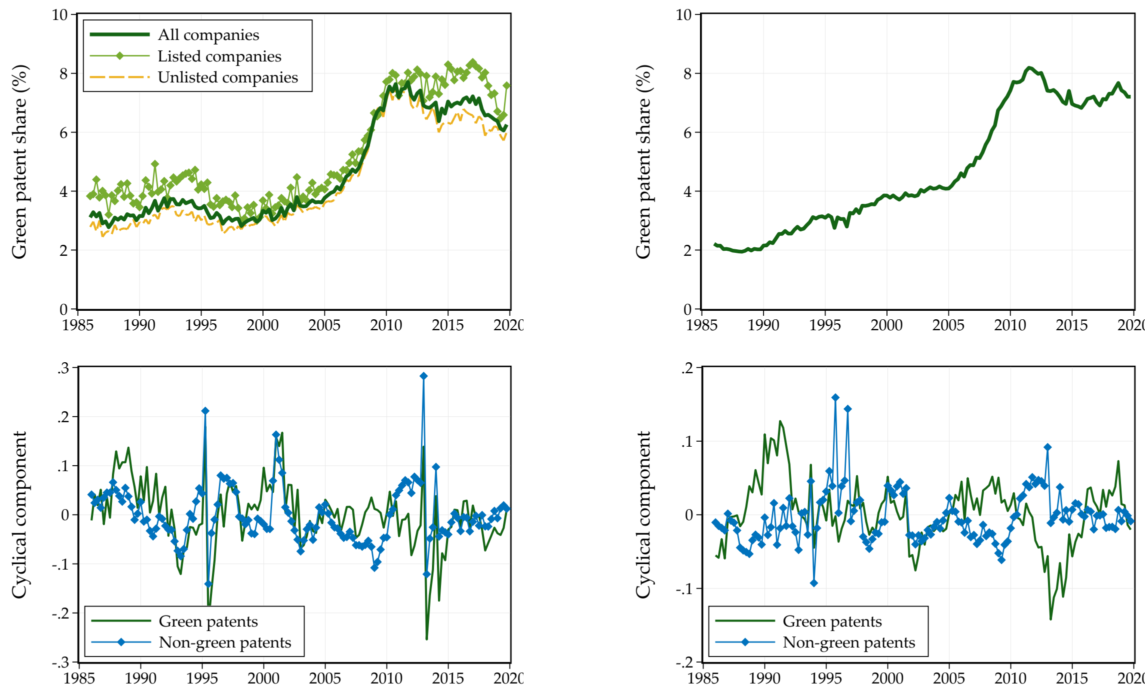

Notes: Trends and cycles in green and non-green patenting. Left: United States. Right: OECD countries. The top panels show the share of green patents, based on our selection of Y02 subclasses. For the U.S., we report the overall green patent share as well as separate shares for listed and unlisted firms. The bottom panels display the cyclical components of green and non-green patent counts, extracted using the Hodrick-Prescott filter with $\lambda = 1,600$. Appendix Figure B.3 shows the cyclical components of U.S. patents by listed and unlisted firms.

Dechezleprêtre (2016) produces very similar results, see Appendix B.10.

Since a patent family is typically associated with many classification codes, we consider it green when any of the codes meet our criteria. We treat the remaining patents as non-green (or gray). Table A.3 in the Appendix includes some examples of green patents.

Aggregate trends and fluctuations. Based on our patent database, we compute aggregate patent application counts. While our primary focus is on patenting in the United States, we also report comparable statistics for OECD countries.[2]

The top panels of Figure 1 show how the share of green patents relative to total patents filed in the U.S. and the OECD evolves from the mid-1980s until the end of 2019. We observe a stark increase in the green patent share over this period, largely driven by a big

[2]Among OECD countries, patents filed with the USPTO account for 21% of total patents and 22% of green patents.

surge between 2005 and 2010. Green patenting starts at a relatively low level—around 3% in the U.S. and 2% in the OECD—reaches a peak at around 8% in 2011, and has stabilized or even decreased slightly since. The trends are broadly similar in the U.S. and the OECD, and align with findings in the existing literature (see e.g. Aghion et al., 2024).

The trends in inventive activity mask the pervasive cyclical fluctuations in patenting. To shed light on these dynamics, the bottom panels of Figure 1 show the cyclical components of green and non-green patent filings in the United States and OECD countries, extracted using the Hodrick-Prescott filter. Both types of patents vary meaningfully over the business cycle. Strikingly, however, green and non-green patents do not co-move very strongly: while non-green patents tend to be procyclical—declining during the early 1990s recession and the 2008 global financial crisis—green patents filings appear countercyclical, displaying an increase during those same downturns.

Firm-level statistics. Which firms account for the bulk of green and non-green patenting? To better understand the key innovators, we merge the PATSTAT dataset with corporate balance sheet data. For firm-level financials, we use Compustat North America, covering the universe of publicly listed companies in the United States. To link the patent data, we rely on two leading datasets that connect patents to firms. The first is Orbis Intellectual Property, which provides global patent portfolios linked to Orbis companies (see Hémous et al., 2025); we match these to Compustat using ISIN identifiers. The second is the dataset by Arora, Belenzon, and Sheer (2021), which extends the NBER patent database (Hall, Jaffe, and Trajtenberg, 2001) and directly links USPTO patents to Compustat firms.

We use the unique patent application number common to both datasets to merge them with information from PATSTAT. In total, we successfully match 1.7 million distinct patent families—including approximately 93,000 green patents—to over 2,100 Compustat firms. Reassuringly, the overlap in matched patents across the two sources is high (see Appendix A for details).

Who are the main players in green innovation? We find that a substantial share of green patents—on average, 42% of quarterly green patent filings—are filed by listed firms. Among these, Table 1 presents descriptive statistics on green patenting by firm size. The bulk of green patenting in the U.S. is concentrated in the largest companies (top size quartile), accounting for more than four out of five green patents filed between 1986 to 2019. While smaller and younger firms patent relatively more in green technology classes, the bottom half of the size distribution accounts for less than 7% of the green patents in our sample. By contrast, the 20 largest green innovators account for close to 50% of green

Table 1: Green patenting and firm size

	Firm size quartiles			
	First	Second	Third	Fourth
Number of green patents	2,241	4,560	9,248	82,816
Green patent share (%)	22.04	11.66	8.96	10.46
Size	40	244	1,214	16,750
Age	14.89	17.56	22.78	30.98
Book to market ratio	0.26	0.45	0.42	0.38
GHG emission intensity	38.17	34.62	81.93	316.07

Notes: The table reports the total number of green patents and the average share of green patents across four quartiles of the firm size distribution. Firm size is measured by average total assets (in millions of 2017 USD) as reported in Compustat from 1986 to 2019. Average firm age is based on incorporation dates from Worldscope. Average GHG emissions intensity is calculated as Scope 1 emissions relative to revenue, using data from Trucost.

patent filings (see Table B.1 in the Appendix).

Thus, large firms appear to be important drivers behind green innovation in the United States.[3] Interestingly, these firms are not particularly green according to conventional metrics. As shown in Table 1, larger firms exhibit a substantially higher GHG emissions intensity than smaller ones. Their patent portfolios are also less weighted toward green technology classes (see also Fornaro, Guerrieri, and Reichlin, 2024). This pattern is consistent with recent evidence in Cohen, Gurun, and Nguyen (2020) showing that utilities and energy companies are important drivers of green innovation.

As expected, firm size is positively correlated with firm age. When examining the book-to-market ratio, growth firms are primarily concentrated in both the smallest and largest size quartiles, while value firms are more evenly distributed across the middle of the size distribution.

Due to data limitations, our focus is on listed firms. However, an important question is how patenting activity in listed firms compares to that in unlisted firms. To explore this, we construct a green patent share based on the sample of patents that cannot be

[3] Importantly, this relationship may differ across countries. For instance, Aghion et al. (2024) document that smaller firms account for a large share of green patenting in German data. However, firms in our sample tend to be substantially larger—a firm at the 90th percentile of their fixed asset distribution (97 million EUR) would fall into the bottom quartile of our total asset distribution—complicating a direct comparison.

linked to listed firms, which we attribute to unlisted firms.[4] As shown in the top-left panel of Figure 1, trends in green patenting among unlisted firms are broadly similar to those observed for listed firms.

2.2. The Cyclicality of Green Innovation at the Macro Level

How does green and non-green innovation fluctuate over the business cycle? Theoretically, the cyclicality of innovation is ambiguous. According to the Schumpeterian view, economic downturns and the associated fall in wages reduce the opportunity cost of innovative activity and induce higher long-term productivity growth (Aghion and Saint-Paul, 1998). However, the effect can be overturned in the presence of financial constraints (Aghion et al., 2010). Thus, the direction and amplitude of the cyclicality of innovation is an empirical question.

To shed light on this, we perform two complementary exercises. First, we study how patenting changes after "business cycle shocks" by analyzing the dynamic correlation between patenting measures and unexpected changes in GDP or other business cycle indicators. Second, we estimate the dynamic causal effects of monetary policy shocks—used here as a stand-in for well-identified demand shocks—on patenting. These shocks also have the desirable property of moving output and interest rates in opposite directions, which will be informative of the underlying mechanisms at play.

Unconditional cyclicality. To assess how patenting varies with the cycle, we estimate simple local projections à la Jordà (2005) on business cycle "shocks" in the spirit of Angeletos, Collard, and Dellas (2020). Specifically, we estimate

$$y_{t+h} = \alpha^h + \psi^h bc_t + \boldsymbol{\beta}_x^h \mathbf{x}_{t-1} + \varepsilon_{t+h}, \tag{1}$$

where y_{t+h} is the innovation measure of interest, h-quarters ahead, bc_t is a business cycle indicator, $\mathbf{x}_{t-1}$ is a vector of controls and ε_{t+h} is a potentially serially correlated error term. As the relevant innovation measures, we consider the number of overall patents filed, the number of green and non-green patents (all expressed in logs), and the green patent share.[5] In our baseline, we use real GDP growth as the business cycle indicator. However, our results are robust to using alternative indicators (see Appendix B.2).

[4] According to Kahle and Stulz (2017), Compustat covers 97–99% of the market capitalization of all listed U.S. firms between 1975 and 2015. Because we assign patent nationality based on the original patent office, we expect filings by foreign corporations to be modest.

[5] We apply a one-quarter backward-looking moving average to the patent counts to address volatility in patent filings. However, the results are robust to using raw counts, see Appendix B.6.

Figure 2: Green and non-green patenting responses to business cycle shock

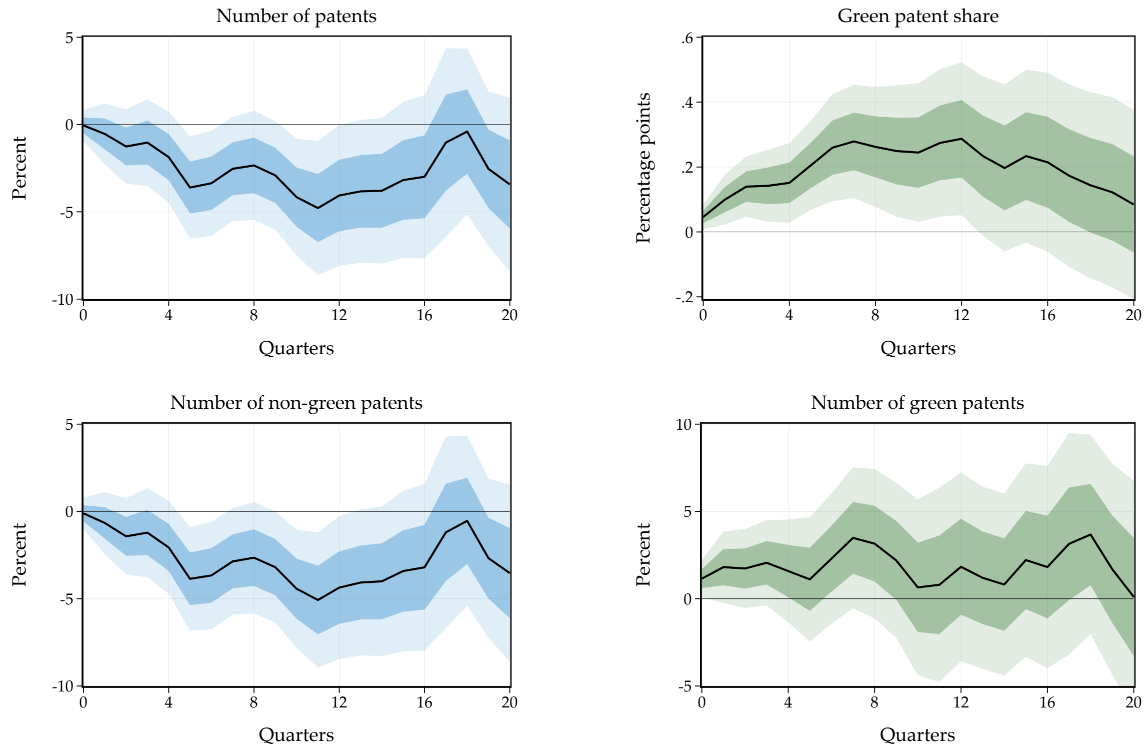

Notes: Impulse responses of green and non-green patenting in the United States to a recessionary innovation to GDP growth, estimated based on the reduced-form local projections (1). The shock is normalized to decrease GDP growth by 1% on impact. Solid line: point estimate. Dark and light shaded areas: 68 and 95% confidence bands based on lag-augmented standard errors.

Our controls include 4 lags of the business cycle indicator and the patenting measure. Moreover, we include quarterly dummy variables and a linear time trend to account for seasonality and trending behavior.[6] By controlling for lags of GDP growth and the patenting measure, we isolate an innovation in GDP that is not forecastable by past economic and innovative activity.[7] The coefficients ψ^h are the dynamic effects of interest: they capture how an unexpected change in GDP affects patenting both contemporaneously and over future periods. It is important to note that these are dynamic correlations and do not have a causal interpretation. Standard errors are computed using the lag-augmentation approach (Montiel Olea and Plagborg-Møller, 2021).

[6]The U.S. patent data exhibits spikes in patent filings in 1995Q2 and 2013Q1, driven by changes in U.S. patent law associated with the Uruguay Round Agreements Act and the America Invents Act, which we account for using two additional dummy variables. The results are robust to omitting these controls.

[7]In this way, we recover a "shock" that maximizes variations in GDP on impact—a special case of the approach in Angeletos, Collard, and Dellas (2020) who target variations over a finite short-run horizon.

We estimate equation (1) based on U.S. data. Our estimation sample spans the period from 1986Q1, when consistent reporting in the Compustat data begins, and ends in 2019Q4, before the onset of the Covid pandemic. Due to substantial reporting lags in the PATSTAT data, extending the sample to more recent periods is challenging.

Figure 2 presents the results. Focusing on total innovation activity, we find that patenting is procyclical—that is, the number of patents filed tends to rise during economic expansions and decline during downturns. This pattern is consistent with the view that tighter credit conditions, lower revenues, and reduced profits in recessions lead firms to cut R&D spending, resulting in fewer patent filings (Aghion et al., 2010; Aghion et al., 2012).

Comparing the cyclicality of green and non-green patents reveals a striking result: the green patent share increases significantly following an economic downturn. This increase is not only statistically but also economically significant. A fall in GDP by 1% leads to an increase in the green patent share by close to 0.3 percentage points. What is driving the relative increase in green patenting? A comparison of the responses in the bottom panels reveals that non-green patent applications decline more strongly than the total, whereas green patenting even tends to rise. This suggests that green patenting is not only less cyclical than non-green patenting, but may even be *countercyclical*—though the increase is not very precisely estimated.

Cyclicality conditional on monetary policy shocks. While the unconditional time-series evidence is informative, it may confound the impacts of the different underlying shocks driving the business cycle. Therefore, it is important to establish the cyclicality of green patenting *conditional* on structural economic shocks.

Over our sample period of interest, business cycles are thought to be mainly demand driven. Credibly identifying demand shocks is challenging though. We focus on monetary policy shocks, as a well-identified instance of a demand shock. Another appealing feature of these shocks is that they imply an opposing effect on interest rates and output, which will help to shed light on the underlying transmission channels. In Appendix B.7, we study the robustness of the results when conditioning on other shocks such as oil price shocks.

To identify monetary policy shocks, we rely on high-frequency identification techniques (Gertler and Karadi, 2015; Nakamura and Steinsson, 2018). We employ the monetary surprises constructed by Bauer and Swanson (2023), purged from macroeconomic and financial data.[8] Using these surprises as an instrument, we estimate the dynamic causal effects of a monetary policy shock on green patenting. Specifically, we run a series of instrumental variable-local projections:

$$y_{t+h} = \alpha^h + \theta^h r_t + \boldsymbol{\beta}_x^h \mathbf{x}_{t-1} + \varepsilon_{t+h}, \tag{2}$$

where y_{t+h} again corresponds to the innovation measure of interest h-quarters ahead, r_t is the policy rate, which we instrument using monetary surprises, and $\mathbf{x}_{t-1}$ is a vector of controls to account for macroeconomic and financial conditions. We use the federal funds rate as the relevant monetary policy indicator, but account for the zero lower bound using a dummy variable. Using the one-year rate instead produces very similar results. The controls include 4 lags of the policy rate, log real GDP, the unemployment rate, log GDP deflator, and the excess bond premium from Gilchrist and Zakrajšek (2012). We keep including quarterly dummy variables and a linear time trend to account for seasonality and trending behavior. The key object of interest is θ^h, the dynamic causal effect of a monetary policy shock on the innovation measure.

Reassuringly, the effective F-statistic in the first stage is above 10, suggesting that there is no weak instrument problem at hand. We thus proceed by conducting standard inference. Before looking at the patenting responses, we also confirm that the responses of U.S. macroeconomic variables to our identified monetary policy shocks are consistent with existing empirical evidence, see Appendix B.3. Throughout, we normalize the monetary policy shock to increase the Fed funds rate by 25 basis points.

Figure 3 shows the results. In line with the unconditional evidence, we find that overall patenting is procyclical: a contractionary monetary policy shock leads to a significant fall in aggregate patenting. This finding is consistent with the evidence in Ma and Zimmermann (2023).

Next, we turn to the responses of green and non-green patenting. We confirm that green patenting is countercyclical, even conditional on monetary policy shocks. A contractionary monetary policy shock leads to a significant and persistent increase in the green patent share, with a peak effect of 0.3 percentage points after 15 quarters. The number of non-green patents declines substantially—slightly more than the decline in overall patenting—while the number of green patents rises. This increase is more pronounced and statistically significant compared to the unconditional evidence.

Why is green patenting less cyclical than non-green—and even tends to be counter-

[8]Our results are robust to using the monetary surprises from Jarociński and Karadi (2020), see Appendix B.7.

Figure 3: Green and non-green patenting responses to a monetary policy shock

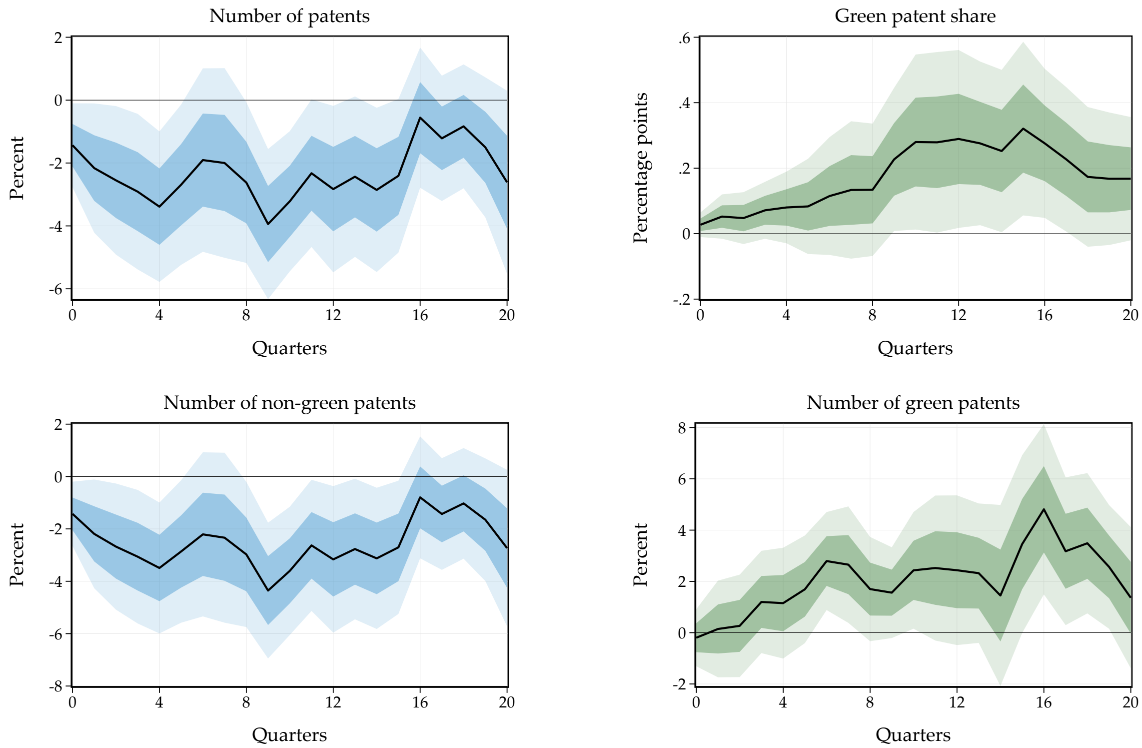

Notes: Impulse responses of green and non-green patenting in the United States to a monetary policy shock, estimated based on the local projections model (2) using high-frequency monetary surprises as an instrument. The shock is normalized to increase the federal funds rate by 25 basis points on impact. Solid line: point estimate. Dark and light shaded areas: 68 and 95% confidence bands based on lag-augmented standard errors.

cyclical? A key difference lies in the timing of expected profits. Green patents tend to generate returns further in the future, whereas non-green patents have a more front-loaded profit structure. Indeed, as we show in Appendix B.8, green patents are significantly more likely to be renewed, consistent with the notion of more backloaded returns. Since business cycle shocks primarily affect short-term economic conditions, this makes the value of green patents—and thus the intensity of green patenting—less sensitive to cyclical fluctuations.

There are two distinct channels that can rationalize this insight: a *cash flow* channel and a *discount rate* channel. The first channel captures that, at fixed discount rates, the cash flows of green patents are less affected by short-term business cycle fluctuations because of their backloaded profile. The second channel captures the notion that discount rates tend to fall in recessions, and thus the more distant cash flows of green patents are discounted by less, making green patent values less cyclical.

Our evidence conditional on monetary policy shocks helps shed light on the relative importance of these channels. Monetary policy shocks imply a negative co-movement between discount rates and output: discount rates increase after a contractionary monetary policy shock. Thus, in this case the discount rate channel would predict more cyclical and not less cyclical green innovation. Our finding that both business cycle and monetary policy shocks generate similar cyclical patterns in green and non-green patenting suggests that the cash flow channel dominates the discount rate channel.

Sensitivity. We perform a number of sensitivity and robustness checks. First, we show that the estimated effects extend beyond the sample of U.S. patents. Figure 4 presents the response of the green patent share in OECD countries and globally to a contractionary U.S. monetary policy shock. Interestingly, we find a similar increase in green patenting as in the U.S. sample. This pattern is consistent with the well-documented global spillovers of U.S. monetary policy (Miranda-Agrippino and Rey, 2020). In Appendix B.5, we further show that the rise in the green patent share in other geographies is similarly driven by an increase in the number of green patents and a decline in the number of non-green patents.

Second, we analyze whether the cyclicality of green patenting differs between listed and unlisted U.S. firms. To this end, we construct the green patent share separately for two samples: patents linked to listed firms and the remaining patents, which we attribute to unlisted firms. The lower panels in Figure 4 present the results. We find a relative increase in green patenting in both groups, although the response for unlisted firms is estimated less precisely. Interestingly, the green patent share rises more quickly among listed firms, while the increase among unlisted firms takes longer to materialize—consistent with the idea that listed firms, with larger R&D departments, can respond more rapidly to economic conditions.

Finally, we consider alternative channels that could help explain the countercyclicality of green innovation. One possibility is that green patenting responds to commodity prices—particularly oil prices. If a recession is triggered by an oil price shock, higher oil prices may incentivize directed technical change (Popp, 2002; Hassler, Krusell, and Olovsson, 2021). However, as we are focusing on demand shocks—business cycle and monetary policy shocks—this channel is unlikely to be driving our results. Indeed, we find similar patterns when examining patenting responses to oil supply shocks, which lead to significant increases in oil prices, suggesting that mechanisms other than energy prices are at play (see Appendix B.7).

Another potential channel relates to physical climate risks. If economic contractions are triggered by natural disasters, this could increase demand for technologies in climate

Figure 4: Sensitivity with respect to geography and type of firm

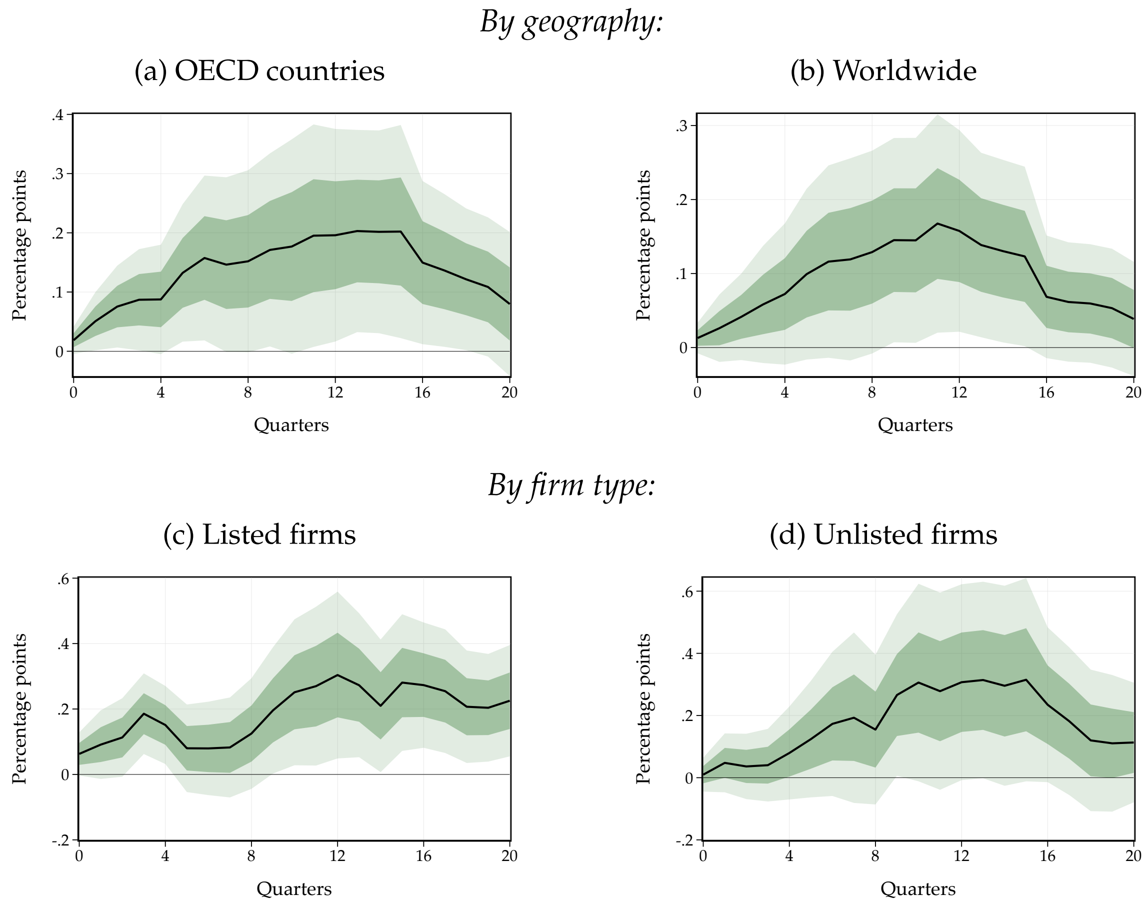

Notes: Impulse responses of the green patent share to a U.S. monetary policy shock for different geographies and firm types, estimated based on the local projections model (2) using high-frequency monetary surprises as an instrument. Upper panels: responses based on patents filed in OECD countries and patents filed worldwide, respectively. Lower panels: responses for patenting by listed and unlisted firms. The shock is normalized to increase the federal funds rate by 25 basis points on impact. Solid line: the point estimate. Dark and light shaded areas: 68 and 95% confidence bands based on lag-augmented standard errors.

mitigation. To account for that possibility, we control for the climate news index by Engle et al. (2020)—a text-based measure of climate change–related news coverage. Figure 5 shows that our results remain robust.

Another possible explanation is that countercyclical fiscal policy and automatic stabilizers disproportionately benefit the green sector. For example, the American Recovery and Reinvestment Act of 2009 included substantial green components—such as investments in renewable energy, energy efficiency, and clean technology—aimed at both stimulating the economy and advancing the low-carbon transition (Chen et al., 2021). Such

Figure 5: Controlling for investor demand and green government spending

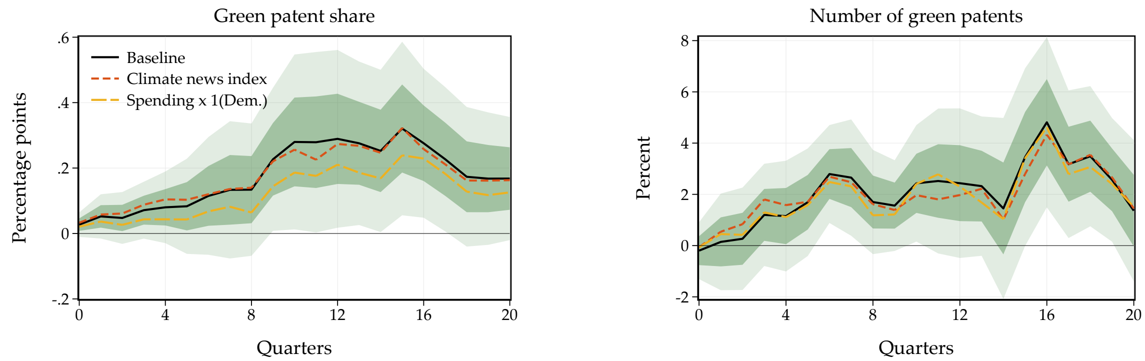

Notes: Sensitivity of green patenting responses to a monetary policy shock, estimated based on the local projections model (2) using high-frequency monetary surprises as an instrument. The orange dotted line is from a specification controls for the climate news index by Engle et al. (2020), and the yellow dashed line controls for government spending interacted with a Democrat dummy. The shock is normalized to increase the federal funds rate by 25 basis points on impact. Lines: point estimates. Dark and light shaded areas: 68 and 95% confidence bands for baseline estimates based on lag-augmented standard errors.

measures can help sustain green innovation during downturns, potentially contributing to its observed countercyclicality. To assess the relevance of this channel, we control for government spending, interacted with a dummy indicating whether the federal government was Democrat-led, reflecting that pro-green fiscal measures have predominantly been enacted under Democratic administrations during our sample period. As shown in Figure 5, this does not change our results materially.

Finally, we perform a number of robustness checks with regards to the measurement of green innovation. Specifically, the results are robust to using alternative green patent classifications, relying exclusively on USPTO data, and controlling for patent quality (see Appendices B.10, B.13, and B.12, respectively).

2.3. The Cyclicality of Green Innovation at the Firm Level

The evidence based on aggregate patent data suggests that green patenting is countercyclical. Is this pattern driven by a subset of firms that specialize in green technologies and respond differently to the cycle, or is there some reallocation from non-green to green patenting even within firms?

To examine this, we study firm-level patenting responses in a large panel of listed U.S.

companies. Formally, we estimate a panel version of the local projections in equation (2):

$$y_{i,t+h} = \alpha_i^h + \theta^h r_t + \boldsymbol{\beta}_{xi}^h \mathbf{x}_{i,t-1} + \boldsymbol{\beta}_x^h \mathbf{x}_{t-1} + \varepsilon_{i,t+h}, \tag{3}$$

where $y_{i,t+h}$ now corresponds to the outcome variable of firm i, h-quarters ahead. As outcome variables, we consider firms' overall number of patents filed, the green patent share, and the number of green or non-green patents. In this specification, we also control for firm fixed effects, α_i^h, to absorb any time-invariant firm characteristics. To allow for general forms of cross-sectional and temporal dependence in the panel data, we compute standard errors using the Driscoll and Kraay (1998) approach.

We restrict our sample to companies that are consistently observed for 20 quarters and exclude firms in the finance, insurance, real estate or public administration sectors. We also drop firms without any green patent over our sample period.[9] Our final sample consists of 166,000 firm-quarter observations, covering more than 2,100 companies and about 93,000 green patents between 1986Q1 and 2019Q4.

A challenge in the firm-level estimations is the sparseness of the patent data. The presence of many zeros, especially in green patent counts, implies missing values when expressing patent counts in logs. We approach this problem in two ways. First, we apply a backward-looking 3-quarter moving average to our firm-level patenting measures. Second, we do not estimate the responses of patent counts in logs. Instead, we use raw patent counts and normalize the impulse responses using the average patent count to obtain percent changes.

Figure 6 shows the firm-level patenting responses to a contractionary monetary policy shock. The estimated responses align well with the aggregate evidence, both qualitatively and quantitatively. In line with the aggregate estimates, we find a significant fall in overall and non-green patents and an increase in the number of green patents. We also document an increase in the firm-level green patent share, which peaks at around 0.4 percentage points and persists for close to 20 quarters. This is striking, because it suggests a shift from non-green to green patenting even *within* a given firm.

An alternative approach to deal with the sparesness in the patent data is to employ a Pseudo-Poisson Maximum Likelihood (PPML) estimator (see e.g. Aghion et al., 2024):

$$\mathrm{E}(\sum_{h=1}^{20} y_{i,t+h}) = \exp(\alpha_i + \theta r_t + \boldsymbol{\beta}_{xi}^h \mathbf{x}_{i,t-1} + \boldsymbol{\beta}_x^h \mathbf{x}_{t-1} + \varepsilon_{i,t+h}), \tag{4}$$

[9] This assumption follows Hémous et al. (2025), but is not critical for our results.

Figure 6: Green and non-green patenting responses of U.S. firms

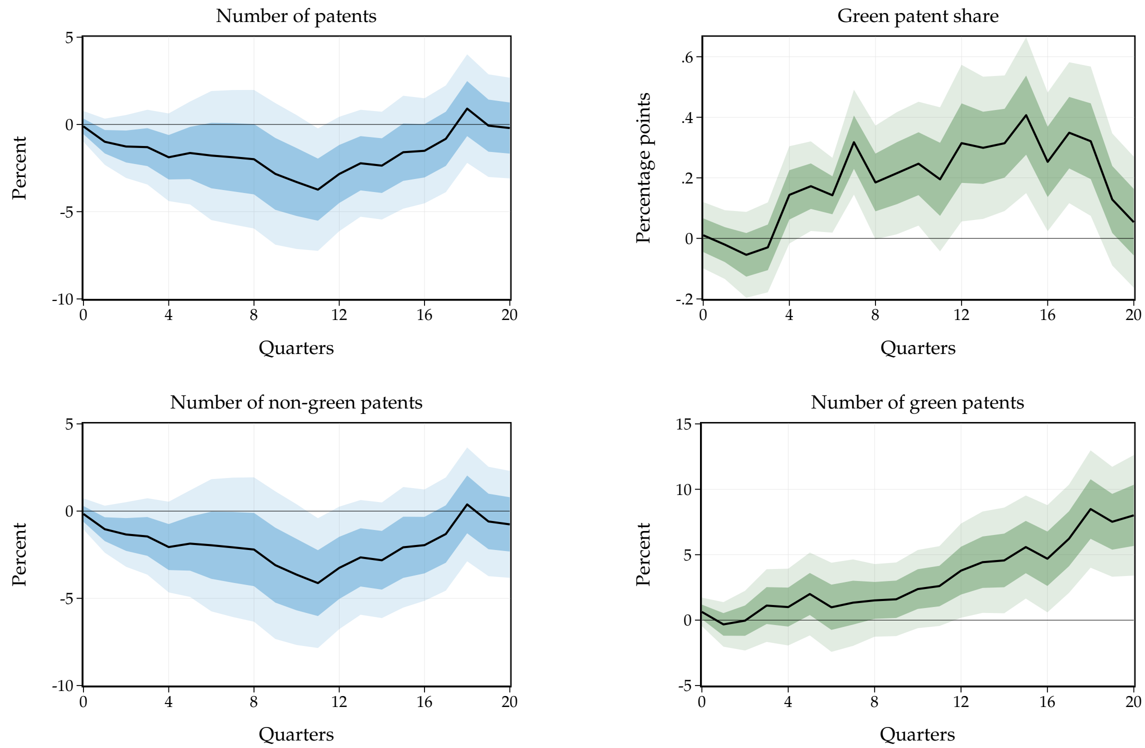

Notes: Impulse responses of firm-level patenting measures in the United States to a monetary policy shock, estimated based on the panel local projections model (3) using high-frequency monetary surprises as an instrument. The shock is normalized to increase the federal funds rate by 25 basis points on impact. Solid line: point estimate. Dark and light shaded areas: 68 and 95% confidence bands based on Driscoll and Kraay (1998) standard errors.

where $\sum_{h=1}^{20} y_{i,t+h}$ captures firm i's cumulative number of green and non-green patents, 20 quarters ahead. By focusing on cumulative patents, we allow for a sufficiently long lag between R&D expenditures and patent applications, in line with Hémous et al. (2025). As before, we instrument the Fed funds rate using monetary surprises and include a set of (lagged) controls and firm fixed effects.

Firm-level heterogeneity. How does the patenting response vary with firm-level characteristics? Do firms with a more backloaded profit structure display a stronger green patenting response? Based on the more parsimonious PPML specification, we study how monetary policy shocks interact with lagged firm-level characteristics of interest, $d_{i,t-1}$:

$$\mathrm{E}\Big(\sum_{h=1}^{20} y_{i,t+h}\Big) = \exp(\alpha_i + \delta_t + \gamma r_t d_{i,t-1} + \boldsymbol{\beta}_{xi}^h \mathbf{x}_{i,t-1} + \varepsilon_{i,t+h}). \tag{5}$$

Table 2: Heterogeneity by firms' profit structures

Dep. var.:	Green patents$_{it+h}$					Non-green patents$_{it+h}$				
	(1)	(2)	(3)	(4)	(5)	(6)	(7)	(8)	(9)	(10)
r_t	1.82***	1.75***		1.57***		-3.43***	-3.41***		-4.70***	
	(0.36)	(0.35)		(0.36)		(0.52)	(0.52)		(0.55)	
$r_t \times btm_{it-1}$		-0.21**	-0.19***				0.26**	0.41***		
		(0.10)	(0.05)				(0.12)	(0.07)		
$r_t \times \overline{gps}_i$				1.34***	1.28***				-0.43	-0.35
				(0.38)	(0.31)				(0.79)	(0.16)
Observations	83,041	82,304	82,304	72,045	72,045	82,966	82,231	82,231	72,841	72,841
Firms	1,552	1,549	1,549	1,397	1,397	1,552	1,549	1,549	1,397	1,397
Time FE	No	No	Yes	No	Yes	No	No	Yes	No	Yes

Notes: The table shows the patenting semi-elasticities, based on the PPML model (4). The dependent variables are a firm's cumulative, 20-quarter ahead number of green and non-green patents, respectively. r_t is the policy rate, instrumented using monetary surprises. We consider a 25 basis point increase. We include interaction terms with the lagged, standardized book-to-market ratio and a firm's initial green patent share. Bootstrapped standard errors clustered at the time-level in parentheses. Significance levels denoted by *** $p < 0.01$, ** $p < 0.05$, * $p < 0.10$.

We use two measures to proxy for firms' profit structures. The first is the book-to-market value with the idea being that growth firms—i.e. firms with low book-to-market—have a more backloaded profit structure. Second, we consider firms' green patent shares. To the extent that green patents have more backloaded returns, a firm with a high share of green patents will also have a more backloaded cash flows. Given the sparseness of the green patent data, we rely on the firm-level average computed over the first 20 quarters of each firm's observation period, $\overline{gps}_i$, to assess this margin.

The interaction term allows us to control for time fixed effects, δ_t, which helps to sharpen the identification of the (relative) effects of monetary policy shocks. To conduct inference, we rely on bootstrapped standard errors clustered at the time level.

Table 2 presents the results. The baseline estimates for green and non-green patenting are shown in columns (1) and (6). Consistent with the local projections, we find a significant increase in the number of green patents and a decrease in the number of non-green patents. Quantitatively, a 25 basis point monetary policy shock is associated with a 1.8% rise in the cumulative number of green and a 3.4% decline in the number of non-green patents over the horizon of 20 quarters. Thus, the magnitude of the contraction in non-green patenting is comparable to the local projections estimates.

In columns (2)-(5) and (7)-(10), we report the interaction effects with the book-to-market value and the green patent share, respectively. To facilitate interpretation, we standardize the interaction terms. Consistent with our purported mechanism, we find that growth firms and firms with a high green patent share display a significantly more positive green patenting response. These effects are also economically meaningful: firms with a green patent share one standard deviation above the mean show around a 1.7 times larger increase in the number of green patents. The interaction effects are robust to including time fixed effects. Similarly, the base effects are largely unchanged when introducing the interactions.

Table 3: Heterogeneity by firms' financial constraints

Dep. var.:	Green patents$_{it+h}$					Non-green patents$_{it+h}$				
	(1)	(2)	(3)	(4)	(5)	(6)	(7)	(8)	(9)	(10)
r_t	1.57***	0.81*	2.09***	1.83***	1.76***	-4.09***	-4.60***	-5.11***	-3.51***	-3.45***
	(0.38)	(0.46)	(0.59)	(0.36)	(0.37)	(0.52)	(0.55)	(0.64)	(0.53)	(0.53)
$r_t \times$ leverage$_{it-1}$	0.31					-0.47				
	(1.30)					(3.90)				
$r_t \times$ age$_{it-1}$		-0.25					-0.11			
		(0.29)					(0.09)			
$r_t \times$ size$_{it-1}$			0.06					0.10		
			(0.26)					(0.21)		
$r_t \times$ st debt$_{it-1}$				0.06					0.05	
				(0.04)					(0.05)	
$r_t \times$ tobinsq$_{it-1}$					0.06					0.02
					(0.05)					(0.04)
Observations	78,899	74,555	82,643	80,298	81,402	78,915	74,372	82,590	80,354	81,400
Firms	1,552	1,291	1,552	1,510	1,544	1,552	1,291	1,552	1,510	1,544

Notes: The table shows patenting semi-elasticities for additional interaction terms with proxies for firms' financial constraints, estimated based on the PPML model (4). The dependent variables are a firm's cumulative, 20-quarter ahead number of green and non-green patents, respectively. r_t is the policy rate, instrumented using monetary surprises. We consider a 25 basis point increase. We include interaction terms with lagged, standardized variables proxying for financial constraints: the leverage ratio, age, size (log assets), share of short-term debt and Tobin's Q. Bootstrapped standard errors clustered at the time-level in parentheses. Significance levels denoted by *** $p < 0.01$, ** $p < 0.05$, * $p < 0.10$.

Do the patenting responses also vary with other firm-level characteristics? In particular, are the effects driven by firms that are more financially constrained? To explore this, Table 3 presents interaction effects with a range of firm-level proxies for financial constraints, including leverage, firm age, size, short-term debt and Tobin's Q. We find little evidence that the effects of monetary policy shocks on firms' innovative activity depend on firms' financial constraints. This contrasts with the evidence in Aghion et al. (2024), which points to an important role for financial constraints in a large sample of German firms. Note, however, that we focus exclusively on listed firms, which tend to be larger and more mature, and therefore less likely to be financially constrained. In contrast, financial constraints are likely to play a more important role for smaller, younger, and unlisted firms, as Aghion et al. (2024) show.

We have presented both aggregate and firm-level evidence showing that green innovation is less cyclical—consistent with the idea that green profits are realized further in the future and are therefore more insulated from short-term fluctuations. Moreover, the fact that generic business cycle and monetary policy shocks lead to similar responses in patenting suggests that the countercyclicality operates mainly through the cash flow rather than the discount rate channel. In the next section, we develop a business cycle model with endogenous green and non-green innovation that can account for these stylized facts by formalizing the backloaded profit structure of green pattens along the climate transition.

3. A Green Business Cycle Model

What is driving the countercyclical nature of green innovation? We have seen evidence that suggests an important role for the backloaded profit structure of green innovations. How far can we get with a model featuring this simple channel to account for the empirical responses, both qualitatively and quantitatively?

To answer these questions, we develop a dynamic stochastic general equilibrium (GE) model with endogenous green and non-green innovation. The model consists of three building blocks: a production block, an innovation block, and a household block with endogenous labor supply and consumption decisions.

We begin by describing the problem of the firm in Section 3.1, taking overall innovation and labor outcomes as given. This partial equilibrium setting allows us to isolate some of the key mechanisms. In Section 3.4, we embed the production block into a full general equilibrium model and discuss the potential role of general equilibrium effects.

3.1. Firms

The production economy features a final good that uses both material and energy composites as inputs. The energy input itself is a composite of fossil fuels and green energy.

Final good producer. There is a representative firm that produces final good by employing unskilled labor L_t, a material composite M_t, and an energy composite E_t:

$$Y_t = (Z_t L_t)^{\alpha_L} M_t^{\alpha_M} E_t^{1-\alpha_L-\alpha_M}, \tag{6}$$

where Z_t is an aggregate labor productivity, evolving as

$$\log Z_t = \rho_z \log Z_{t-1} + \sigma_z \varepsilon_t^z. \tag{7}$$

We think of the material composite as the gray, or non-green, input. The energy composite E_t consists of fossil fuel f_t and a green energy composite G_t, which are combined by the final goods producer using a CES technology:

$$E_t = \left(f_t^{\frac{\rho-1}{\rho}} + G_t^{\frac{\rho-1}{\rho}} \right)^{\frac{\rho}{\rho-1}}. \tag{8}$$

The parameter ρ is crucial: it governs the elasticity of substitution between fossil fuel and the green energy composite. We assume $\rho > 1$, indicating that f_t and G_t are substitutes.

The green energy composite G_t and the materials composite M_t each aggregate a continuum of differentiated inputs:

$$M_t = \left(\int_0^{A_t^M} m_{ht}^{\frac{1}{\mu_M}} \, dh \right)^{\mu_M}, \qquad G_t = \left(\int_0^{A_t^G} g_{jt}^{\frac{1}{\mu_G}} \, dj \right)^{\mu_G}, \tag{9}$$

where, as in Romer (1990), A_t^G and A_t^M denote the number of available green energy and materials varieties, respectively.

The final good producer's optimization problem is:

$$\max_{L_t, \{m_{ht}\}, f_t, \{g_{jt}\}} P_t \left[(Z_t L_t)^{\alpha} M_t^{\beta} E_t^{1-\alpha-\beta} \right] - \int_0^{A_t^M} p_{ht}^m \, m_{ht} \, dh - \int_0^{A_t^G} p_{jt}^g \, g_{jt} \, dj - P_t^f f_t. \tag{10}$$

Solving this problem yields the following demand equations:

$$m_{ht} = \left(\frac{p_{ht}^m}{P_t^M} \right)^{\frac{\mu_M}{1-\mu_M}} M_t, \qquad g_{jt} = \left(\frac{p_{jt}^g}{P_t^G} \right)^{\frac{\mu_G}{1-\mu_G}} G_t, \tag{11}$$

where $P_t^M = \left(\int_0^{A_t^M} (p_{ht}^m)^{\frac{1}{1-\mu_M}} \, dh \right)^{1-\mu_M}$ and $P_t^G = \left(\int_0^{A_t^G} (p_{jt}^g)^{\frac{1}{1-\mu_G}} \, dj \right)^{1-\mu_G}$ are the corresponding price indices of M_t and G_t.

Intermediate input producers. Intermediate input producers—firms that produce non-green and green varieties, m_{ht} and g_{jt}—maximize profits subject to the demand equations in (11).

Green energy varieties. The green energy varieties are produced by a continuum of firms operating under monopolistic competition. Each green variety g_{jt} is indexed by $j \in [0, A_t^G]$. Consider a generic variety j, its production uses a linear production technology: each unit of green energy variety j requires one unit of final good

$$g_{jt} = Y_t^j, \tag{12}$$

where Y_t^j represent the final good used as inputs by variety j.

The profit maximization problem for producing this green energy variety is:

$$\Pi_{jt}^G = \max_{p_{jt}^g} \left(p_{jt}^g \, g_{jt} - g_{jt} \right), \tag{13}$$

subject to the demand equation in (11).

We assume that each period, there is a fixed probability $1 - \phi$ that the variety becomes obsolete. This is a reduced-form way to capture the notion that some varieties will be replaced by better varieties over time. In Appendix C.12, we endogenize this to allow for creative destruction in the spirit of Aghion and Howitt (1992).[10]

The value of owning the intellectual property (IP) right to produce the green variety j, V_{jt}^G, is thus given by:

$$V_{jt}^G = \sum_{s=0}^{\infty} \phi^s \, \mathbb{E}_t \left[\Lambda_{t,t+s} \, \Pi_{j,t+s}^g \right], \tag{14}$$

where Π_{jt}^G is the period profit, as defined in (13). Given this setup, the value of owning a green patent today is the expected sum of future profits Π_{jt+s}^G, discounted using the discount factor $\Lambda_{t,t+s}$ and adjusted by the survival probability ϕ^s.

IP values determine innovators' incentives to innovate. We postpone the discussion of innovators' optimization problems to Section 3.3.

Non-green material varieties. Non-green material varieties are produced and sold similarly

[10] All our results go through in the quality ladder model, but the tractability of the expanding varieties model allows us to derive some propositions in closed form. Specifically, when we endogenize the obsolescence rate, we are no longer able to obtain closed-form solutions for the allocation of skilled labor across green and non-green innovation activities. See Appendix C.12 for more details.

to green energy varieties. Each variety m_{ht} is indexed by $h \in [0, A_t^M]$ and produced via a linear technology:

$$m_{ht} = Y_t^h, \tag{15}$$

where Y_t^h represents the final good used as inputs by non-green variety h.

The profit maximization problem for producing the non-green variety h is:

$$\Pi_{ht}^m = \max_{p_{ht}^m} \left(p_{ht}^m m_{ht} - m_{ht} \right), \tag{16}$$

subject to the demand equation in (11). Similar to green varieties, each non-green variety becomes obsolete with probability $1 - \phi$.

The value of holding the IP rights to a non-green variety h satisfies:

$$V_{ht}^M = \sum_{s=0}^{\infty} \phi^s \, \mathbb{E}_t \left[\Lambda_{t,t+s} \, \Pi_{h,t+s}^m \right]. \tag{17}$$

Fossil fuel. We follow Acemoglu et al. (2016) to model the oil market as follows. Fossil fuel is extracted by a set of competitive firms using final goods as the sole input. Extraction follows a linear technology:

$$f_t = \xi_f \cdot y_t^f, \tag{18}$$

where f_t denotes the quantity of fossil fuel extracted in period t, $\xi_f > 0$ governs the productivity, and y_t^f is the amount of final good allocated to extraction.

Let R_t denote the oil reserves at time t. The evolution of oil reserves is described by the equation:

$$R_{t+1} = R_t - f_t, \tag{19}$$

which indicates that oil reserves decrease over time as a result of extraction. The resource constraint requires the oil reserves in the long run is non-negative:

$$\lim_{t \to \infty} R_t \geq 0. \tag{20}$$

This is a simple, reduced-form way of modeling the oil market. We assume fixed marginal extraction costs, resulting in a constant fossil fuel price. Thus, any change in the relative price of green energy arises from changes in the price of green energy itself.

As robustness checks, we consider two alternative specifications of the oil market. In Appendix C.10, we consider an extension that allows for technological progress in fossil fuel extraction, following Aghion et al. (2016). This introduces some dynamic pricing considerations, similar in spirit to Bornstein, Krusell, and Rebelo (2023). In Appendix C.11, we implement an alternative formulation of extraction costs following Bornstein, Krusell, and Rebelo (2023), in which costs are convex in the extraction rate. These extensions illustrate that our results generalize to more realistic fossil market structures.

3.2. Green Is in the Future

The partial equilibrium setting allows us to distill some of the key mechanisms driving the cyclicality of green and non-green patenting. We asssume that final and intermediate goods firms maximize their profits, taking the evolution of A_t^M and A_t^G as given. We restrict our analysis to an economy on a balanced growth path (BGP) where A_t^M and A_t^G share the same long-run growth rate. For now, we assume that such a path exists. We will discuss the existence and occurrence of a BGP when we move to the general equilibrium setting.

We consider an economy undergoing a green transition. Along this transition path, A_t^G rises, leading to an increase in the green share of energy, $\frac{G_t}{E_t}$—despite the fact that fossil reserves are not exhausted.

Lemma 3.1 (Condition for the Green Transition). *Define the green transition as the process in which the green share of energy, $\frac{G_t}{E_t}$, increases during the transition period. The economy undergoes the green transition if and only if $\frac{P_t^f}{P_t^G}$ increases over time, where $P_t^G = \mu_G (A_t^G)^{1-\mu_G}$.*

Proof. See Appendix D. ■

The intuition for the above lemma is straightforward: the green share of energy increases over time if and only if the price of green energy, relative to the price of fossil fuel, declines over time. In a Romer (1990)-type growth model, the total number of varieties reflects productivity in the economy. Analogously, in our framework, A_t^G captures the productivity of green inputs. As a result, green innovations that increase A_t^G raise the productivity of green energy, lower its relative price, and induce final goods producers to substitute toward green energy inputs.

Under our assumptions, this condition is trivially satisfied as the price of fossil energy is fixed while the price of green decreases as A_t^G increases. During the green transition, the following proposition holds:

Proposition 3.1 (**Green Is in the Future**). *During the green transition:*

(1) *The equilibrium market share of green energy, given by* $\frac{P_t^G G_t}{P_t Y_t}$, *increases over time.*

(2) *The relative profits of green varieties compared to non-green varieties, measured by* $\frac{\Pi_t^G}{\Pi_t^M}$, *increase over time.*

Proof. See Appendix D. ■

Proposition 3.1 shows that, during the green transition, the equilibrium market share of G_t, denoted by $\frac{P_t^G G_t}{P_t Y_t}$, increases over time, and, green patents generate higher profits in the future. We label this phenomenon as *green is in the future*. The intuition for this result is as follows. As the share of green energy in total energy use rises, the overall market share of green energy in the economy increases. This shift leads final good producers to substitute away from fossil fuel toward green energy inputs. As a result, the demand faced by each green input producer rises over time.[11]

Under monopolistic competition, this increase in demand translates into higher profits. Consequently, the profitability of producing green inputs becomes increasingly concentrated in the future. This implies that the value of a green patent, V_t^G, which reflects the discounted sum of future profits, is more backloaded relative to that of non-green patents.

The backloaded profit structure of green patents suggests that V_t^G is less affected by an exogenous, transitory disturbance to Y_t than V_t^M—holding discount rates and other prices fixed. The key intuition is that business-cycle shocks operate at much shorter horizons and thus do not affect cash flows further out in the future. Proposition 3.2 formalizes this insight: the relative value of producing g_{jt}, defined as $\frac{V_t^G}{V_t^M}$, exhibits countercyclicality.

Proposition 3.2 (**Cyclicality during the Green Transition**). *During the green transition, and holding the discount factor constant, the relative value of producing* g_{jt}, *defined as* $\frac{V_t^G}{V_t^M}$, *exhibits countercyclicality. Formally,* $\frac{d\log V_t^G}{d\log Y_t} < \frac{d\log V_t^M}{d\log Y_t}$, *or equivalently* $\frac{d\log\left(V_t^G/V_t^M\right)}{d\log Y_t} < 0$.

Proof. See Appendix D. ■

So far, we have kept discount rates fixed. How do changes in discount rates affect the

[11] In a standard Romer (1990)-type model, the increase in aggregate demand due to the declining price index is exactly offset by the increase in the number of varieties, so that the demand faced by each individual variety producer remains constant. In contrast, in our model, green inputs gain an additional source of demand by replacing fossil fuel in the energy mix. As a result, the demand for each green input producer increases over time during the green transition.

cyclicality of innovation? To shed light on this, we employ the following decomposition:

$$\frac{d\log V_t^k}{d\log Y_t} = \underbrace{\sum_{s=0}^{\infty} \phi^s \frac{\Lambda_{t,t+s,ss}\Pi_{t+s,ss}^k}{V_{t,ss}^k} \frac{d\log \Pi_{t+s}^k}{d\log Y_t}}_{\text{Cash flow channel}} + \underbrace{\sum_{s=0}^{\infty} \phi^s \frac{\Lambda_{t,t+s,ss}\Pi_{t+s,ss}^k}{V_{t,ss}^k} \frac{d\log \Lambda_{t,t+s}}{d\log Y_t}}_{\text{Discount rate channel}}, \tag{21}$$

for $k = \{M, G\}$, where $X_{t,ss}$ captures the evolution of X along the transition, absent any shocks, and $\Lambda_{t,t+s,ss} = \beta\frac{U'(C_{t+s,ss})}{U'(C_{t,ss})}$ is the value of the stochastic discount factor (SDF) along the transition path with no shocks. The first component captures the effect of changes in cash flows, holding the discount factor fixed (see Proposition 3.2). The second component captures changes in the discount rate, keeping the cash flows at the trajectory absent any shocks.

While the cash flow channel unambiguously generates countercyclicality in V_t^G/V_t^M, the discount rate channel depends on the cyclicality of the SDF. As we show in Appendix C.4, a procyclical stochastic discount factor dampens the countercyclicality of the relative valuation of green patents while a countercyclical SDF amplifies it. The intuition is straightforward. If the discount factor falls in a recession—making agents discount the future more—the IP values of green innovations are hurt *more* and not less than those of non-green innovations because of the more backloaded structure.

The cyclicality of the SDF depends on the underlying shock driving the business cycle. Our empirical evidence conditional on monetary policy shocks, suggests that the cash flow channel dominates: such shocks imply a procyclical SDF, which works against the countercyclicality of green innovation. In Section 3.5, we allow for the SDF to be endogenously determined and show that the cash flow channel generally dominates the discount rate channel.

The cyclicality of the green and non-green patent values determine the incentives to innovate over the cycle. In the next section, we study the corresponding problem of the innovators.

3.3. Innovators

There is a continuum of innovators indexed by $i \in [0, 1]$. Each existing green or non-green variety, as described in the previous section, is created by one of these innovators. Because the innovation decisions for each variety are independent of one another, we need not track which innovator creates and owns which variety.

In each period, each innovator i engages in R&D to *create* new varieties. Upon successfully developing a new variety, the innovator sells its IP rights at a price proportional to the value of owning the right to produce. We now describe this innovation process in more detail.

Let $L^S_{it,M}$ and $L^S_{it,G}$ denote the skilled labor employed in R&D by innovator i for materials and green-energy innovation, respectively. φ^M_t and φ^G_t are the number of new technologies that each unit of skilled labor can create. Following Romer (1990), we assume the innovation productivity depends on aggregate conditions, meant to capture knowledge spillover effects:

$$\varphi^M_t = \zeta_M A^M_t \left(L^S_{t,M}\right)^{-(1-\nu)} \tag{22}$$

$$\varphi^G_t = \zeta_G A^G_t \left(L^S_{t,G}\right)^{-(1-\nu)} \tag{23}$$

where the terms A^M_t and A^G_t capture positive externalities from knowledge accumulation, respectively. There is also a congestion externality: as more firms engage in R&D, each one's contribution becomes less effective due to competition for similar innovation targets. This stength of this congestion externality is governed by $\nu \in [0, 1)$ and prevents corner solutions in which all innovation is concentrated in a single type.

We assume that innovators pay a fixed setup cost, $cV^m_{t,ss}$ or $cV^g_{t,ss}$, for each unit of new innovation. These costs are proportional to the counterfactual value of intellectual property in the absence of aggregate shocks. Specifically, $V^m_{t,ss}$ and $V^g_{t,ss}$ represent the expected discounted value of IP rights, where the production profits are evaluated along the transition path of the economy in the absence of aggregate shocks. This modeling choice, similar to the calibration strategy in Barlevy (2007), allows the model to generate realistic cyclical responses of innovation investment while maintaining internal consistency between setup costs and expected value. In the following, we denote $\mathcal{V}^m_t = V^m_t - cV^m_{t,ss}$ and $\mathcal{V}^g_t = V^g_t - cV^g_{t,ss}$.

In summary, an innovator i's optimization problem can be expressed as:

$$\max_{L^S_{it,M}} \quad \varphi^M_t L^S_{it,M} \mathcal{V}^m_t - W^s_t L^S_{it,M}, \tag{24}$$

$$\max_{L^S_{it,G}} \quad \varphi^G_t L^S_{it,G} \mathcal{V}^g_t - W^s_t L^S_{it,G}, \tag{25}$$

taking wages W^s_t and innovation productivity φ^M_t, φ^G_t as given.

Aggregation. Let $S^M_t = \varphi_{t,M} L_{t,M}$ and $S^G_t = \varphi_{t,G} L_{t,G}$ denote the aggregate successful innovation for materials and green energy, respectively. The total amount of varieties then evolves as:

$$A^M_{t+1} = \phi A^M_t + S^M_t, \tag{26}$$
$$A^G_{t+1} = \phi A^G_t + S^G_t. \tag{27}$$

3.4. General Equilibrium

We now embed the production and innovation blocks into a general equilibrium setting. This allows us to incorporate business cycle shocks, as examined in the empirical part of the paper, and to analyze the cyclicality of innovation *outcomes*, rather than just their incentives. More importantly, within this general equilibrium setting, a key mechanism emerges that explains the striking countercyclical pattern of the numer of green patents uncovered in our empirical analysis. To close the economy, we detail the household sector and discuss market clearing.

Households. All households are identical, which is why we focus on the problem of a representative household. The household derives utility over consumption C_t and labor. They maximize lifetime utility

$$\mathbb{E}_t \sum_{t=0}^{\infty} \beta^t \left(\varrho^D_t \log C_t - \frac{\bar{\omega}}{1+\eta} L_t^{1+\eta} - \frac{\bar{\omega}^s}{1+\psi} (L^s_t)^{1+\psi} \right), \tag{28}$$

where ϱ^D_t is the time-preference shock which follows:

$$\log \varrho^d_t = \rho_d \log \varrho^d_{t-1} + \sigma_d \varepsilon^d_t. \tag{29}$$

The household faces the following budget constraint:

$$P_t C_t + Q_t B_{t+1} = B_t + W_t L_t + W^s_t L^s_t + D_t. \tag{30}$$

Here, L_t is the supply of unskilled labor and L^s_t is the supply of skilled labor with corresponding wages W_t and W^s_t, B_t is a risk-free bond and D_t are transfers.

Market clearing. In general equilibrium, all markets have to clear. Labor market clearing of skilled labor requires:

$$\int_0^1 \left(L^S_{it,G} + L^S_{it,M} \right) \, di = L^S_t \tag{31}$$

Final good market market clearing:

$$C_t + \int_0^{A_t^M} m_{ht}\, dh + \int_0^{A_t^G} g_{jt}\, dj + \xi_f^{-1} f_t = Y_t. \tag{32}$$

The remaining markets clear by Walras' law.

Balanced growth. We assume that a BGP exists and that the economy is on a green transition path. In other words, we assume that the conditions stated in Lemma 3.1 hold. This assumption is not restrictive. In our model, we will always be on a green transition path in the absence of technological obsolescence—i.e., when $\phi = 1$. With technological obsolescence ($\phi < 1$), the green transition condition requires that the parameters governing green innovation are such that the pace of green innovation exceeds the rate of obsolescence. In our quantitative analysis, we confirm that this condition holds for empirically plausible calibrations. In Appendix C.2, we provide a detailed discussion on existence.

3.5. The Role of General Equilibrium Effects

We now study the cyclicality of green and non-green patenting in general equilibrium. We first start with our real model and consider preference ϱ_t^d and TFP shocks Z_t. In a next step, we introduce nominal rigidities and also study monetary policy shocks.

A key prediction form our partial equilibrium analysis is that the relative value of green varieties is countercyclical during the green transition. As long as the SDF is countercyclical—as implied by preference shocks under plausible parameterizations—this is also always true in general equilibrium. The countercyclicality of green patent values then implies that firms' R&D investment in green, relative to non-green, is also countercyclical. As a result, the green share of new varieties, $\frac{S_t^G}{S_t^G + S_t^M}$, is itself countercyclical. Proposition 3.3 formalizes this result.

Proposition 3.3 (Countercyclical Green Share of New Varieties). *During the green transition, the green share of new varieties, $\frac{S_t^G}{S_t^G + S_t^M}$, is countercyclical conditional on both, preference and TFP shocks.*

Proof. See Appendix D. ■

Proposition 3.3, however, does not only apply for shocks that imply a countercyclical SDF: it also holds for technology and preference shocks that imply a procyclical SDF in our model. In these cases, the discount rate channel could potentially overturn the cash flow channel. However, we show that the cash flow channel always dominates.[12] Key to this result is the assumption of log utility. If the intertemporal elasticity of substitution is much lower, the discount rate channel becomes more powerful and the result could be potentially overturned. In Section 4.1, we show that under empirically plausible parameterizations, the discount rate channel is dominated.

So far, we showed that the green is in the future channel can account for the countercyclical share of green varieties. However, this channel alone is not enough to explain the countercyclicality in the *number* of green varieties.

In general equilibrium, there is an additional effect at play, driven by changes in equilibrium skilled wages. During recessions, skilled wages decline due to both increased labor supply—households' endogenous response to reduced consumption—and diminished labor demand, resulting from lower non-green innovation. The lower wage reduces the cost of green R&D, incentivizing firms to undertake more green innovation and thereby offsetting the partial-equilibrium effect. Proposition 3.4 shows that, if the wage elasticity of skilled labor with respect to output is sufficiently large, the number of new green varieties becomes countercyclical in general equilibrium.

Proposition 3.4 (**General Equilibrium Effects**). *During the green transition, there exists a threshold $\bar{\epsilon}_x > 0$ such that green innovation is countercyclical, i.e.,*

$$\frac{\partial \log S_t^G}{\partial \log X_t} < 0$$

if and only if the wage elasticity of skilled labor, $\frac{\partial \log W_t^s}{\partial \log X_t}$ exceeds $\bar{\epsilon}_x$ for $X = Z,\ \varrho^d$. By contrast, non-green innovation is procyclical, that is, $\frac{\partial \log S_t^M}{\partial \log X_t}$. Moreover, the threshold $\bar{\epsilon}_x$ is decreasing in the degree of countercyclicality in the relative valuation of green versus non-green innovation, $\mathcal{V}_t^G / \mathcal{V}_t^M$.

Proof. See Appendix D. ■

For green innovation to be countercyclical, as observed in the data, the general equilibrium effects through wages must offset the partial equilibrium effect of a recession on the value of green patents. The latter depends on the strength of the *Green Is in the Future* mechanism. Therefore, the condition is more easily satisfied when the relative value of green varieties exhibits greater countercyclicality.

[12] To formally prove this, Appendix C.4 derives Proposition 3.2 within the general equilibrium model featuring an endogenously determined stochastic discount factor.

To further build intuition, Corollary 3.1 provides a *sufficient* condition, showing that when the supply of skilled labor is sufficiently inelastic—that is, when the labor supply curve is steep—the general equilibrium effect dominates, rendering the number of new green varieties countercyclical.

Corollary 3.1. *During the green transition, there exists a threshold $\overline{\psi}_x$. If the Frisch elasticity of labor supply ψ^{-1} is less than $\overline{\psi}_x^{-1}$, then in equilibrium:*

$$\frac{\partial \log S_t^M}{\partial \log X_t} > 0, \qquad \frac{\partial \log S_t^G}{\partial \log X_t} < 0 \tag{33}$$

for $X = Z,\ \varrho^d$.

Proof. See Appendix D. ■

Monetary policy shocks. So far, we have focused on a real economy in which money is neutral. To be able to study the effects of monetary policy shocks, we extend the model to include nominal rigidities, with retailers facing Rotemberg price adjustment costs (see Appendix C.1 for details). We introduce monetary policy through a Taylor rule and incorporate a monetary shock ϱ_t, which follows an AR(1) process:

$$\log \varrho_t^m = \rho_m \log \varrho_{t-1}^m + \sigma_m \varepsilon_t^m. \tag{34}$$

A result similar to Proposition 3.4 holds conditional on monetary policy shocks:

Corollary 3.2. *During the green transition, there exists a threshold $\overline{\epsilon}_m > 0$. If the wage elasticity to output of skilled labor, $\frac{\partial \log W_t^s}{\partial \log \varrho_t^m}$, is greater than $\overline{\epsilon}_m$, then in equilibrium:*

$$\frac{\partial \log S_t^M}{\partial \log \varrho_t^m} < 0, \qquad \frac{\partial \log S_t^G}{\partial \log \varrho_t^m} > 0. \tag{35}$$

Proof. See Appendix D. ■

4. Evaluating Model Predictions

The previous section analytically demonstrates that the model can qualitatively rationalize our empirical findings. In this section, we assess the model's predictions quantitatively. First, we show that under standard calibrations, the model can quantitatively match the empirical findings. Second, we confront key model predictions with the data and provide direct evidence supporting the model mechanisms.

4.1. A Quantitative Exploration

To assess the quantitative predictions of the model, we calibrate the model to the U.S. economy.

Calibration. We set the discount factor β to match a 2% annual interest rate. The final good technology parameters α_L, α_M are set to 0.5 and 0.45, respectively, which corresponds to a 50% income share of intermediate inputs (Comin and Gertler 2006) and matches a 5% energy share of income (Hassler, Krusell, and Olovsson 2021). The markup parameters μ_M and μ_G are set to 2 to ensure the existence of a balanced growth path.

Following Acemoglu et al. (2012), we set the elasticity of substitution between green energy and fossil fuels, ρ, to 3. The marginal cost of fossil fuel ξ_f is normalized to 1. The congestion externality parmeter ν is set to 0.5, following Anzoategui et al. (2019). The technology obsolescence rate is set to 0.03, consistent with Comin and Gertler (2006) and recent estimates from Ma (2021).

For labor supply elasticities, we set the Frisch elasticity of labor supply, $1/\eta$, to 2, in line with standard RBC calibrations (Kydland and Prescott 1982; King and Rebelo 1999), to generate meaningful business cycle fluctuations. The inverse Frisch elasticity of skilled labor supply—the key parameter determining the strength of the GE effects—is set to $\psi = 2$. This is motivated by Chetty et al. (2011) and Elminejad et al. (2023) that estimate a low labor supply elasticity for skilled, higher-wage workers. The scale parameter of labor $\bar{\omega}$ and $\bar{\omega}^s$ is set to normalize the skilled and unskilled labor to 1 on the BGP.

Following Ottonello and Winberry (2020), we set $\varphi = 90$ and $\sigma = 10$. The Taylor rule parameters are set to $\phi_\pi = 1.69$ and $\phi_A = 1$, the latter fully offsetting fluctuations in the medium-term component. We assume that supply and demand shocks are equally important in driving the business cycle. For the underlying contributions of demand shocks, we assume that preference shocks make up for 45% and monetary policy shocks for 5%. We assume that all shocks are equally persistent, with $\rho_x = 0.6$. To jointly generate a 1.2% standard deviation of output at business cycle frequency, we calibrate the standard deviations of the shocks to $\sigma_z = 0.01$, $\sigma_d = 0.005$, and $\sigma_m = 0.0005$.

We internally calibrate ζ_M, ζ_G to match a 3% GDP growth rate on the BGP. The fixed setup cost for innovation, $c = 0.9$, is calibrated to match a 2% standard deviation in aggregate R&D expenditures from the national accounts at business cycle frequencies. We start the green transition at an initial state where fossil fuel consumption accounts for 80% of the total energy consumption—a value comparable to the figure reported by the U.S. Energy Information Administration.

Figure 7: Green and non-green patenting responses in the model

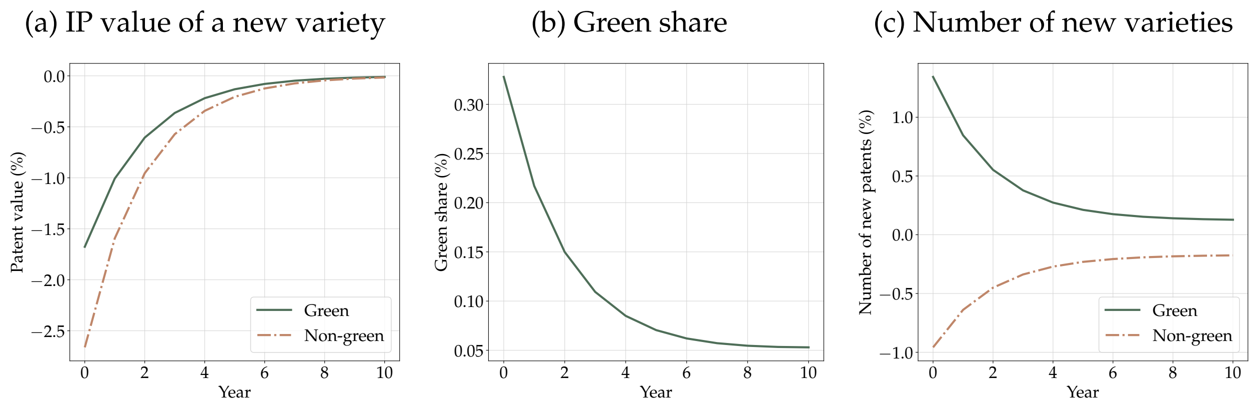

Notes: Impulse responses of the value and number of varieties of green and non-green patents to a 25 basis point monetary policy shock, based on the green business cycle model calibrated to the U.S. economy.

Impulse responses. We now turn to the model's quantitative predictions. We focus on the effects of a monetary policy shock for more direct comparison with the empirical evidence. Figure 7 shows the impulse responses of green and non-green patenting to a 25 basis point monetary policy shock.

The IP value of a non-green new variety is significantly more sensitive to shocks than that of a green variety, falling by over 1.5 times more after a contractionary monetary policy shock. This result demonstrates the quantitative significance of our green is in the future channel underlying Proposition 3.3.

Consistent with the change in the relative values of green and non-green varieties, the green share among new varieties increases. The magnitude of this increase is around 0.3% at peak—in line with the empirical response in Figure 3. Importantly, these moments are not targeted in our calibration, illustrating the quantitative success of the model.

The model not only produces the countercyclicality of the green share, it also generates the countercyclical response of the number of green varieties and the procyclical response of the number of non-green varieties.[13] This is the additional general equilibrium effect via the inelastic supply of skilled labor at play. After a recessionary shock, innovative activity falls, with a disproportionately larger drop in the non-green sector. This reduces the demand for skilled labor, leading to a decline in wages for skilled workers. The lower wages in turn decrease the cost of green R&D, incentivizing firms to undertake more green innovation.

[13] Since there is no clear quantitative mapping between new varieties and new patents, we cannot directly compare the magnitude of these responses to their empirical counterparts.

Figure 8: Decomposition: Cash flow v.s. discount factor channel

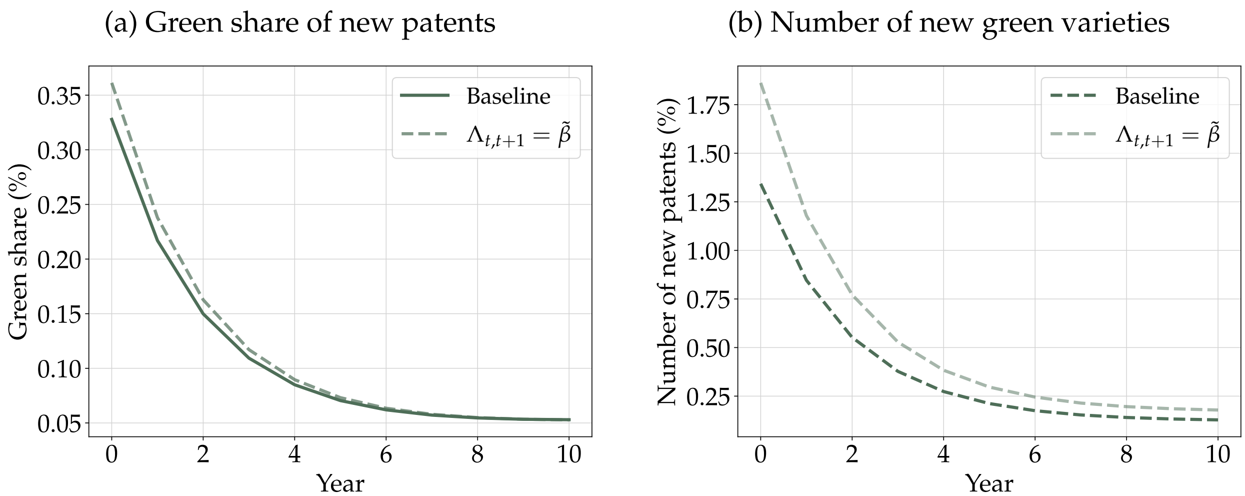

Notes: Impulse responses of the green share of new varieties and the number of new green varieties to a 25 basis point monetary policy shock. We compare the baseline model (with both cash flow and discount factor channels) to a counterfactual in which the discount factor channel is shut down.

How powerful is the discount rate channel in our simulations? To shed light on this, we perform a counterfactual exercise where we keep the discount rate fixed at its no-shock trajectory.[14]

Figure 8 shows the results. We see that the discount rate channel works against the green countercyclicality, conditional on monetary policy shocks. The reason is that these shocks imply a procyclical SDF. When we shut the discount rate channel down, the green share increases by over 0.35%, around 0.03 percentage points more relative to our baseline response. The difference is even more pronounced when we look at the response of the number of new green varieties.

Overall, these results illustrate that while the discount factor channel goes against the cash flow channel, its quantitative impact is relatively modest. In Appendix C.6, we examine the sensitivity of these results with respect to the intertemporal elasticity of substitution. We show that the results are robust when we use a lower intertemporal elasticity of substitution of 0.5, even though the magnitudes are somewhat smaller due to the amplified discount rate channel.

In Appendix C.7, we study the responses to alternative shocks. Preference shocks are of particular interest, as they can generate a countercyclical SDF such that the discount

[14]Specifically, we solve the model under the same equilibrium conditions using the calibrated parameters, but impose an additional restriction that the discount factor in the value of innovation does not respond to business cycle shocks.

rate channel reinforces the green countercyclicality. We find that a negative preference shock increases the degree of countercyclicality relative to a similarly sized contractionary monetary policy shock—but only by about 8%—reaffirming that the cash flow channel remains the dominant driver of the countercyclical pattern in green innovation (see Appendix Figure C.3).

How does the green is in the future channel depend on the starting point and speed of the transition? In our baseline simulations, the economy begins its transition in 2010, and our calibration implies that after 60 years, the transition is halfway completed. The further along in the transition, the weaker the countercyclicality of the green patent share. Interestingly, however, this relationship is not monotonic—the strongest countercyclicality occurs roughly 25 years into the transition. Early on, the pace of green innovation is slower and only picks up over time, making the increase in green profits more pronounced later. Because of discounting, the slope of the profit profile matters: countercyclicality is stronger when 'green is in the more immediate future'. See Appendix C.8 for details. For similar reasons, the countercyclicality of the green patent share is also amplified when the overall speed of the transition is accelerated, see Appendix C.9.

Until now, we have considered a model with an exogenous obsolescence rate. In Appendix C.12, we extend the analysis to a quality-ladder model with creative destruction, where the obsolescence rate is endogenous. Reassuringly, this extended model yields very similar results, both qualitatively and quantitatively.

4.2. Evidence Supporting the Model Mechanism

In this section, we provide direct empirical evidence supporting the key mechanisms of our model. We start by looking into the green is in the future channel. As discussed in Section 3.2, this channel is active when the values of green patents are less cyclical than those of non-green patents. This is a testable prediction that we can confront with the data.

To test this prediction, we require information on the value of green and non-green patents. We draw on the dataset by Kogan et al. (2017), who construct market-implied value of patents filed with the USPTO based on the stock market response to news about patents. We merge the information on patent values to our PATSTAT dataset (see Appendix A for more details).

Based on this data, we can then test the model's prediction about the cyclicality of patent values. We conduct two complementary exercises. First, we exploit panel variation in the patent data to estimate the relative cyclicality of green and non-green patent values:

$$\text{value}_{j,i,t} = \alpha_i + \delta_t + \theta \text{r}_t \times \text{green}_{j,i,t} + \varepsilon_{j,i,t}, \tag{36}$$

where $\text{value}_{j,i,t}$ corresponds to the (log) real value of patent j filed by firm i. We focus on the federal funds rate, instrumented using high-frequency monetary surprises, but also report results using GDP growth instead without conditioning on a specific shock. α_i and δ_t denote firm and time fixed effects, respectively. Since our goal is to estimate the relative cyclicality of green and non-green patent values, captured by θ, the inclusion of time fixed effects allows us to flexibly control for any time-varying common shocks. As quality is homogeneous in the model, we include dummy variables for biadic patents, as well as for patents with at least one citation.

Table 4: Relative cyclicality of green and non-green patent values in the data

	Dependent variable: $100\times\log(\text{patent value}_{j,i,t})$			
	(1)	(2)	(3)	(4)
$\Delta\text{GDP}_t \times \text{green}_{j,i,t}$	-2.12***	-2.05***		
	(0.48)	(0.61)		
$\text{r}_t \times \text{green}_{j,i,t}$			2.48***	2.47***
			(0.52)	(0.52)
Observations	1,256,917	1,256,917	1,256,917	1,256,917
Firm fixed effects	Yes	Yes	Yes	Yes
Time fixed effects	Yes	Yes	Yes	Yes
Quality controls	No	Yes	No	Yes

Notes: The relative cyclicality of green and non-green patent values, estimated based on the patent-level regressions (36). Real patent values are sourced from Kogan et al. (2017), expressed in logs. ΔGDP_t corresponds to real GDP growth and r_t is the policy rate, instrumented using high-frequency monetary surprises. $\text{green}_{j,i,t}$ is a dummy variable denoting green patents. We consider a 1 percentage point increase in GDP growth and a 25 basis point increase in the policy rate. Quality controls include dummy variables for biadic patents and patents with at least one citation. Robust standard errors in parentheses, significance levels denoted by *** $p < 0.01$, ** $p < 0.05$, * $p < 0.10$.

Table 4 reports the estimated coefficients. Consistent with the model's prediction, green patent values are less cyclical than non-green patent values: after a recessionary shock, the value of green patents falls by significantly less than that of non-green patents. This holds true both unconditionally using the GDP growth as well as when conditioning on monetary policy shocks. Moreover, the results are robust to excluding the quality controls.

Second, we construct firm-level patent valuations by tracking the market-implied value of firms' stock of green and non-green patents over time. Using these valuations, we estimate firm-level green and non-green patent value responses to monetary policy shocks based on the panel local projections model (3). To control for quality, we focus only on biadic patents that received at least one citation in the construction of the firm-level value indices.

Figure 9 shows that non-green patent values fall significantly and persistently after a contractionary monetary policy shock. By contrast, the values of green patents are much less affected: while they also tend to decline, the response is weaker and not statistically significant. Notably, the magnitudes are roughly comparable to those obtained in our calibrated model, as shown in Figure 7a.

Figure 9: Impulse responses of U.S. firms' green and non-green patent values

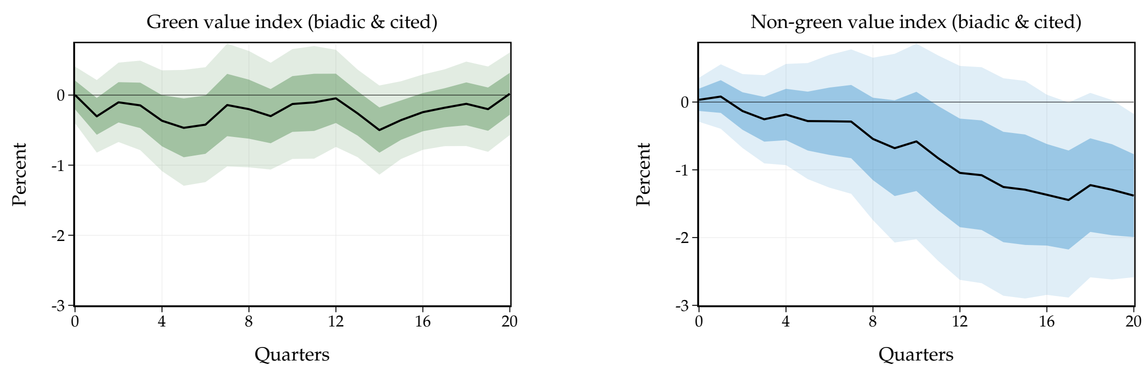

Notes: Impulse responses of firms' green and non-green patent values in the United States to a monetary policy shock, estimated based on the panel local projections model (3) using high-frequency monetary surprises as an instrument. The dependent variable is the cumulative real value of firm-level patents, sourced from Kogan et al. (2017), separately computed for green and non-green patents and expressed in logs. The shock is normalized to increase the federal funds rate by 25 basis points on impact. Solid line: point estimate. Dark and light shaded areas: 68 and 95% confidence bands based on Driscoll and Kraay (1998) standard errors.

Next, we aim to shed light on the general equilibrium effects via the market of skilled labor. Our model predicts a decline in non-green patenting during business cycle downturns, depressing wages of skilled workers and thus making it cheaper for firms to engage in green innovation. To test this prediction in the data, we use PATSTAT data on inventors referenced in patent filings. This allows us to classify green and non-green inventors based on what patents they worked on.

Equipped with these data, we aggregate the number of green and non-green inventors at the firm-level and construct the share of green inventors. We then trace their dynamic responses to monetary shocks, using the panel local projections model (3). Figure 10 shows a significant increase in the number and share of green inventors. We find that at least part of this increase is driven by new inventors, i.e. inventors that have not patented at the firm previously (see Appendix B.9). These results are consistent with the general equilibrium effects via the skilled labor market that operate in our model.

Figure 10: Firm-level responses of green inventors

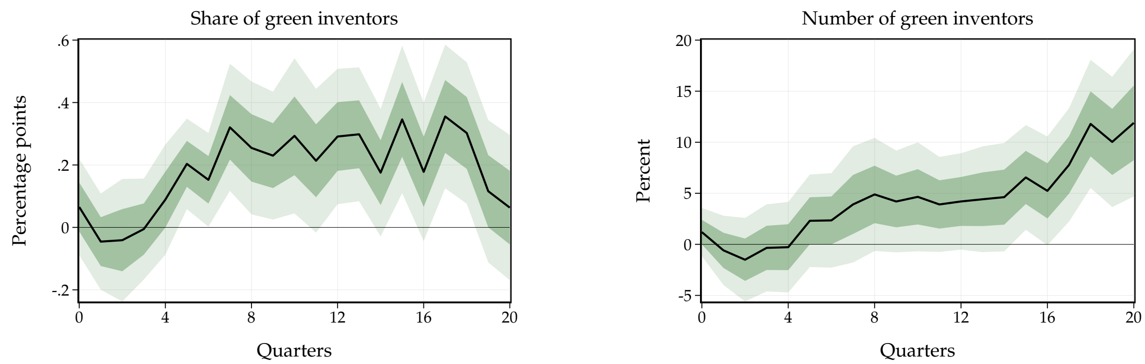

Notes: Responses of the share and number of green inventors in U.S. firms to a monetary policy shock, estimated based on the panel local projections model (3) using high-frequency monetary surprises as an instrument. The shock is normalized to increase the federal funds rate by 25 basis points on impact. Solid line: point estimate. Dark and light shaded areas: 68 and 95% confidence bands based on Driscoll and Kraay (1998) standard errors.

Overall, this evidence corroborates our model mechanisms that allow us to generate the countercyclicality of the green patent share and the number of green patents.

5. Conclusion

This paper documents a novel empirical fact: while non-green innovation is procyclical, green innovation is countercyclical. Not only is green patenting less affected by recessionary shocks, the number of green patents even tends to rise during downturns. This pattern holds across aggregate and firm-level data, within the U.S. and internationally, and persists when conditioning on different types of macroeconomic shocks. These findings challenge the conventional view that innovation declines uniformly in recessions and call for a deeper understanding of the distinct economic forces shaping green technological progress.

To explain these patterns, we develop a business cycle model with endogenous green and non-green innovation. At the core of the model is the green is in the future channel: along the transition, green patents yield profits that are more backloaded than non-green ones, making their value less sensitive to transitory macroeconomic shocks. In general equilibrium, this effect is reinforced through reallocation in the skilled labor market. When downturns depress non-green innovation, the resulting decline in skilled wages lowers the cost of green R&D, further boosting green innovation. Our model not only accounts for the relative and absolute cyclicality observed in the data but is also supported by direct evidence on underlying mechanisms—specifically, the weaker cyclicality of green patent values and the reallocation of inventors toward green technologies during recessions.

Our results underscore the importance of understanding how macroeconomic fluctuations interact with the green transition. While green innovation is often framed as a long-run structural challenge, our findings highlight its sensitivity to short-run dynamics. This has several important implications. First, it matters for interpreting progress on the green transition in the data: business cycle fluctuations may lead to temporary slowdowns or accelerations in green innovation that do not reflect changes in long-run fundamentals. Misinterpreting these short-term fluctuations could lead policymakers to draw incorrect conclusions about the pace of the transition. Second, our findings shed light on the transmission mechanism of climate change policies, including carbon pricing. If such policies have contractionary effects on the broader economy, these forces could amplify the positive impact on green innovation according to our findings. Finally, because recessionary shocks can spur green innovation, it is important to account for macroeconomic conditions when estimating the causal effects of climate policies—otherwise, business cycle dynamics may confound the interpretation of empirical evidence.

References

Acemoglu, Daron, Philippe Aghion, Lint Barrage, and David Hémous (2023). *Climate change, directed innovation, and energy transition: The long-run consequences of the shale gas revolution*. Tech. rep. National Bureau of Economic Research.

Acemoglu, Daron, Philippe Aghion, Leonardo Bursztyn, and David Hémous (2012). "The environment and directed technical change". *American Economic Review* 102.1, pp. 131–166.

Acemoglu, Daron, Ufuk Akcigit, Douglas Hanley, and William Kerr (2016). "Transition to clean technology". *Journal of Political Economy* 124.1, pp. 52–104.

Aghion, Philippe, George-Marios Angeletos, Abhijit Banerjee, and Kalina Manova (2010). "Volatility and growth: Credit constraints and the composition of investment". *Journal of Monetary Economics* 57.3, pp. 246–265.

Aghion, Philippe, Philippe Askenazy, Nicolas Berman, Gilbert Cette, and Laurent Eymard (2012). "Credit constraints and the cyclicality of R&D investment: Evidence from France". *Journal of the European Economic Association* 10.5, pp. 1001–1024.

Aghion, Philippe, Antonin Bergeaud, Maarten De Ridder, and John Van Reenen (2024). "Lost in transition: Financial barriers to green growth".

Aghion, Philippe, Antoine Dechezleprêtre, David Hémous, Ralf Martin, and John Van Reenen (2016). "Carbon taxes, path dependency, and directed technical change: Evidence from the auto industry". *Journal of Political Economy* 124.1, pp. 1–51.

Aghion, Philippe and Peter Howitt (1992). "A model of growth through creative destruction". *Econometrica* 60.2.

Aghion, Philippe and Gilles Saint-Paul (1998). "Uncovering some causal relationships between productivity growth and the structure of economic fluctuations: a tentative survey". *Labour* 12.2, pp. 279–303.

Angeletos, George-Marios, Fabrice Collard, and Harris Dellas (2020). "Business-cycle anatomy". *American Economic Review* 110.10, pp. 3030–3070.

Antolin-Diaz, Juan and Paolo Surico (2022). *The long-run effects of government spending*. Centre for Economic Policy Research.

Anzoategui, Diego, Diego Comin, Mark Gertler, and Joseba Martinez (2019). "Endogenous technology adoption and R&D as sources of business cycle persistence". *American Economic Journal: Macroeconomics* 11.3, pp. 67–110.

Arora, Ashish, Sharon Belenzon, and Lia Sheer (2021). "Knowledge spillovers and corporate investment in scientific research". *American Economic Review* 111.3, pp. 871–898.

Barlevy, Gadi (Sept. 2007). "On the Cyclicality of Research and Development". *American Economic Review* 97.4, pp. 1131–1164.

Bauer, Michael D. and Eric T. Swanson (2023). "A reassessment of monetary policy surprises and high-frequency identification". *NBER Macroeconomics Annual* 37.1, pp. 87–155.

Benigno, Gianluca and Luca Fornaro (2018). "Stagnation traps". *The Review of Economic Studies* 85.3, pp. 1425–1470.

Bianchi, Francesco, Howard Kung, and Gonzalo Morales (2019). "Growth, slowdowns, and recoveries". *Journal of Monetary Economics* 101, pp. 47–63.

Bilal, Adrien and Diego R. Känzig (2024). *The Macroeconomic Impact of Climate Change: Global vs. Local Temperature*. Tech. rep. National Bureau of Economic Research.

Bornstein, Gideon, Per Krusell, and Sergio Rebelo (2023). "A world equilibrium model of the oil market". *The Review of Economic Studies* 90.1, pp. 132–164.

Burke, Marshall, Mustafa Zahid, Noah Diffenbaugh, and Solomon M Hsiang (2023). *Quantifying climate change loss and damage consistent with a social cost of greenhouse gases*. Tech. rep. National Bureau of Economic Research.

Calel, Raphael and Antoine Dechezleprêtre (2016). "Environmental policy and directed technological change: evidence from the European carbon market". *Review of Economics and Statistics* 98.1, pp. 173–191.

Chen, Ziqiao, Giovanni Marin, David Popp, and Francesco Vona (2021). "The Employment Impact of Green Fiscal Push: Evidence from the American Recovery and Reinvestment Act". *Brookings Papers on Economic Activity*.

Chetty, Raj, Adam Guren, Day Manoli, and Andrea Weber (2011). "Are micro and macro labor supply elasticities consistent? A review of evidence on the intensive and extensive margins". *American Economic Review* 101.3, pp. 471–475.

Cohen, Lauren, Umit G. Gurun, and Quoc H. Nguyen (2020). *The ESG-innovation disconnect: Evidence from green patenting*. Tech. rep. National Bureau of Economic Research.

Colmer, Jonathan, Ralf Martin, Mirabelle Muûls, and Ulrich J. Wagner (2024). "Does pricing carbon mitigate climate change? Firm-level evidence from the European Union Emissions Trading System". *Review of Economic Studies*, rdae055.

Comin, Diego and Mark Gertler (2006). "Medium-term business cycles". *American Economic Review* 96.3, pp. 523–551.

Driscoll, John C. and Aart C. Kraay (1998). "Consistent covariance matrix estimation with spatially dependent panel data". *Review of Economics and Statistics* 80.4, pp. 549–560.

Elminejad, Ali, Tomas Havranek, Roman Horvath, and Zuzana Irsova (2023). "Intertemporal substitution in labor supply: A meta-analysis". *Review of Economic Dynamics* 51, pp. 1095–1113.

Engle, Robert F., Stefano Giglio, Bryan Kelly, Heebum Lee, and Johannes Stroebel (2020). "Hedging climate change news". *The Review of Financial Studies* 33.3, pp. 1184–1216.

Fornaro, Luca, Veronica Guerrieri, and Lucrezia Reichlin (2024). *Monetary policy for the energy transition*. Tech. rep. Technical report, Working Paper.

— (2025). "Monetary policy for the green transition".

Furlanetto, Francesco, Antoine Lepetit, Ørjan Robstad, Juan Rubio-Ramırez, and Pål Ulvedal (2025). "Estimating hysteresis effects". *American Economic Journal: Macroeconomics* 17.1, pp. 35–70.

Gertler, Mark and Peter Karadi (2015). "Monetary policy surprises, credit costs, and economic activity". *American Economic Journal: Macroeconomics* 7.1, pp. 44–76.

Gilchrist, Simon and Egon Zakrajšek (2012). "Credit spreads and business cycle fluctuations". *American Economic Review* 102.4, pp. 1692–1720.

Gornemann, Nils, Pablo Guerrón-Quintana, and Felipe Saffie (2021). "Real Exchange Rates and Endogenous Productivity".

Hall, Bronwyn H., Adam B. Jaffe, and Manuel Trajtenberg (2001). *The NBER patent citation data file: Lessons, insights and methodological tools*.

Hassler, John, Per Krusell, and Conny Olovsson (2021). "Directed technical change as a response to natural resource scarcity". *Journal of Political Economy* 129.11, pp. 3039–3072.

Hémous, David, Morten Olsen, Carlo Zanella, and Antoine Dechezleprêtre (2025). "Induced Automation Innovation: Evidence from Firm-level Patent Data".

Ilzetzki, Ethan (2024). "Learning by necessity: Government demand, capacity constraints, and productivity growth". *American Economic Review* 114.8, pp. 2436–2471.

Jarociński, Marek and Peter Karadi (2020). "Deconstructing monetary policy surprises—the role of information shocks". *American Economic Journal: Macroeconomics* 12.2, pp. 1–43.

Jordà, Òscar (2005). "Estimation and inference of impulse responses by local projections". *American Economic Review* 95.1, pp. 161–182.

Jordà, Òscar, Sanjay R. Singh, and Alan M. Taylor (2024). "The long-run effects of monetary policy". *Review of Economics and Statistics*, pp. 1–49.

Kahle, Kathleen M. and René M. Stulz (2017). "Is the US public corporation in trouble?" *Journal of Economic Perspectives* 31.3, pp. 67–88.

Känzig, Diego R. (2023). “The unequal economic consequences of carbon pricing”. *Available at SSRN 3786030*.

King, Robert G. and Sergio T. Rebelo (1999). “Resuscitating real business cycles”. *Handbook of macroeconomics* 1, pp. 927–1007.

Kogan, Leonid, Dimitris Papanikolaou, Amit Seru, and Noah Stoffman (2017). “Technological innovation, resource allocation, and growth”. *The Quarterly Journal of Economics* 132.2, pp. 665–712.

Kung, Howard and Lukas Schmid (2015). “Innovation, growth, and asset prices”. *The Journal of Finance* 70.3, pp. 1001–1037.

Kydland, Finn E. and Edward C. Prescott (1982). “Time to build and aggregate fluctuations”. *Econometrica: Journal of the Econometric Society*, pp. 1345–1370.

Ma, Song (2021). *Technological obsolescence*. Tech. rep. National Bureau of Economic Research.

Ma, Yueran and Kaspar Zimmermann (2023). *Monetary policy and innovation*. Tech. rep. National Bureau of Economic Research.

Migotto, Mauro and Ivan Haščič (2015). “Measuring environmental innovation using patent data”. *OECD Environment Working Papers* 89.89, pp. 1–59.

Miranda-Agrippino, Silvia and Hélene Rey (2020). “US monetary policy and the global financial cycle”. *The Review of Economic Studies* 87.6, pp. 2754–2776.

Montiel Olea, José Luis and Mikkel Plagborg-Møller (2021). “Local projection inference is simpler and more robust than you think”. *Econometrica* 89.4, pp. 1789–1823.

Nagaoka, Sadao, Kazuyuki Motohashi, and Akira Goto (2010). “Patent statistics as an innovation indicator”. *Handbook of the Economics of Innovation*. Vol. 2. Elsevier, pp. 1083–1127.

Nakamura, Emi and Jón Steinsson (2018). “High-frequency identification of monetary non-neutrality: The information effect”. *The Quarterly Journal of Economics* 133.3, pp. 1283–1330.

Ottonello, Pablo and Thomas Winberry (2020). “Financial heterogeneity and the investment channel of monetary policy”. *Econometrica* 88.6, pp. 2473–2502.

Popp, David (2002). “Induced innovation and energy prices”. *American Economic Review* 92.1, pp. 160–180.

Queralto, Albert (2020). “A model of slow recoveries from financial crises”. *Journal of Monetary Economics* 114, pp. 1–25.

Romer, Paul M. (1990). “Endogenous technological change”. *Journal of Political Economy* 98.5, Part 2, S71–S102.

Wang, Lixing and Donghai Zhang (2025). "A Theory of Lumpy Innovation and Aggregate Dynamics". *Available at SSRN 4818040*.

Online Appendix

Green Business Cycles

Diego R. Känzig
Maxilian Konradt
Lixing Wang
Donghai Zhang

Contents

A. Data

In this appendix, we provide additional information on the sources and the construction of our sample. We discuss the sources for the patent and firm-level data as well as how we match patents to firms. Finally, we provide details on how we aggregate the patent data, as well as the supplementary macroeconomic and financial data used in our analyses.

A.1. Patent Data

Our main source of patent data is the World Patent Statistical Database (PATSTAT), which encompasses bibliographic information for close to the universe of patents globally. We use the autumn 2023 edition (version 5.22).

We follow the previous literature (e.g. Hémous et al., 2025) to focus on patent families, i.e. patents representing the same innovation filed at different patent offices. For each patent family we use the original application date to capture the time of the innovation and assign nationality based on the respective filing office.

To measure green innovation, we use International Patent Classification (IPC) and Co-operative Patent Classification (CPC) codes. Specifically, we apply the OECD definition (Migotto and Haščič, 2015) to classify patent families in subclass Y02 of the C/IPC, which includes technologies that reduce greenhouse gases. Following Acemoglu et al. (2023), we exclude technologies that do not directly compete with fossil-fuel technologies, including those aimed at reducing pollution from fossil-fuel electricity generation (Y02E20), improving grid efficiency (Y02E40) or storage (Y02E60). We classify patent families with multiple C/IPC codes as green if any of the respective codes meet our criteria. We treat the remaining patent (families) as non-green.

Table A.1: Green patents by CPC code, 1986-2019

CPC code	Description	Number of patents	Share of sample
Y02E	Production, distribution and transport of energy	109,682	35.93
Y02T	Transportation	63,053	20.66
Y02P	Industry and agriculture	61,760	20.23
Y02A	Adaptation to climate change	34,258	11.22
Y02B	Buildings	32,598	10.68
Y02D	ICT aiming at reduction of own energy use	31,350	10.27
Y02W	Wastewater treatment or waste management	14,995	4.91
Y04S	Smart grids	9,832	3.22
Y02C	Capture and storage of greenhouse gases	4,416	1.45

Notes: Based on USPTO patent families.

What are the most salient green subclasses? Table A.1 shows that the majority of green patent filings in our data are associated with production, distribution and transport of energy (Y02E), transportation (Y02T), and industry and agriculture (Y02P).

Table A.2: Example of a green patent family by Hitachi Ltd.

Patent number	Patent name	Filing date	CPC codes
US7185722	Power transmission apparatus of motor vehicles	01.09.2000	B60W 20/00, B60K 6/442, B60K 6/48, B60K 6/547, B60W 10/02, B60W 10/06, B60W 10/08, B60W 10/10, F16D 25/0638, F16H 3/089, F16H 61/0437, Y02T 10/6221, Y02T 10/6234, Y02T 10/6286, Y10S 903/914, Y10S 903/917, Y10S 903/919, Y10S 903/945, Y10S 903/946, Y10T 74/19014, Y10T 74/19242, Y10T 74/19284, Y10T 477/23
EP1122111	A power transmission apparatus for hybrid vehicles	04.09.2000	B60K 6/442, B60K 6/48, B60K 6/547, B60W 10/02, B60W 10/06, B60W 10/08, B60W 10/10, B60W 20/00, F16H 3/089, F16H 61/0437, Y10S 903/945, Y10S 903/946, Y10S 903/914, Y10S 903/917, Y10S 903/919, Y10T 74/19014, Y10T 74/19284, Y10T 74/19242, Y02T 10/62, B60K 2006/268, B60K 17/02, F16D 25/0638
DE000060021163	Antriebsübertragungsvorrichtung für Hybridfahrzeuge	04.09.2000	B60K 6/442, B60K 6/48, B60K 6/547, B60W 10/02, B60W 10/06, B60W 10/08, B60W 10/10, B60W 20/00, F16H 3/089, F16H 61/0437, Y10S 903/945, Y10S 903/946, Y10S 903/914, Y10S 903/917, Y10S 903/919, Y10T 74/19014, Y10T 74/19284, Y10T 74/19242, Y02T 10/62, B60K 2006/268, B60K 17/02, F16D 25/0638
KR1020010077862	Power transmission apparatus of motor vehicles	04.09.2000	B60W 20/00, B60K 6/442, B60K 6/48, B60K 6/547, B60W 10/02, B60W 10/06, B60W 10/08, B60W 10/10, F16D 25/0638, F16H 3/089, F16H 61/0437, Y02T 10/6221, Y02T 10/6234, Y02T 10/6286, Y10S 903/914, Y10S 903/917, Y10S 903/919, Y10S 903/945, Y10S 903/946, Y10T 74/19014, Y10T 74/19242, Y10T 74/19284, Y10T 477/23
EP1122110	A power transmission apparatus of motor vehicles	02.02.2001	B60K 6/442, B60K 6/48, B60K 6/547, B60W 10/02, B60W 10/06, B60W 10/08, B60W 10/10, B60W 20/00, F16H 3/089, F16H 61/0437, Y10S 903/945, Y10S 903/946, Y10S 903/914, Y10S 903/917, Y10S 903/919, Y10T 74/19014, Y10T 74/19284, Y10T 74/19242, Y02T 10/62, B60K 2006/268, B60K 17/02, F16D 25/0638
US20010042647	Power transmission apparatus of motor vehicles	02.02.2001	B60W 20/00, B60K 6/442, B60K 6/48, B60K 6/547, B60W 10/02, B60W 10/06, B60W 10/08, B60W 10/10, F16D 25/0638, F16H 3/089, F16H 61/0437, Y02T 10/6221, Y02T 10/6234, Y02T 10/6286, Y10S 903/914, Y10S 903/917, Y10S 903/919, Y10S 903/945, Y10S 903/946, Y10T 74/19014, Y10T 74/19242, Y10T 74/19284, Y10T 477/23
KR1020010078264	Power transmission apparatus of motor vehicles	02.02.2001	B60W 20/00, B60K 6/442, B60K 6/48, B60K 6/547, B60W 10/02, B60W 10/06, B60W 10/08, B60W 10/10, F16D 25/0638, F16H 3/089, F16H 61/0437, Y02T 10/6221, Y02T 10/6234, Y02T 10/6286, Y10S 903/914, Y10S 903/917, Y10S 903/919, Y10S 903/945, Y10S 903/946, Y10T 74/19014, Y10T 74/19242, Y10T 74/19284, Y10T 477/23
JP2001287555	Power transmission of automobile	02.02.2001	Y02T 10/62, Y02T 10/7072

Notes: For more information, see https://patentscope.wipo.int/search/en/detail.jsf?docId=US41976272.

To illustrate how we handle patent families, Table A.2 provides an example of a patent family related to a power transmission apparatus for hybrid vehicles by Hitachi Ltd. filed at five different patent offices. The patent family is classified as green because it includes multiple CPC codes in subclass Y02T. Because the first patent was filed with the USPTO, we treat it as a U.S. patent and use September 2000 as the relevant date.

Finally, in Table A.3, we provide a number of additional examples of green patents, specifically related to photovoltaic and solar technologies.

Table A.3: Examples of green patents related to photovoltaic and solar technologies

Patent number	Patent name	Applicant	Filing date	CPC codes
US5959787	Concentrating coverglass for photovoltaic cells	The Boeing Company	26.11.1996	Y02E
US6461947	Photovoltaic device and making of the same	Hitachi, Ltd.	07.09.2000	Y02E, Y02P
US20070267290	Photovoltaically powered cathodic protection system for automotive vehicle	Ford Global Technologies, LLC	16.05.2006	Y02T
US20180054064	Smart main electrical panel for energy generation systems	Tesla, Inc.	29.09.2016	Y02B, Y02E

PATSTAT also reports information on patent citations. We compute citation counts at the family level, excluding any self citations within the same family. To measure quality, we additionally define biadic patents, filed with at least two of the three major patent offices (USPTO, EPO and JPO).

A.2. Firm Data

We rely on Compustat North America for accounting data on listed U.S. companies. Following Cloyne et al. (2023) we exclude Compustat companies in the finance, insurance, real estate and public administration sectors and drop firms which report data for fewer than 20 quarters, or have missing investment or sales figures for more than 20 quarters. We measure firm age using the date of incorporation, which we supplement from Thomson Reuter's WorldScope.

In contrast to Cloyne et al. (2023), we only exclude firms with negative or missing age when we explicitly study firm heterogeneity, including the effects on younger and older firms. Otherwise, we retain firms even if the age variable is negative.[1] We limit our

[1] The age data are noisy, e.g. because of firm mergers and acquisitions. The firm-level estimates are consistent when we apply more restrictive criteria.

attention to years with consistent reporting, starting in 1986Q1.

Table A.4 shows how we construct the key firm-level variables of interest based on the Compustat data. To limit the impact of outliers, we winsorize the book-to-market ratio at the 1^{st} and 99^{th} percentile in each year. We also merge data on firm-level emissions from Trucost using company ISIN codes. We focus on the Scope 1 GHG emission intensity (scaled by revenue), which is available for roughly half of the companies in our dataset.

Table A.4: Definitions of firm-level variables

Variable	Compustat definition
Size	atq
Investment	capxq/ppentq
Leverage ratio	(dlcq+dlttq)/atq
Book-to-market	ceqq/(prccq*cshoq)
R&D intensity	xrdq/atq
Short term debt	dlcq/(dlcq+dlttq)
Tobin's Q	(tq + prccq*cshoq - ceqq + txditcq) / atq

A.3. Matching Patents to Firms

Measuring U.S. firms' innovation activity requires matching patents to firm-level data. To maximize the number of successful matches, we rely on two different datasets. The first is Orbis Intellectual Property, which links global patent portfolios to Orbis companies (see Hémous et al., 2025). We map Orbis to Compustat companies using the ISIN identifier, which implies we are measuring innovation at the U.S. group level.

Second, we also employ the mapping by Arora, Belenzon, and Sheer (2021), which establishes a link between USPTO patents and Compustat firms based on a fuzzy matching approach and extends the NBER patent database (Hall, Jaffe, and Trajtenberg, 2001).[2] Combining the matches in both datasets we are able to link 1.7 million distinct patent families to Compustat firms, including about 93,000 green patents.[3]

We use the unique patent application number encompassed in both datasets to merge the relevant information from PATSTAT. In particular, we construct firm-level patent counts for green and non-green patents at quarterly frequency. To that end, we retain patents filed with the USPTO and international filings.

[2] For more details on the approach, see Arora et al. (2024).

[3] Reassuringly, the two mappings overlap significantly: Orbis identifies 1.296 million total (73,600 green) patents, while applying Arora, Belenzon, and Sheer (2021) results in 1.094 million total (58,000 green) matched patents.

In addition to patent counts, we are also interested in quantifying patent values. We therefore match our firm-level data with market-implied patent value data constructed by Kogan et al. (2017), extended to 2020. Consistent with our earlier definition, we focus on the first patent in a patent family to infer its value, but verify that taking an average value does not impact our results. Lastly, to dynamically study the value of firms' innovation, we construct cumulative value indices for green and non-green patents at the firm-level.

A.4. Aggregate Patent Counts

In order to assess the correlation of innovation activity with the business cycle, we compute aggregate patent counts. First, we construct separate series for U.S. green and non-green patents based on USPTO filings. Second, we compute similar patent counts for OECD countries, including filings with the respective national offices and the EPO. For the OECD, we also include international applications filed under the Patent Cooperation Treaty, but verify that excluding them does not impact our estimates. Finally, we construct counts at the global level, exploiting all available information in PATSTAT.

Third, since Compustat covers close to the universe of listed companies in the U.S., we can also aggregate our matched firm-level patents to compute separate counts for listed and unlisted U.S. firms. Compustat accounts for 97-99% of market capitalization of all listed firms in the U.S. between 1975-2015 according to Kahle and Stulz (2017). Because we assign patent nationality based on the original patent office, we expect that filings by foreign corporations are modest.

To control for potential seasonality, we apply an X-11 filter to our constructed aggregate patent counts.

A.5. Macroeconomic Data

We complement the innovation and firm-level data with a set of aggregate macroeconomic and financial variables, listed in Table A.5.

Table A.5: Macro data description and sources

Variable	Description	Source
U.S. data		
Monetary surprise	Purified high-frequency monetary surprises from Bauer and Swanson (2023)	Michael Bauer's website
Excess bond premium	Gilchrist and Zakrajšek (2012)	FRB website
Monetary surprise	Jarociński and Karadi (2020)	Marek Jarocinski's website
Oil supply shock	Känzig (2021)	Diego Känzig's website
TFP	Fernald (2014)	San Francisco Fed
Climate policy news index	Gavriilidis et al. (2025)	mimeo
Climate news index	Engle et al. (2020)	Johannes Stroebel's website
Federal funds rate	FEDFUNDS	FRED
Real GDP	GDPC1	FRED
GDP deflator	GDPDEF	FRED
Unemployment rate	UNRATE	FRED
Industrial production	INDPRO	FRED
1-year rate	GS1	FRED
Investment	A008RA3Q086SBEA	FRED
Oil price	WTISPLC	FRED
Government spending	GCEC1	FRED
OECD data		
Industrial production	Global IP index by Baumeister and Hamilton (2019)	Christiane Baumeister's website
Real GDP	Based on 19 OECD countries	OECD
GDP deflator	Based on 19 OECD countries	OECD
Unemployment rate	Based on 9 OECD countries with consistent data	OECD

Notes: Due to data limitations, we construct the unemployment series based on data from 9 major OECD countries that consistently report since 1986. These countries include the United States, Germany, Japan, Australia, the United Kingdom, New Zealand, Chile and Canada.

B. Additional Charts and Tables

In this appendix, we report a number of additional results, as well as robustness checks.

B.1. Green Innovation by the 20 Largest Green U.S. Innovators

Table B.1: Green patenting by the 20 largest green innovators

	Patenting measure		
Company	Total patents	Green patents	Green patent share
RTX CORP	35,780	6,197	17.32
FORD MOTOR CO	24,275	5,839	24.05
GENERAL MOTORS CO	29,376	5,148	17.52
INTEL CORP	60,630	4,116	6.79
INTL BUSINESS MACHINES CORP	129,491	3,797	2.93
QUALCOMM INC	39,358	3,235	8.22
BOEING CO	20,761	2,824	13.60
CATERPILLAR INC	12,321	1,890	15.34
HP INC	52,319	1,872	3.58
APPLE INC	26,243	1,711	6.52
DU PONT (E I) DE NEMOURS	19,877	1,569	7.89
EXXON MOBIL CORP	11,152	1,429	12.81
MOTOROLA SOLUTIONS INC	27,752	1,255	4.52
MICROSOFT CORP	55,076	1,192	2.16
CUMMINS INC	4,350	1,181	27.15
TEXAS INSTRUMENTS INC	25,256	1,176	4.66
CORNING INC	12,311	983	7.98
ADVANCED MICRO DEVICES	16,560	901	5.44
APPLIED MATERIALS INC	15,821	889	5.62
LOCKHEED MARTIN CORP	10,154	812	8.00

Notes: The table reports patent measures for the 20 largest innovators in the U.S. between 1986–2019, based on green patent counts.

B.2. Unconditional Cyclicality using Alternative Economic Indicators

Figure B.1: Patenting responses to business cycle shock

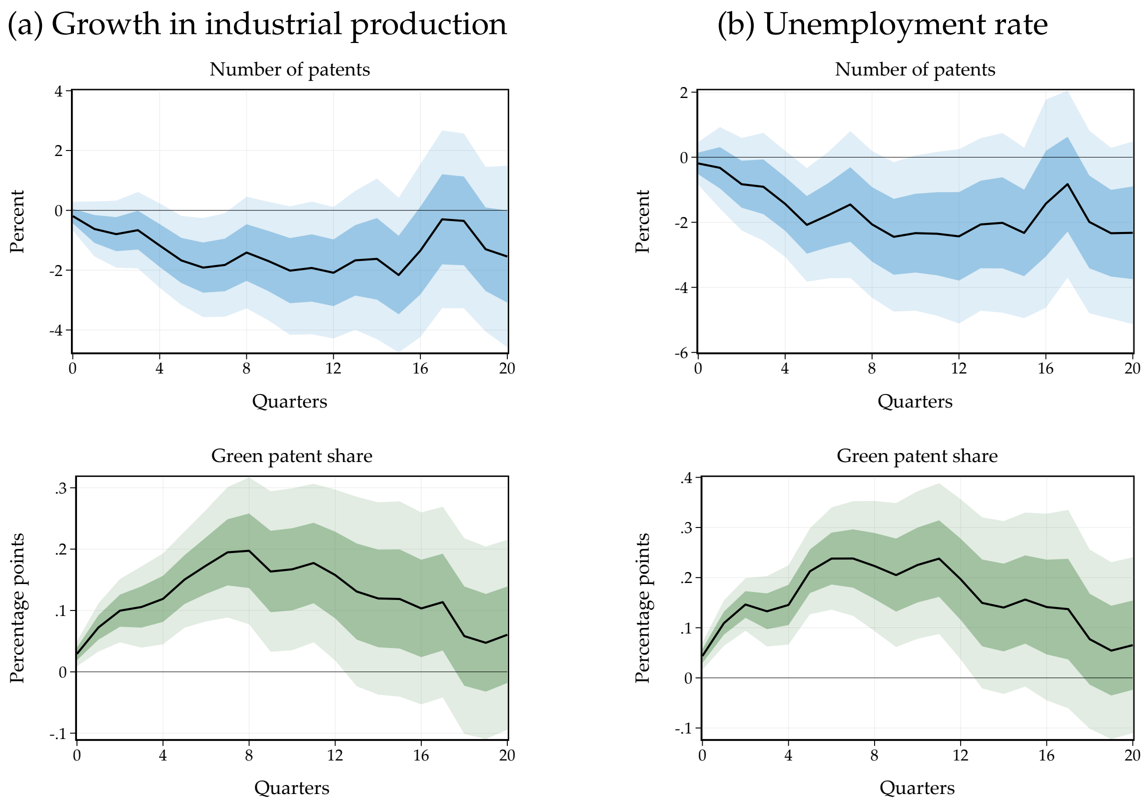

Notes: Impulse responses of total patents and the green patent share in the United States to a recessionary innovation to industrial production (normalized to decrease growth in IP by 1%) and the unemployment rate (normalized to increase the unemployment rate by 25 basis points), estimated based on the reduced-form local projections (1). Solid line: point estimate. Dark and light shaded areas: 68 and 95% confidence bands based on lag-augmented standard errors.

B.3. Responses of Macroeconomic Variables to Monetary Policy Shock

Figure B.2: Macroeconomic effects of a U.S. monetary policy shock

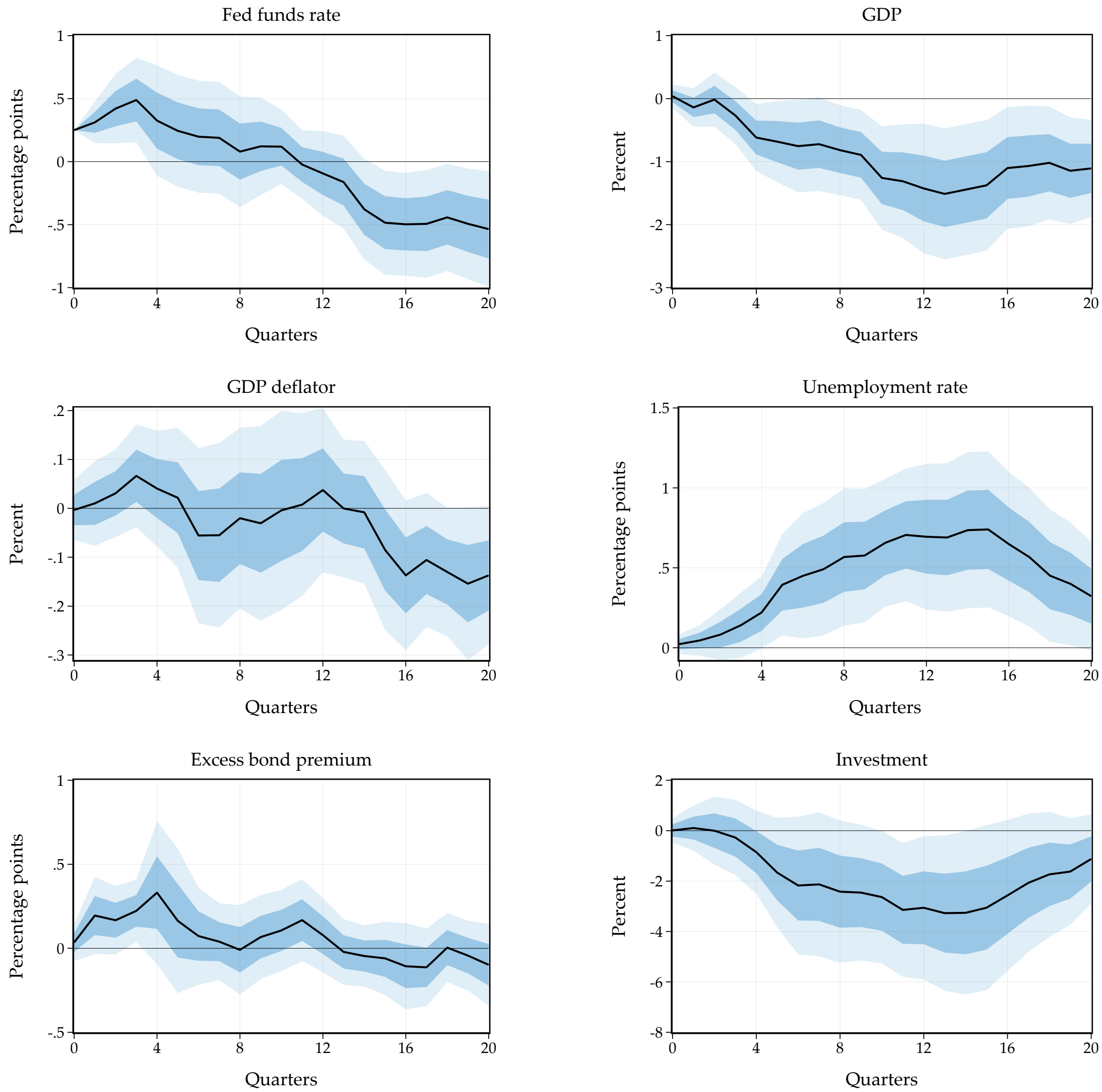

Notes: Macroeconomic effects of a U.S. monetary policy shock, estimated based on the local projections model (2) using high-frequency monetary surprises as an instrument. The shock is normalized to increase the federal funds rate by 25 basis points on impact. Solid line: point estimate. Dark and light shaded areas: 68 and 95% confidence bands based on lag-augmented standard errors.

B.4. Additional Results for Listed and Unlisted U.S. Firms

Figure B.3: Cyclical component of green and non-green patents by U.S. companies

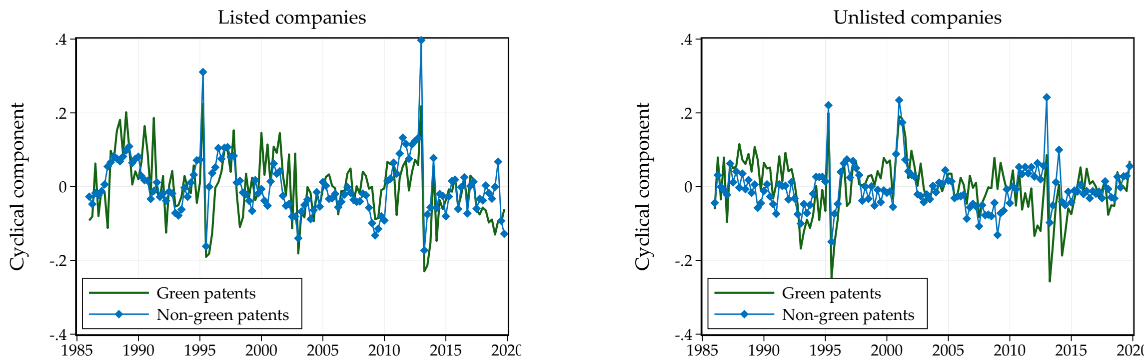

Notes: Cycles in green and non-green patenting for listed (left panel) and unlisted (right panel) U.S. companies. The panels display the cyclical components of green and non-green patent counts, extracted using the Hodrick-Prescott filter with $\lambda = 1,600$.

Figure B.4: Green and non-green patenting responses for listed and unlisted U.S. firms

(a) Listed firms (b) Unlisted firms

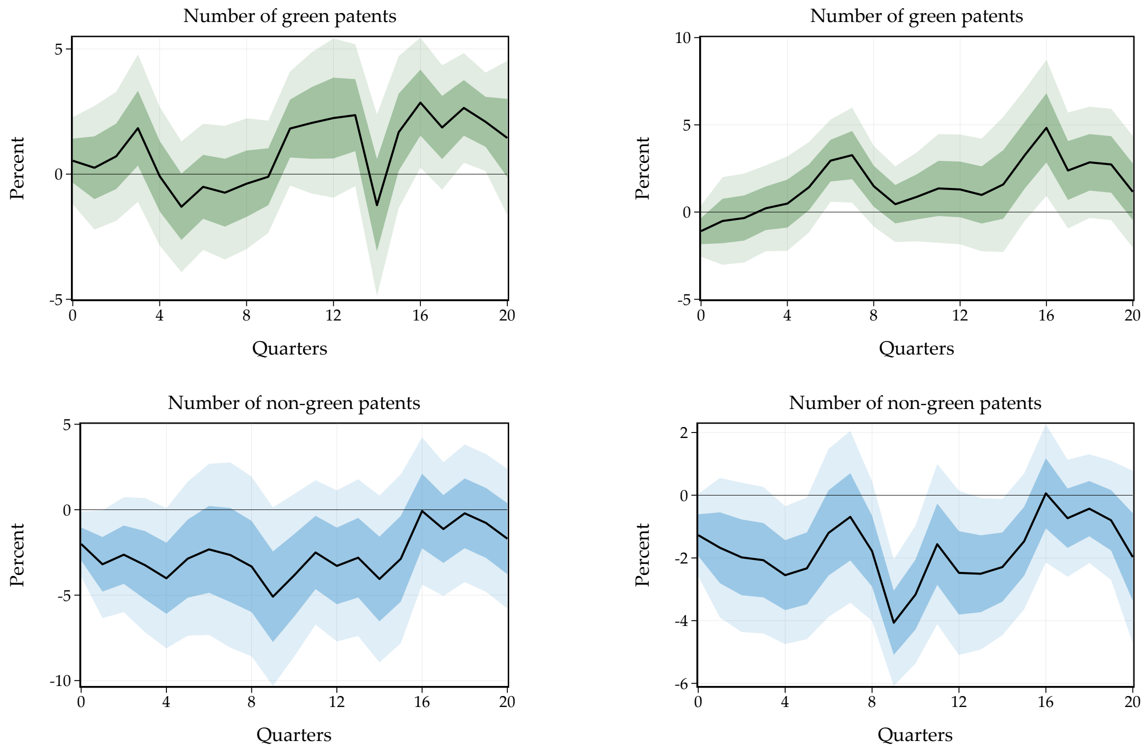

Notes: Impulse responses of green and non-green patents by listed and unlisted U.S. firms to a monetary policy shock, estimated based on the local projections model (2) using high-frequency monetary surprises as an instrument. The shock is normalized to increase the federal funds rate by 25 basis points on impact. Solid line: point estimate. Dark and light shaded areas: 68 and 95% confidence bands based on lag-augmented standard errors.

B.5. Additional Results for OECD Countries and Global Patents

Figure B.5: Green and non-green patenting responses in different geographies

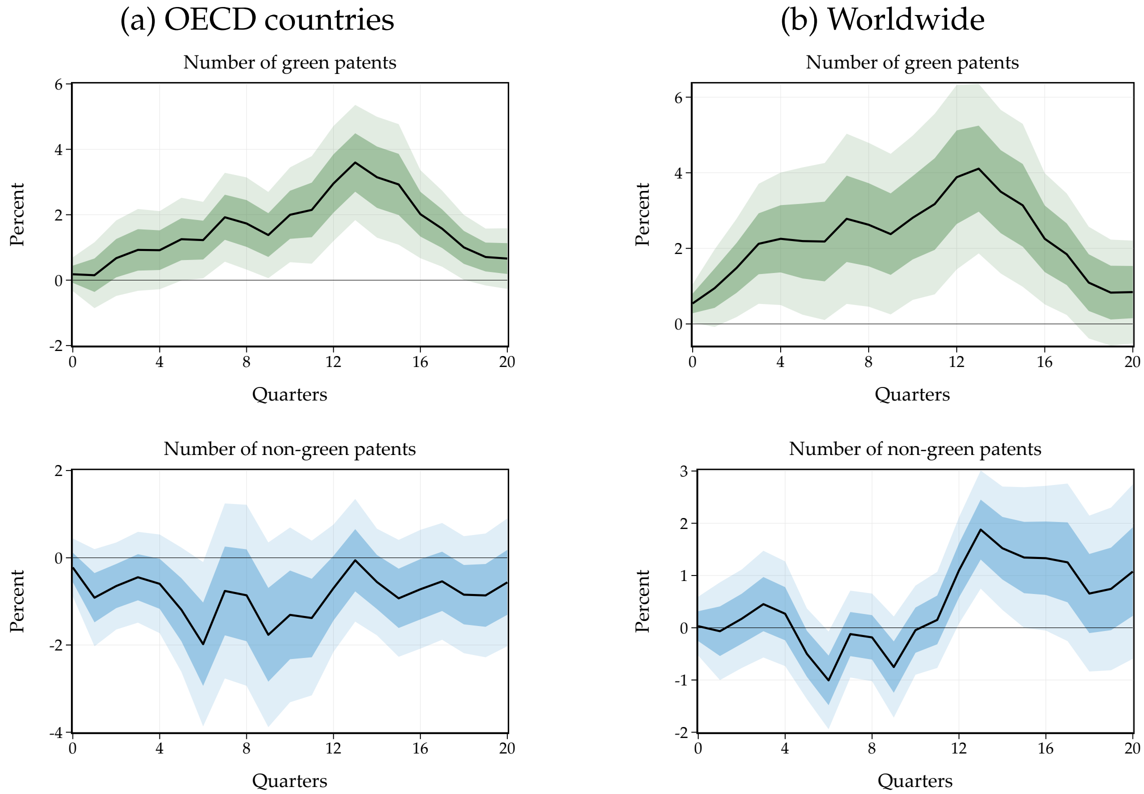

Notes: Impulse responses of green and non-green patents in different geographies to a U.S. monetary policy shock, estimated based on the local projections model (2) using high-frequency monetary surprises as an instrument. Left panels: OECD countries. Right panels: patents worldwide. The shock is normalized to increase the federal funds rate by 25 basis points on impact. Solid line: point estimate. Dark and light shaded areas: 68 and 95% confidence bands based on lag-augmented standard errors.

B.6. Additional Results Using Raw Patent Counts

In our baseline analysis, we apply a one-quarter moving average to the aggregate patent counts to mitigate noise in the patent data. Here, we estimate the local projection models (1) and (2) based on the raw patent counts. As Figures B.6 and B.7 show that the impulse responses to the business cycle and monetary policy shocks are robust to using raw patent counts.

Figure B.6: Patenting responses to business cycle shocks using raw patent counts

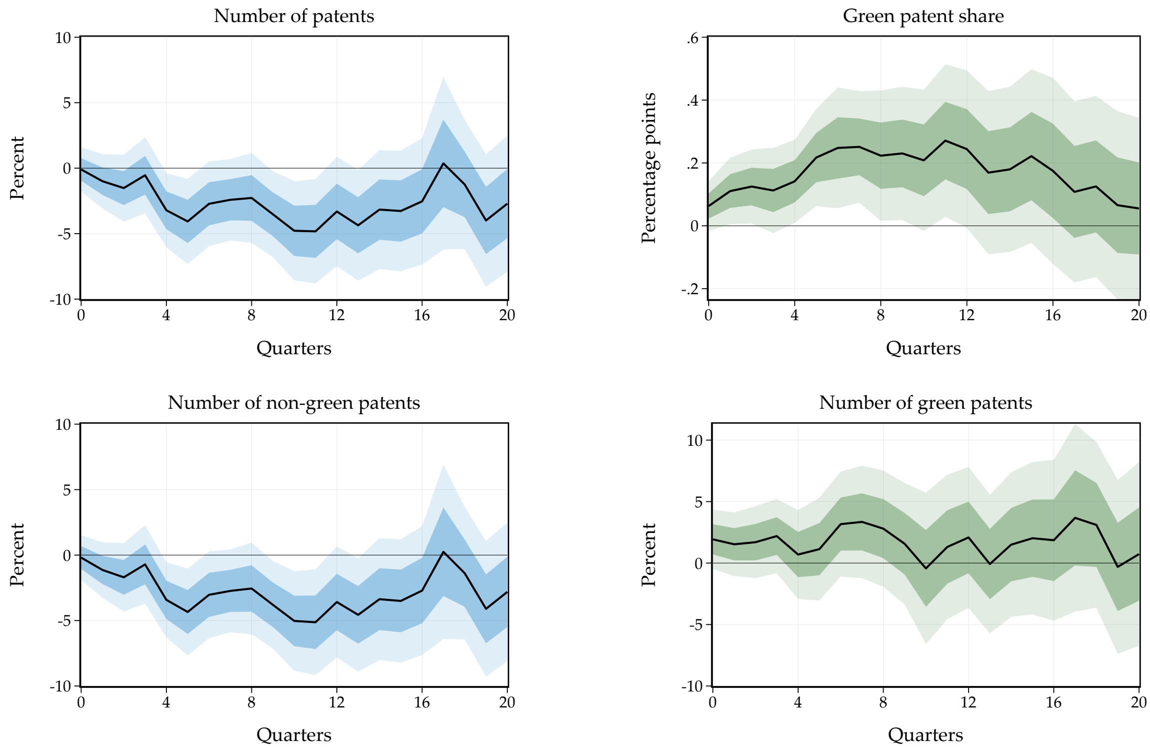

Notes: Impulse responses of green and non-green patents using raw patent counts, estimated based on the reduced-form local projections (1). The shock is normalized to decrease GDP growth by 1% on impact. Solid line: point estimate. Dark and light shaded areas: 68 and 95% confidence bands based on lag-augmented standard errors.

Figure B.7: Patenting responses to monetary policy shocks using raw patent counts

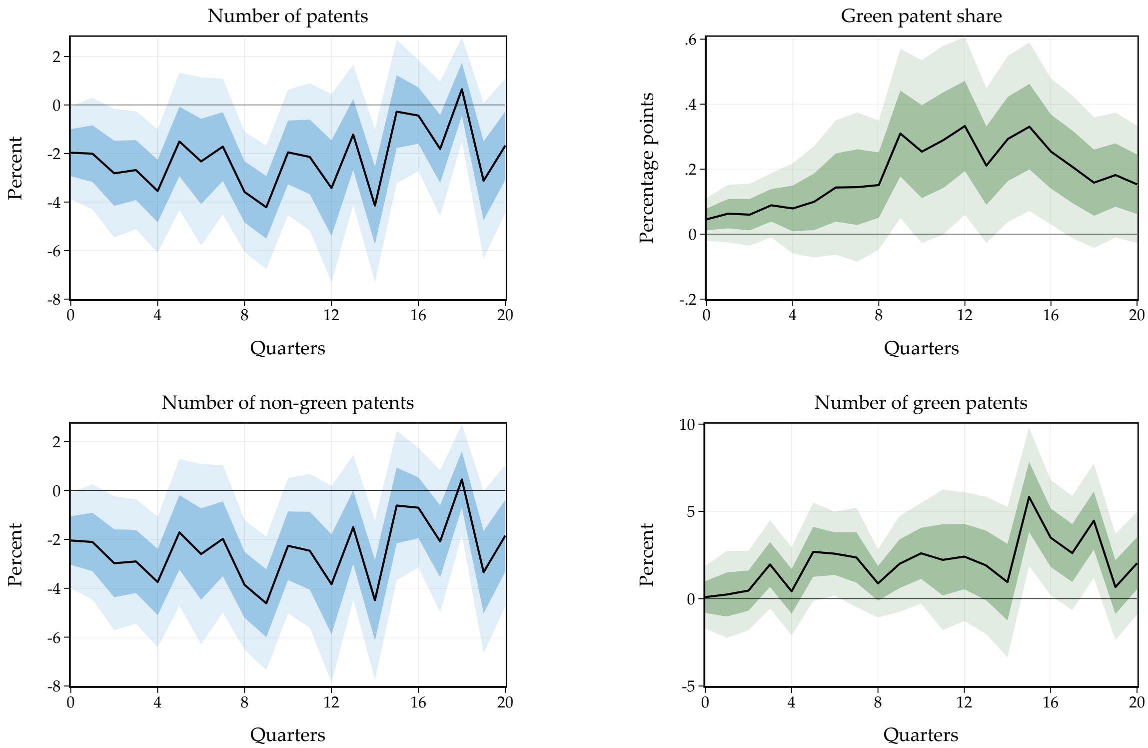

Notes: Impulse responses of green and non-green patents using raw patent counts, estimated based on the local projections model (2) using high-frequency monetary surprises as an instrument. The shock is normalized to increase the federal funds rate by 25 basis points on impact. Solid line: point estimate. Dark and light shaded areas: 68 and 95% confidence bands based on lag-augmented standard errors.

B.7. Alternative Shock Measures

Our baseline analysis relies on a local projections approach using the monetary surprises by Bauer and Swanson (2023) as an instrument. The left panel in Figure B.8 shows similar dynamic responses of the U.S. green patent share, estimated using the monetary surprises by Jarociński and Karadi (2020) as an instrument.

As alternative shock measures, the right panel in Figure B.8 considers the impacts of oil supply shocks on the green patent share. Specifically, we use the oil supply shock identified in Känzig (2021) as an instrument for the real oil price in an otherwise identical empirical setup. The responses, normalized to increase the real oil price by 10 USD, display a similarly persistent increase as in our main analysis.

Figure B.8: Patenting responses to alternative macroeconomic shocks

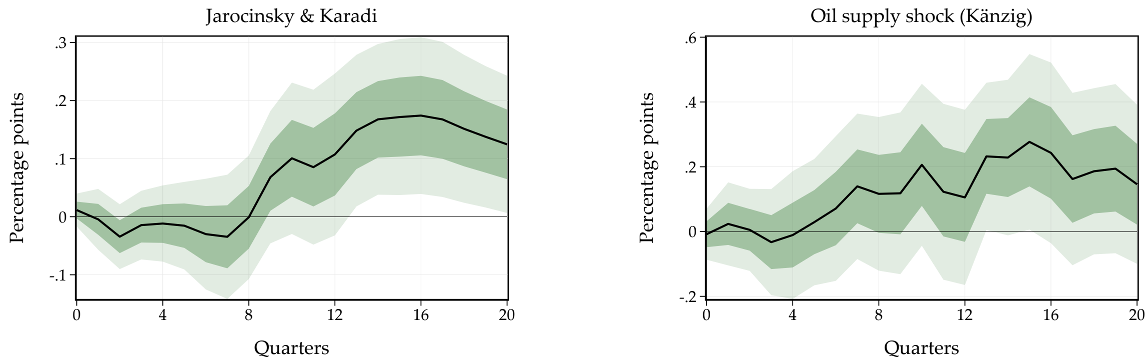

Notes: Green patenting responses to alternative monetary policy and oil supply shocks. Left panel: monetary policy shock, identified using the Jarociński and Karadi (2020) monetary surprises, normalized to increase the policy rate by 25 basis points. Right panel: Oil supply news shock, identifed using the OPEC surprise series by Känzig (2021), normalized to increase the (real) WTI crude price by 10 USD. Solid line: point estimate. Dark and light shaded areas: 68 and 95% confidence bands based on lag-augmented standard errors.

B.8. Evidence on USPTO Patent Renewals

We argue that green patents have a more backloaded profit structure along the green transition. To corroborate this assumption, we exploit information on the maintenance fee payments maintained by the USPTO. Patents need to be renewed after 3.5, 7.5 and 11.5 years in order to remain active. Therefore, patent renewal decisions reflect the value that firms assign to a given innovation over time.

We begin by estimating a logistic regression at the patent-level:

$$\mathrm{P}(\text{renewal})_{i,t} = \alpha + \delta_t + \theta \text{green}_{i,t} + \varepsilon_{i,t}, \tag{1}$$

where $\mathrm{P}(\text{renewal})_{i,t}$ corresponds to the probability that patent i filed in quarter t is renewed. δ_t denotes a set of time fixed effects. To control for patent quality, we include dummy variables for biadic patents and patents with at least one citation.

In addition, we estimate OLS regressions using patent duration (expressed in years) as the dependent variable. Lastly, we construct patent maintenance scores, which take on a value between 0 and 3 depending on the number of renewals (Porter et al., 2023). We focus on patents filed before 2010 to allow for up to three recorded renewal decisions.

Table B.2: Evidence on patent renewal decisions

	Logit	OLS	
Dependent variable:	$\mathrm{P}(\text{renewal})_{i,t}$	$\text{Duration}_{i,t}$	$\text{Maintenance score}_{i,t}$
	(1)	(2)	(3)
$\text{green}_{i,t}$	0.36^{***}	0.36^{***}	0.09^{***}
	(0.01)	(0.01)	(0.00)
Observations	3,652,350	3,652,350	3,652,350
Pseudo R^2	0.07	0.06	0.06
Quality controls	Yes	Yes	Yes
Time fixed effects	Yes	Yes	Yes

Notes: The table shows coefficients from a regression of patent renewal metrics on a dummy variable, $\text{green}_{i,t}$ denoting green patents. Column (1) is estimated using a logistic regression, (2)-(3) are based on OLS. Quality controls include dummy variables for biadic patents and patents with at least one citation. All regressions include a constant, with the coefficient not reported for brevity. Robust standard errors in parentheses, significance levels denoted by *** $p < 0.01$, ** $p < 0.05$, * $p < 0.10$.

Table B.2 presents the results. We find that green patents are more likely to be renewed and remain active for longer relative to non-green patents, controlling for patent quality.

These results suggest that green patents carry a higher value at later stages of their life cycle compared to non-green patents.

B.9. Evidence on Green Inventors

One key insight from the model is that during business cycle downturns, a decline in non-green patenting depresses wages of skilled workers, making it cheaper for firms to engage in green innovation. We have seen some evidence that the share and number of non-green inventors increases at the firm-level.

One drawback of this approach is that it does not distinguish between existing and new green inventors. To address this issue, we separately analyze the number of new green inventors who are linked to a green patent for the first time in a given quarter. Lastly, we construct the share of new green inventors relative to the total number of inventors who have not been linked to a green patent before. Consistent with the channel emphasized in the model, Figure B.9 suggests an increase in both measures in response to a monetary shock.

Figure B.9: Firm-level responses of new green inventors

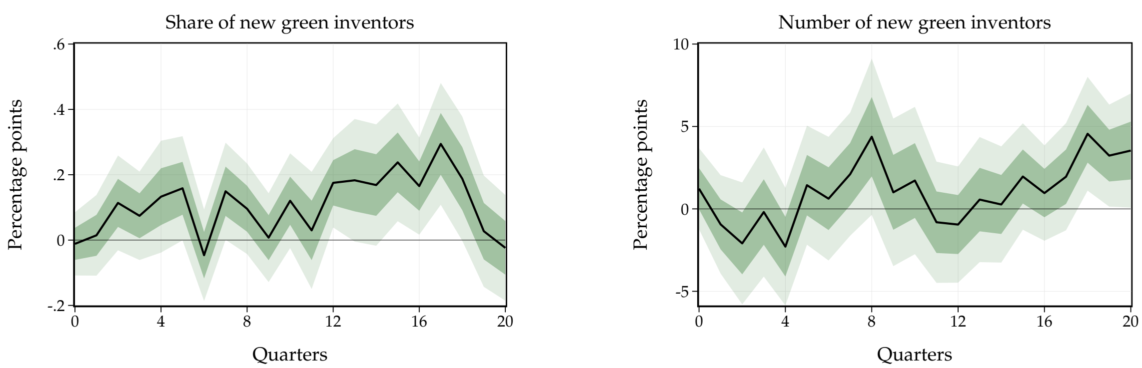

Notes: Responses of new green inventors to a monetary policy shock, estimated based on the panel local projections model (3) using high-frequency monetary surprises as an instrument. The measures are restricted to inventors who have not been linked to a green patent before. The shock is normalized to increase the federal funds rate by 25 basis points on impact. Solid line: point estimate. Dark and light shaded areas: 68 and 95% confidence bands based on lag-augmented standard errors.

B.10. Alternative Green Patent Classifications

Our baseline classification of green patents follows Acemoglu et al. (2023) to include Y02, excluding Y02E20, Y02E40 and Y02E60. Figure B.10 verifies that the responses in the U.S. are robust to alternative classifications. First, we include all Y02E subclasses of the CPC, which leads to comparable responses. Second, following Calel and Dechezleprêtre (2016), we check that including smart grid technologies (CPC class Y04S) does not meaningfully impact our estimates.

Figure B.10: Patenting responses using alternative green patent classifications

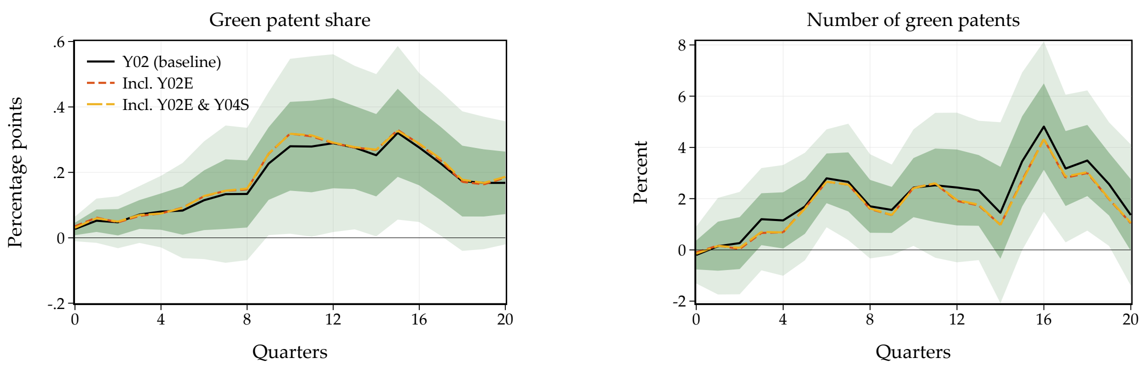

Notes: Impulse responses of the share and number of green patents to a monetary policy shock for alternative definitions of green patents. Responses are estimated based on the local projections model (2) using high-frequency monetary surprises as an instrument. The orange dotted lines include Y02E and yellow dashed lines include Y02E and Y04S as green. The shock is normalized to increase the federal funds rate by 25 basis points on impact. Lines: point estimate. Shaded areas: 68 and 95% confidence bands for the baseline estimates.

B.11. Controlling for Fiscal Policy and Investor Demand

In our local projections, we flexibly capture prevailing macro-financial conditions with a set of control variables. In this appendix, we expand on the robustness checks in Section 2 to rule out two additional, potentially confounding channels related to changes in demand for green technologies and fiscal policy.

First, changing opinions on climate change and environmental policies could be a driver of green innovation. We include two indices, Engle et al. (2020) and Gavriilidis et al. (2025), that capture mentions of climate change (policies) in major US newspapers. We also control for the oil price, which could influence firms' decisions to invest in green technologies. The top two panels of Figure B.11 show that the estimated impulse responses are comparable.

Second, we rule out that the U.S. fiscal policy stance, which increasingly tries to promote green investments (such as Obama's American Recovery and Reinvestment Act of 2009, or Biden's Inflation Reduction Act of 2022) impacts our estimates. To that end, we separately include government spending, a dummy for democratic presidents (which are more likely to prioritize green spending), as well as their interaction in the local projections. The responses are close to the baseline estimates (bottom panel of Figure B.11).

Figure B.11: Robustness with respect to patent quality

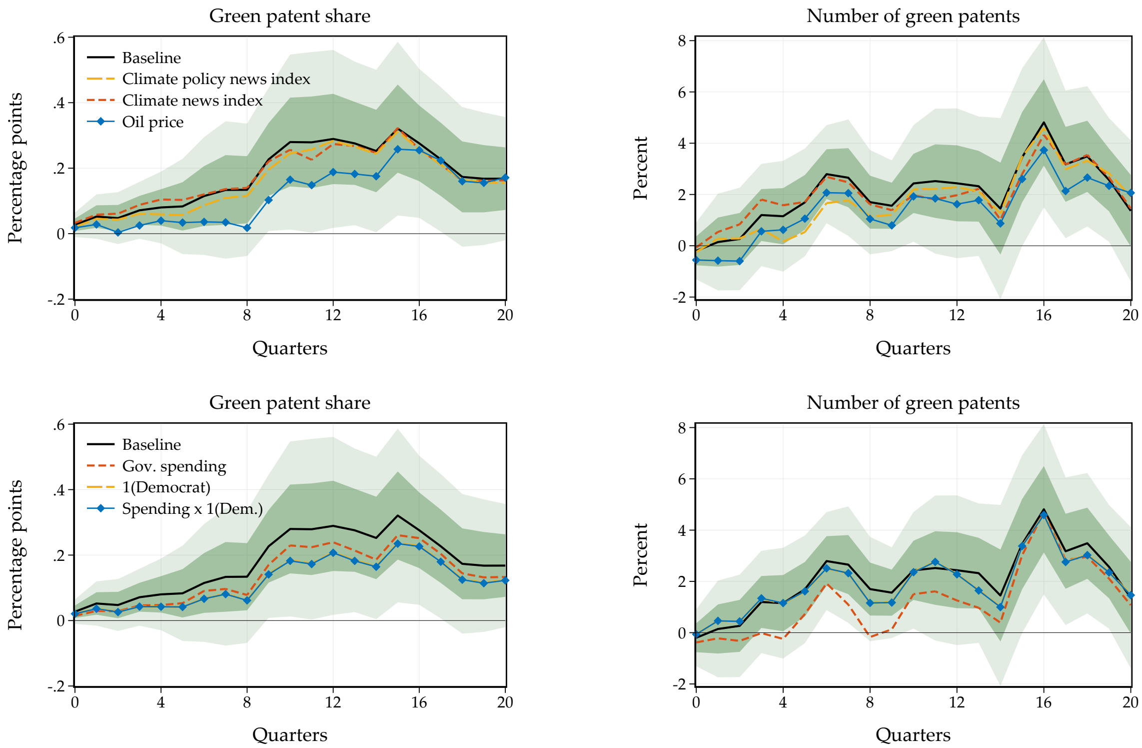

Notes: Green patenting responses to a monetary policy shock with alternative set of controls. Responses are estimated based on the local projections model (2) using high-frequency monetary surprises as an instrument. Top panels: controlling for the climate news index by Engle et al., 2020 (yellow dashed line), the climate policy news index (orange dotted line) and the oil price (blue line). Bottom panels: controlling for government spending (orange dotted line), a dummy for democratic presidents (yellow dashed line) and their interaction (blue line). The shock is normalized to increase the federal funds rate by 25 basis points on impact. Lines: point estimates. Shaded areas: 68 and 95% confidence bands for baseline model.

B.12. Distinguishing between Patent Quality

In the baseline estimation we include all patent families, irrespective of their quality. To control for patent quality, we closely follow Hémous et al. (2025) to focus on biadic patents (filed in at least two of the three major patent offices) with at least on citation. Figure B.12 shows that the estimated responses for the U.S. sample are very similar.

Figure B.12: Robustness with respect to patent quality

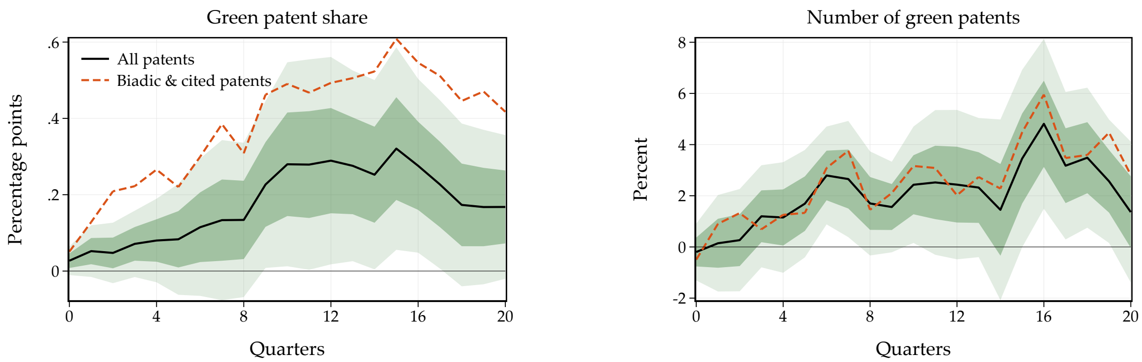

Notes: Green patenting responses to a monetary policy shock when controlling for patent quality. Responses are estimated based on the local projections model (2) using high-frequency monetary surprises as an instrument. We control for quality by only using biadic patent families with at least one citation. The shock is normalized to increase the federal funds rate by 25 basis points on impact. Lines: point estimates. Shaded areas: 68 and 95% confidence bands for baseline model.

B.13. Responses using USPTO Data

We rely on PATSTAT data for our main analysis, but verify that the estimates are comparable when using USPTO data. Patent counts can differ across the two sources, because of different procedures for how patent applications are recorded and the treatment of PCT patent applications. We keep focusing on patent families, but include all families filed with the USPTO (even when the first filing in the family was with a foreign office). Figure B.13 illustrates that the estimated responses in the U.S. are comparable for PATSTAT and USPTO data.

Figure B.13: Patent responses based on USPTO data

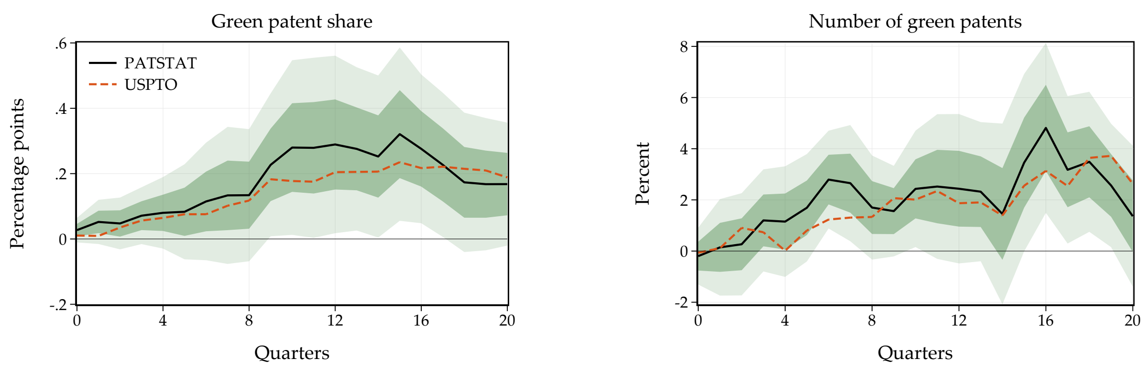

Notes: Green patenting responses to a monetary policy shock based on USPTO data. Responses are estimated based on the local projections model (2) using high-frequency monetary surprises as an instrument. The shock is normalized to increase the federal funds rate by 25 basis points on impact. Lines: point estimates. Shaded areas: 68 and 95% confidence bands for baseline model.

B.14. Robustness to Firm-level Patent Counts

In our main analysis, a patent can be matched to multiple U.S. companies as the result of co-inventions. Figure B.14 shows that our results are not sensitive to this approach, as the estimated impulse responses are comparable when (i) weighting co-invented patents, or (ii) excluding co-invented patents.

Figure B.14: Robustness to co-invented patents

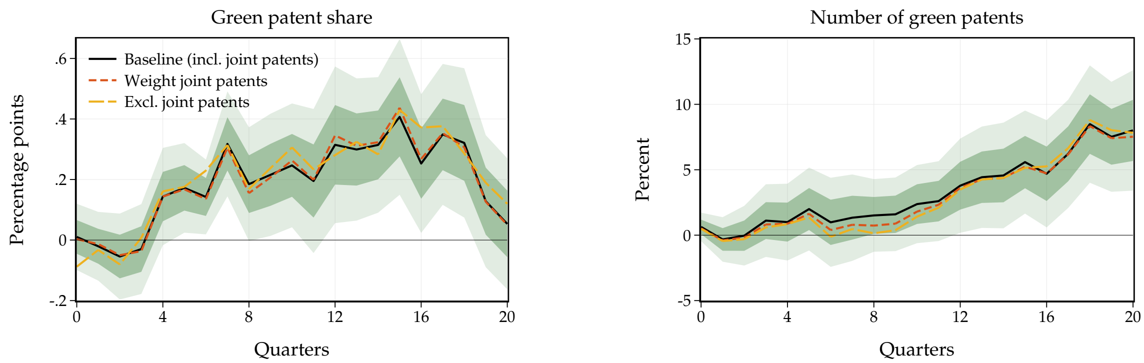

Notes: Green patenting responses to a monetary policy shock under different approaches to deal with co-inventions. Responses are estimated based on the panel local projections model (3) using high-frequency monetary surprises as an instrument. The orange dotted line weighs co-invented patents while the yellow dashed line excludes co-invented patents. The shock is normalized to increase the federal funds rate by 25 basis points on impact. Lines: point estimates. Shaded areas: 68 and 95% confidence bands for baseline model.

C. Model Appendix

This appendix includes derivations, proofs as well as details on the extensions of our dynamic stochastic general equilibrium model with green and non-green innovation.

C.1. General Equilibrium with Monetary Shocks

In this section, we show how we introduce nominal rigidities and monetary policy shocks into our model.

Consider that instead of demanding final goods, households purchase a basket of differentiated retail goods indexed by k:

$$\tilde{Y}_t = \left(\int_0^1 \tilde{y}_{kt}^{\frac{\sigma-1}{\sigma}} \, dk \right)^{\frac{\sigma}{\sigma-1}}, \tag{2}$$

where $\sigma > 1$ is the elasticity of substitution between varieties.

Given the aggregate demand $\tilde{Y}_t$, the demand function for each variety k follows $\tilde{y}_{kt} = \left(\frac{\tilde{p}_{kt}}{\tilde{P}_t}\right)^{-\sigma} \tilde{Y}_t$, where $\tilde{p}_{kt}$ is the price of variety k and $\tilde{P}_t$ is the corresponding price index $\tilde{P}_t = \left(\int_0^1 \tilde{p}_{kt}^{1-\sigma} dk\right)^{\frac{1}{1-\sigma}}$. The household's budget constraint now takes the form:

$$\tilde{P}_t C_t + Q_t B_{t+1} = B_t + W_t L_t + W_t^s L_t^s + D_t. \tag{3}$$

Retailer. A fixed mass of retailers $k \in [0, 1]$ produces differentiated retail goods from the final good producer. The production technology is one-to-one, $\tilde{y}_{kt} = y_{kt}$, where y_{kt} is the amount of final good that the retailer k purchased. Retailers set prices with Rotemberg price adjustment costs:

$$\frac{\varphi}{2} \left(\frac{\tilde{p}_t}{\tilde{p}_{t-1}} - 1 \right)^2 \tilde{Y}_t. \tag{4}$$

Each retailer maximizes its expected discounted profit:

$$\mathbb{E}_t \sum_{s=0}^{\infty} \Lambda_{t,t+s} \left[\left(\tilde{p}_{k,t+s} - P_{t+s} \right) \tilde{y}_{k,t+s} - \frac{\varphi}{2} \left(\frac{\tilde{p}_{k,t+s}}{\tilde{p}_{k,t+s-1}} - 1 \right)^2 \tilde{Y}_{t+s} \right], \tag{5}$$

subject to its demand. The optimal price-setting condition:

$$(1-\sigma)+\sigma\frac{P_t}{\tilde{P}_t}-\varphi\Pi_t\tilde{P}_t^{-1}+\mathbb{E}_t\Lambda_{t,t+1}\varphi\Pi_{t+1}(1+\Pi_{t+1})\tilde{P}_{t+1}^{-1}=0 \tag{6}$$

Monetary policy. The central bank follows a Taylor Rule:

$$R_t=\beta^{-1}\left(\frac{A_{t+1}}{A_t}\right)^{\phi_A}\Pi_t^{\phi_\pi}\varrho_t. \tag{7}$$

where ϱ_t is a monetary shock:

$$\log\varrho_t=\rho^\varrho\log\varrho_t+\sigma^\varrho e_t^\varrho \tag{8}$$

C.2. Balanced Growth Path

In this appendix, we define the notion of balance growth in our model and provide conditions for its existence.

Definition C.1 (Balanced Growth Path)**.** *A **balanced growth path (BGP)** is a sequence of allocations and prices*

- *household allocations:* $\{C_t, L_t, L_t^s, B_{t+1}\}_{t=0}^\infty$,
- *firm allocations:* $\{Y_t, L_t, M_t, E_t, m_{ht}, g_{jt}, f_t\}_{t=0}^\infty$,
- *innovator allocations:* $\{L_{it,M}^S, L_{it,G}^S\}_{t=0}^\infty$,
- *price system:* $\{P_t, \tilde{P}_t, P_t^M, P_t^G, P_t^f, P_t^E, W_t, W_t^s, R_t\}_{t=0}^\infty$,
- *aggregate state variables:* $\{A_t^M, A_t^G\}_{t=0}^\infty$,

such that:

1. *The equilibrium conditions of the model are satisfied at each* t*;*
2. *As* $t\to\infty$*, the aggregate variables* Y_t, C_t, M_t, E_t *grow at a constant rate;*
3. *As* $t\to\infty$*, the input shares*

$$\frac{1}{Y_t}\int_0^{A_t^M} m_{ht}\,dh \quad \textit{and} \quad \frac{1}{Y_t}\int_0^{A_t^G} g_{jt}\,dj$$

converge to constants.

To understand the properties of BGP, consider the limit where the green transition is completed, and the production technology simplifies to:

$$Y_t = L_t^{\alpha_L} M_t^{\alpha_M} G_t^{1-\alpha_L-\alpha_M}. \tag{9}$$

The first-order conditions are given by:

$$\alpha_L \frac{P_t Y_t}{L_t} = W_t, \tag{10}$$
$$\alpha_M \frac{P_t Y_t}{M_t} = P_t^M, \tag{11}$$
$$(1-\alpha_L-\alpha_M)\frac{P_t Y_t}{G_t} = P_t^G. \tag{12}$$

Given the price equations:

$$P_t^M = \left(A_t^M\right)^{1-\mu_M} \mu_M P_t, \tag{13}$$
$$P_t^G = \left(A_t^G\right)^{1-\mu_G} \mu_G P_t, \tag{14}$$

substituting into equations (11) and (12), we obtain:

$$M_t = \frac{\alpha_M}{\mu_M}\left(A_t^M\right)^{\mu_M-1} Y_t, \tag{15}$$
$$G_t = \frac{1-\alpha_L-\alpha_M}{\mu_G}\left(A_t^G\right)^{\mu_G-1} Y_t. \tag{16}$$

Substituting (15) and (16) into (9):

$$Y_t = L_t^{\alpha_L}\left(\frac{\alpha_M}{\mu_M}\left(A_t^M\right)^{\mu_M-1} Y_t\right)^{\alpha_M}\left(\frac{1-\alpha_L-\alpha_M}{\mu_G}\left(A_t^G\right)^{\mu_G-1} Y_t\right)^{1-\alpha_L-\alpha_M}. \tag{17}$$

Rearranging, we obtain:

$$Y_t = \bar{Z} L_t \left(A_t^M\right)^{\frac{\alpha_M(\mu_M-1)}{\alpha_L}}\left(A_t^G\right)^{\frac{(1-\alpha_L-\alpha_M)(\mu_G-1)}{\alpha_L}}, \tag{18}$$

where $\bar{Z} = \left(\frac{\alpha_M}{\mu_M}\right)^{\frac{\alpha_M}{\alpha_L}}\left(\frac{1-\alpha_L-\alpha_M}{\mu_G}\right)^{\frac{1-\alpha_L-\alpha_M}{\alpha_L}}$.

On the balanced growth path, the ratios $\frac{\int_0^{A_t^M} m_{ht}\,dh}{Y_t}$ and $\frac{\int_0^{A_t^G} g_{jt}\,dj}{Y_t}$ must remain constant over time. Moreover, A_t^G, A_t^G have to be growing such that $f_t \to 0$ in the long run.

Assumption C.1. *To ensure the existence of a Balanced Growth Path, the following conditions hold:*

1. *In the long run, A_t^M and A_t^G have to be growing over time.*
2. *In the long run, the technology levels satisfy $A_t^M = \iota A_t^G$.*
3. *The exponents satisfy the constraint:*

$$\frac{\alpha_M}{\alpha_L}(\mu_M - 1) + \frac{1 - \alpha_L - \alpha_M}{\alpha_L}(\mu_G - 1) = 1. \tag{19}$$

C.3. Equilibrium Conditions and Model Solution

We present here the equilibrium conditions under nominal rigidity and monetary policy shocks, in line with the empirical analysis which focuses on the impulse responses to monetary policy shocks. The equilibrium conditions for the RBC version of the model are analogous, but exclude the Taylor rule and the New Keynesian Phillips Curve.

C.3.1. Equilibrium Conditions

Households. The consumption Euler equation:

$$1 = \beta \mathbb{E}_t \left(\frac{\varrho_{t+1}^D C_t}{\varrho_t^D C_{t+1}} \Pi_{t+1}^{-1} R_t \right). \tag{20}$$

Unskilled Labor Supply:

$$\varrho_t^D W_t = \bar{\omega} C_t \tilde{P}_t (L_t^s)^{\eta}. \tag{21}$$

Skilled Labor Supply:

$$\varrho_t^D W_t^s = \bar{\omega}^s C_t \tilde{P}_t (L_t^s)^{\psi}. \tag{22}$$

Final good producer. The optimization of the final good producer yields the following FOCs:

$$\alpha_L \frac{P_t Y_t}{L_t} = W_t \tag{23}$$

$$\alpha_M \frac{P_t Y_t}{M_t} = P_t^M \tag{24}$$

$$(1-\alpha_L-\alpha_M)\frac{P_t Y_t}{E_t} E_t^{\frac{1}{\rho}} f_t^{-\frac{1}{\rho}} = P_t^f \tag{25}$$

$$(1-\alpha_L-\alpha_M)\frac{P_t Y_t}{E_t} E_t^{\frac{1}{\rho}} G_t^{-\frac{1}{\rho}} = P_t^G \tag{26}$$

The final good producer's demand of intermediate good and clean energy input:

$$m_{ht} = \left(\frac{p_{ht}^m}{P_t^M}\right)^{\frac{\mu_M}{1-\mu_M}} M_t, \tag{27}$$

$$g_{jt} = \left(\frac{p_{jt}^g}{P_t^G}\right)^{\frac{\mu_G}{1-\mu_G}} G_t. \tag{28}$$

Because the market of final good is perfectly competitive:

$$P_t = \left(\frac{W_t}{\alpha_L}\right)^{\alpha_L} \left(\frac{P_t^M}{\alpha_M}\right)^{\alpha_M} \left(\frac{P_t^E}{1-\alpha_L-\alpha_m}\right)^{1-\alpha_L-\alpha_m} Z_t^{-\alpha_L}. \tag{29}$$

where by Shephard's Lemma,

$$P_t^E = \left((P_t^f)^{1-\rho} + (P_t^G)^{1-\rho}\right)^{\frac{1}{1-\rho}}. \tag{30}$$

Intermediate good producer.

$$p_{ht}^m = \mu_M P_t, \tag{31}$$

$$p_{jt}^g = \mu_G P_t. \tag{32}$$

Fossil fuel. The price-setting condition of fossil fuel producer:

$$P_t^f = \xi_f^{-1} P_t. \tag{33}$$

Innovation.

$$A_t^M \zeta_M \left(L_{it,M}^S \right)^{\nu-1} \mathcal{V}_t^m = W_t^s. \tag{34}$$

$$A_t^G \zeta_G \left(L_{it,G}^S \right)^{\nu-1} \mathcal{V}_t^g = W_t^s. \tag{35}$$

Retailer.

$$(1-\sigma) + \sigma \frac{P_t}{\tilde{P}_t} - \varphi \Pi_t \tilde{P}_t^{-1} + \mathbb{E}_t \Lambda_{t,t+1} \varphi \Pi_{t+1} (1 + \Pi_{t+1}) \tilde{P}_{t+1}^{-1} = 0 \tag{36}$$

Monetary policy. The central bank follows a Taylor Rule:

$$R_t = \beta^{-1} \left(\frac{A_{t+1}}{A_t} \right)^{\phi_A} \Pi_t^{\phi_\pi} \varrho_t. \tag{37}$$

TFP growth rate. Given equilibrium condition (24) and the auxiliary optimality condition for optimization E_t:

$$(1 - \alpha_L - \alpha_M) \frac{P_t Y_t}{E_t} = P_t^E, \tag{38}$$

we can substituting them into the production technology of the final good:

$$Y_t = \left(\frac{\alpha_M}{\mu_M} \right)^{\frac{\alpha_M}{\alpha_L}} (1 - \alpha_L - \alpha_M)^{\frac{1-\alpha_L-\alpha_M}{\alpha_L}} L_t (A_t^M)^{\frac{\alpha_M}{\alpha_L}(\mu_M - 1)} (P_t / P_t^E)^{\frac{1-\alpha_L-\alpha_M}{\alpha_L}} \tag{39}$$

By the definition of TFP,

$$A_t = (A_t^M)^{\frac{\alpha_M}{\alpha_L}(\mu_M - 1)} (P_t / P_t^E)^{\frac{1-\alpha_L-\alpha_M}{\alpha_L}} \tag{40}$$

C.3.2. Definition of Equilibrium

Given an initial value of (A_0^M, A_0^G) and a sequence of exogenous shocks $\{Z_t, \varrho_t\}_{t=0}^{\infty}$, a Recursive Competitive Equilibrium consists of sequences:

Household allocations:	$\{C_t, L_t, L_t^s, B_{t+1}\}_{t=0}^{\infty}$,
Firm decisions:	$\{Y_t, L_t, M_t, E_t, m_{ht}, g_{jt}, f_t\}_{t=0}^{\infty}$,
Innovation choices:	$\{L_{it,M}^S, L_{it,G}^S\}_{t=0}^{\infty}$,
Price system:	$\{P_t, \tilde{P}_t, P_t^M, P_t^G, P_t^f, P_t^E, W_t, W_t^s, R_t\}_{t=0}^{\infty}$,
Aggregate state variables:	$\{A_t^M, A_t^G\}_{t=0}^{\infty}$,

such that:

1. Households optimize given prices, subject to their budget constraint and first-order conditions for consumption and labor supply;

2. Final good producers maximize profits subject to the production technology and demand for inputs, satisfying the optimality conditions for labor, materials, fossil fuels, and green energy;

3. Intermediate good producers and green energy producers set prices as monopolistic competitors, satisfying the demand functions;

4. Fossil fuel producers set prices competitively, satisfying their cost conditions;

5. Retailers set prices subject to nominal rigidities, satisfying their optimal price-setting condition;

6. Innovators choose R&D effort to maximize expected returns, satisfying their first-order conditions;

7. Monetary policy follows the Taylor rule specified above;

8. The laws of motion for the variety stocks A_t^M and A_t^G are consistent with innovation outcomes and obsolescence;

9. All markets clear: goods, labor (skilled and unskilled), bond, and intermediate inputs.

C.3.3. Solution Method

In solving the model, we adopt the MIT shock approach to study the causal effect of a specific shock on the economy's dynamic transition path. Unlike standard perturbation methods commonly employed in DSGE models, which rely on a fixed steady state around which the system is locally approximated, our framework features an endogenous accumulation of material and green energy varieties, A_t^M and A_t^G, whose dynamics are permanently influenced by shocks. The absence of a fixed steady state makes conventional local linearization techniques not directly applicable. Instead, the MIT shock approach provides a tractable way to characterize the economy's nonlinear adjustment following a shock, conditional on the endogenous evolution of the state variables.

Specifically, the numerical solution proceeds as follows:

1. Initialize iteration index $i = 0$. Given a steady state implied by the balanced growth path (BGP), set an initial guess $(\{A_t^M, A_t^G\}_{t=0}^T)^{(i)}$.

2. **Repeat until convergence:**

   (a) Using the path $(\{A_t^M, A_t^G\}_{t=0}^T)^{(i)}$, along with a specified shock sequence $(1, \rho, \rho^2, \dots)\varepsilon_t$, solve forward for the evolution of all endogenous variables.

   (b) Update the sequence of the number of green and non-green varieties, denoted by $\mathcal{A}_t^M$ and $\mathcal{A}_t^G$, respectively.

   (c) Compute the maximum deviation across time between the updated and previous sequences of varieties:

   $$\xi = \max_t \left(\left| \mathcal{A}_t^M - A_t^{M,(i)} \right| + \left| \mathcal{A}_t^G - A_t^{G,(i)} \right| \right).$$

   (d) **If** $\xi < 10^{-5}$, the algorithm has converged and the procedure terminates.

   (e) **Else**, update the path by setting $(\{A_t^M, A_t^G\}_{t=0}^T)^{(i+1)} = (\mathcal{A}_t^M, \mathcal{A}_t^G)$, increment $i \leftarrow i + 1$, and continue to the next iteration.

C.4. Proposition 3.2 in General Equilibrium

Proposition 3.2 established that, during a green transition, the value of a green variety is unambiguously less cyclical than the value of a non-green variety, holding the discount factor constant.

What is the effect of the stochastic discount factor? The following lemma formalizes how the impact of the discount rate channel depends on the cyclicality of the SDF:

Lemma C.1 (Discount Rate Channel)**.** *Denote the discount rate component in equation* (21)*:*

$$\Xi^k = \sum_{s=0}^{\infty} \phi^s \frac{\Lambda_{t,t+s,ss} \Pi_{t+s,ss}^k}{V_{t,ss}^k} \frac{d \log \Lambda_{t,t+s}}{d \log Y_t} \tag{41}$$

for $k = \{M, G\}$. During the green transition, a procyclical SDF $\left(\frac{\partial \log \Lambda_{t+s,t+s+1}}{\partial \log Y_t} > 0 \text{ for } s \in \mathbb{N}\right)$ implies that $\Xi^G > \Xi^M$, whereas a countercyclical SDF implies that $\Xi^G < \Xi^M$.

This result highlights that when the SDF is countercyclical, the discount rate channel reinforces the cash flow channel. In contrast, a procyclical SDF causes the discount rate channel to act in the opposite direction, thereby dampening the effect of the cash flow channel.

Despite the ambiguity of the discount rate channel, the result of Proposition 3.2 also holds in the general equilibrium model with a stochastic discount factor that is endogenously determined. Corollary C.1 shows that the cash flow channel unambiguously dominates the discount rate channel under the log utility assumption.

Corollary C.1 (Cyclicality during the Green Transition in GE). *During the green transition in the general equilibrium with an endogenous SDF, conditional on both preference and TFP shocks, the relative value of innovation, defined as $\frac{\mathcal{V}_t^G}{\mathcal{V}_t^M}$, exhibits countercyclicality. Formally, $\frac{d \log \mathcal{V}_t^G}{d \log Y_t} < \frac{d \log \mathcal{V}_t^M}{d \log Y_t}$, or equivalently $\frac{d \log\left(\mathcal{V}_t^G / \mathcal{V}_t^M\right)}{d \log Y_t} < 0$.*

Proof. See Appendix D. ■

C.5. Impulse Responses

In the main text, we report the impulse response of green and non-green innovation to a 25 basis point monetary policy shock. To provide a comprehensive overview of the model's quantitative results, Figure C.1 presents the impulse responses of a range of other aggregate variables. The contractionary monetary policy shock leads to a decline in aggregate demand, resulting in a short-term reduction in output and deflationary pressures. Simultaneously, it lowers the profitability of innovation, which reduces the availability of skilled labor for R&D, leading to a lower long-term total factor productivity.

Figure C.1: Model impulse responses

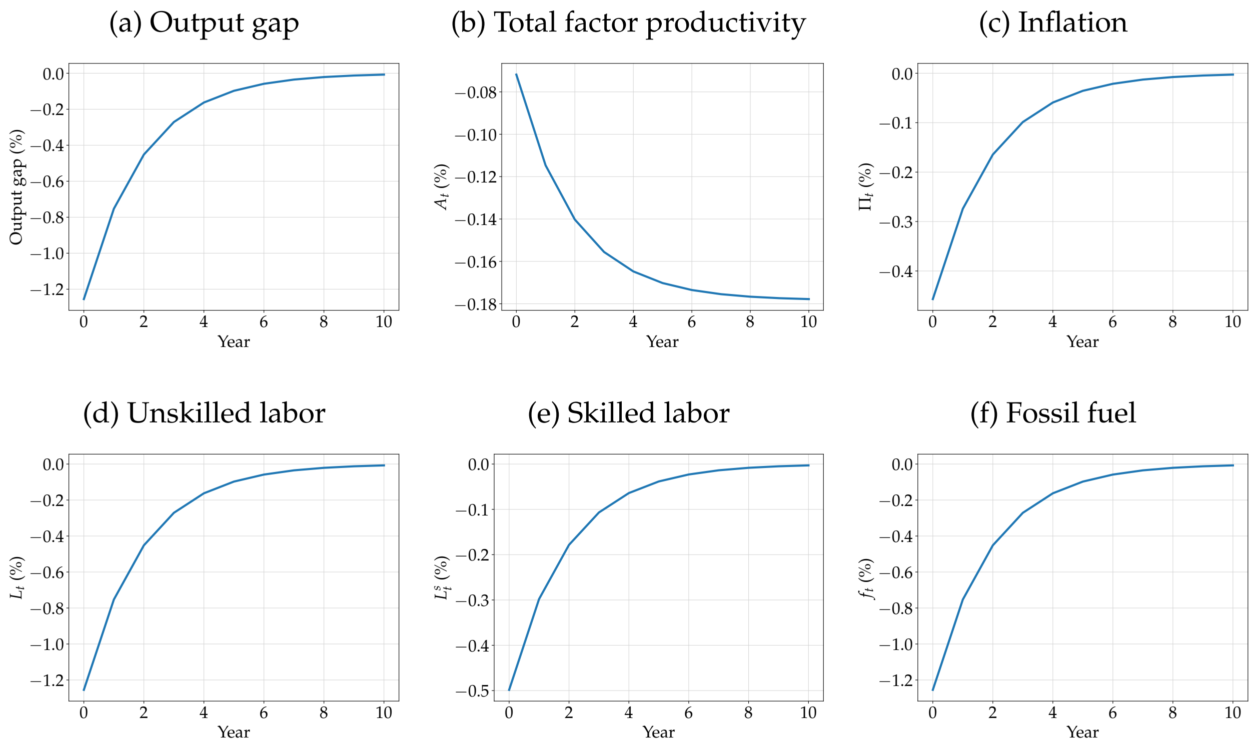

Notes: Figure C.1 illustrates the impulse response of aggregate variables to a 25-basis-point monetary policy shock.

C.6. The Role of Intertemporal Elasticity of Substitution

In Section 3, we demonstrate that under log utility, the cash flow channel dominates the discount rate channel in general equilibrium. In this section, we extend the analysis to a more general CRRA utility specification and examine how different values of the intertemporal elasticity of substitution (IES) influence the cyclicality of green innovation. Specifically, we modify the household's objective to:

$$\mathbb{E}_t \sum_{t=0}^{\infty} \beta^t \left(\varrho_t^D \frac{C_t^{1-\sigma_c}}{1-\sigma_c} - \frac{\bar{\omega}}{1+\eta} L_t^{1+\eta} - \frac{\bar{\omega}^s}{1+\psi} (L_t^s)^{1+\psi} \right), \tag{42}$$

subject to the period-by-period budget constraint:

$$P_t C_t + Q_t B_{t+1} = B_t + W_t L_t + W_t^s L_t^s + D_t, \tag{43}$$

where σ denotes the coefficient of relative risk aversion. All other elements of the model, including equilibrium conditions and calibration targets, remain as specified in Section 3.

Figure C.2: The role of intertemporal elasticity of substitution

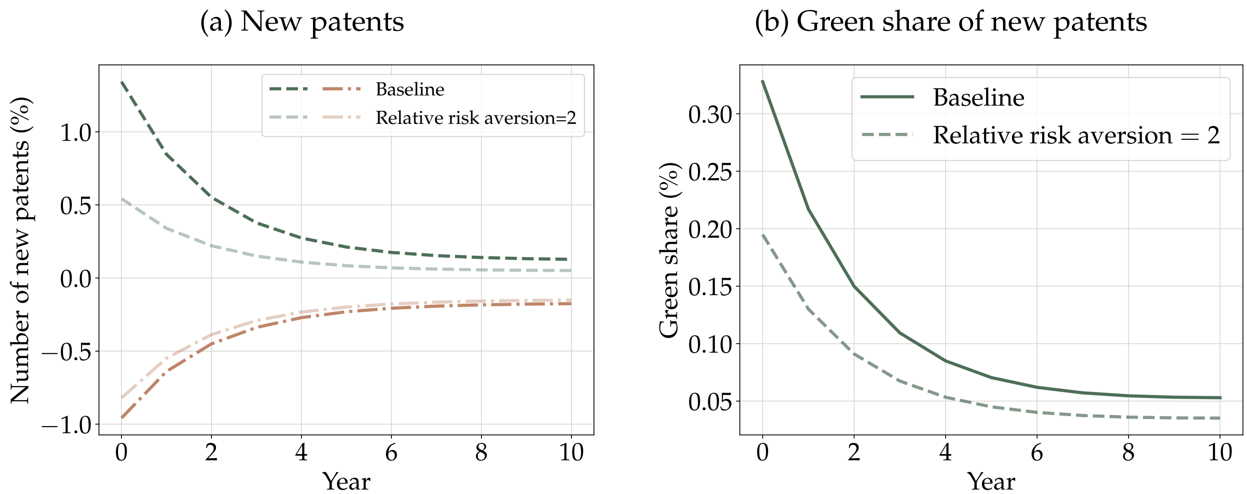

Notes: Impulse responses of the relative patent value and the green share of new patents to a 25 basis point monetary policy shock. We compare the baseline model ($\sigma_c = 1$) to the case where $\sigma_c = 2$, keeping other parameterizations the same.

Figure C.2 compares the results under $\sigma_c = 2$ to the baseline specification with log utility (i.e., $\sigma_c = 1$). Intuitively, a higher value of σ implies a lower intertemporal elasticity of substitution, which strengthens the discount rate channel and thereby dampens the countercyclicality of green innovation. Figure C.2 confirms this prediction.

Panel a shows that when $\sigma_c = 2$, the countercyclicality of new green patenting declines considerably, while the cyclicality of new non-green patents remains largely unchanged. As a result, the countercyclicality of the green share of new patents declines by about 40% under the same parameterization, see Panel b.

C.7. Alternative Shocks from the Demand Side: Preference Shocks

In Section 3, we model monetary shocks as demand-side disturbances to allow for better comparability with the empirical analysis. In this appendix, we look into the implications of the preference shock, altering the marginal utility of consumption.

Unlike monetary shocks, preference shocks influence not only the level of marginal utility but also intertemporal substitution by shifting the relative valuation of consumption today versus in the future. Specifically, the stochastic discount factor becomes:

$$\Lambda_{t,t+1} = \beta \frac{\varrho^D_{t+1} C_t}{\varrho^D_t C_{t+1}}, \tag{44}$$

where changes in ϱ^D_t affect the slope of intertemporal marginal utility.

As a result, the SDF becomes less procyclical—or even countercyclical—compared to the case of TFP or monetary shocks. This distinction implies that the discount rate channel may contribute to countercyclical movements in the relative valuation of intellectual property (IP) associated with green versus non-green technologies.

Figure C.3 compares the responses of green innovation to a preference shock and to a comparable monetary shock.[4]

Figure C.3: Preference shocks

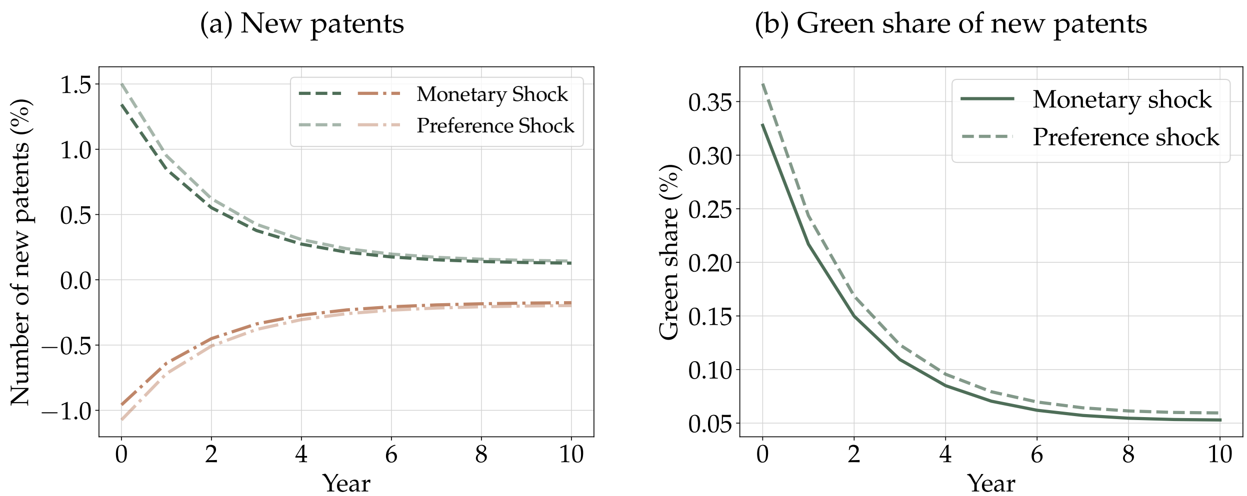

Notes: Impulse responses of the relative patent value and the green share of new patents to a preference shock and a monetary shock that reduces the output by 1% at $t = 0$.

Panel a shows that the countercyclicality of green patenting is modestly stronger under a preference shock, consistent with the intuition that a countercyclical stochastic discount factor—induced by such shocks—gives rise to a discount rate channel that reinforces, rather than offsets, the countercyclicality raised by the cash flow channel.

Panel b presents the response of the green share of new patents, which also increases slightly more under a preference shock. While these results suggest that the discount rate channel moves in the same direction as the cash flow channel in this case, the magni-

[4]Comparable in the sense that both shocks generate an impact decline in aggregate output of approximately one percent.

tude of the difference remains limited, reaffirming that the cash flow channel remains the dominant force behind the countercyclical pattern of green innovation.

C.8. Green Is in the Future Along the Transition Path

In Section 4, we present the impulse response of the green share of patents at $t = 0$, which is calibrated to the green share of energy in the 2010s. The results show that, due to the 'green is in the future' effect, the green share of new patents is countercyclical. How does the green is in the future effect evolve, and how does it affect the countercyclicality of the green share of new patents along the transition path?

Figure C.4a first depicts the green share of energy cost along the transition path. The green energy input gradually takes over the energy market. Panel b plots the cash flow from producing green varieties. Its trend tracks the trajectory of the green transition, initially growing slowly, then accelerating as the transition progresses, and eventually flattening out as green energy dominates the entire energy market. Panel c shows the cumulative impulse response of the green share of new patents to a 25 basis point monetary policy shock along the transition path. The countercyclicality of the green share of new patents exhibits a pattern of first increasing and then decreasing. The initial increase is due to the slower pace at which green energy is capturing the market in the early stages, which results in a weaker green is in the future effect in the short term. As the pace of green energy adoption accelerates, the green is in the future effect strengthens. Ultimately, as green profits stabilize and the transition matures, the green is in the future effect gradually vanishes in the long term.

Figure C.4: The role of the base period along the transition path

(a) Green share of energy (b) Profit of green production (c) Green share of new patents

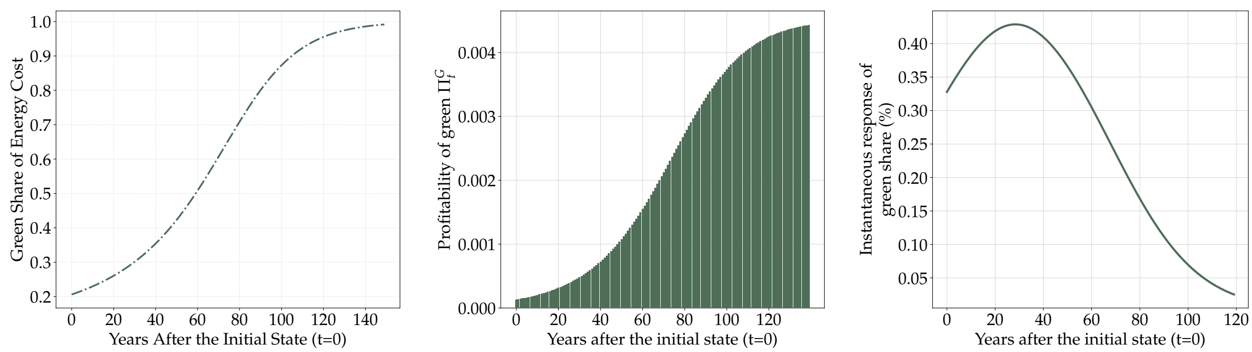

Notes: Sensitivity of the results depending on the initial period t along the transition path when the monetary policy shock hits. Panel a shows the green share of energy cost along the transition path, Panel b depicts the profit of green production $\Pi_t^G = (\mu_G - 1)\bar{g}_t$ and Panel c shows the instantaneous response of the green share of new patents.

C.9. Varying Speed of Green Transition

In Section 4.1, we calibrate the model to U.S. data, and the model suggests that it takes 60 years for the economy to reach a point where green energy occupies half of the energy market. What if the green transition is accelerated? How does an accelerated green transition influence the cyclicality of green innovation? Figure C.5a shows the green transition path based on our baseline calibration, as well as an accelerated path where we increase the scale parameters of innovation ζ_G and ζ_M by 20%. Figure C.5b illustrates the impulse response of the green share of new patents to a 25-basis-point monetary policy shock under both transition scenarios. This figure shows that if the green transition is accelerated, the green share of new patents exhibits stronger countercyclicality. This is because a faster transition means that, within a relatively short period, the proportion of current cash flow to value is smaller, thereby strengthening the green is in the future effect. Figure C.5c plots the cumulative response of the green share of new patents against the years required for the green share of energy cost to reach 50%. We find that the faster the green transition, the stronger the countercyclicality.

Figure C.5: Varying speed of green transition

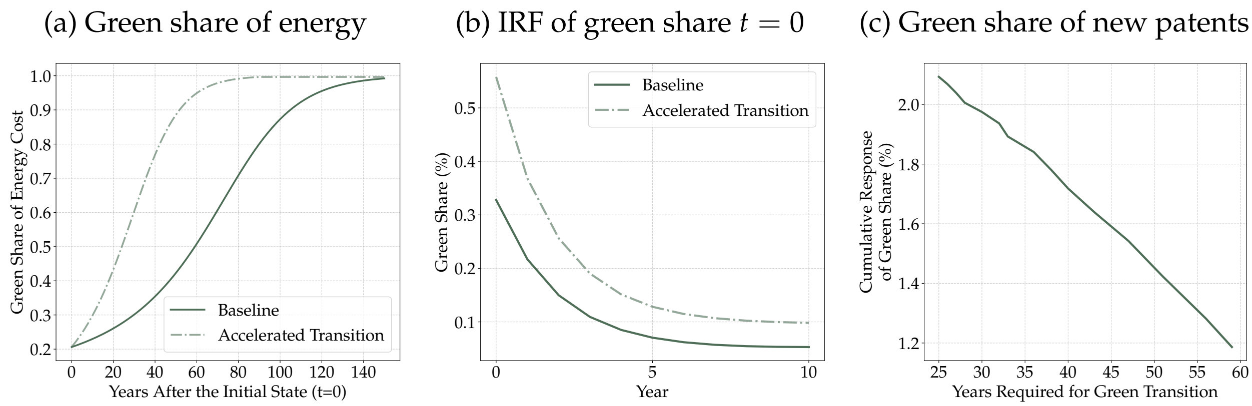

Notes: Sensitivity with respect to the speed of the green transition path. We consider an accelerated path where we increase the scale parameters of innovation ζ_G and ζ_M by 20%. Panel b illustrates the impulse response of the green share of new patents to a 25 basis point monetary policy shock at $t = 0$ under both transition scenarios. Panel c plots the cumulative response of the green share of new patents against the years required for the green share of energy cost to reach 50%.

C.10. Model with Brown Innovation

In Section 3, we abstract from innovation in fossil fuel (brown) inputs. This simplification allows us to focus on the endogenous dynamics of green innovation. However, empirical evidence suggests that a considerable fraction of energy-related innovation continues to target improvements in the efficiency and productivity of traditional fossil fuels. For instance, Aghion et al. (2016) documents that firms facing weak environmental regulation tend to innovate more in brown technologies rather than shifting towards green alternatives. To capture this pattern, we extend the model by allowing for endogenous innovation in brown energy. In this section, we relax the assumption of a fixed measure of brown inputs and introduce entry dynamics for fossil-based energy varieties.

Endogenous brown innovation. We modify the baseline specification by allowing the measure of brown energy varieties to evolve endogenously. The final energy input is produced by aggregating green and brown components through a CES aggregator:

$$E_t = \left(G_t^{\frac{\rho-1}{\rho}} + F_t^{\frac{\rho-1}{\rho}} \right)^{\frac{\rho}{\rho-1}}, \tag{45}$$

where the brown energy component F_t is given by

$$F_t = \left(\int_0^{A_t^F} f_{st}^{\frac{1}{\mu_F}} \, ds \right)^{\mu_F}. \tag{46}$$

From the optimization problem of final good producer, demand for each brown energy variety $s \in [0, A_t^F]$ is given by

$$f_{st} = \left(\frac{p_{ht}^f}{P_t^F} \right)^{\frac{\mu_F}{1-\mu_F}} F_t \tag{47}$$

where P_t^F denotes the associated price index:

$$P_t^F = \left(\int_0^{A_t^F} \left(p_{st}^f \right)^{\frac{1}{1-\mu_F}} \, ds \right)^{1-\mu_F}. \tag{48}$$

The evolution of the fossil reserve is modified to account for the endogenous measure of brown varieties:

$$R_{t+1} = R_t - \int_0^{A_t^F} f_{st} \, ds. \tag{49}$$

Each brown energy variety is produced by a monopolistically competitive firm that sets its price subject to demand from final good producers. The firm chooses p_{st}^f to maximize profits:

$$\Pi_{st}^F = \max_{p_{st}^f} \left\{ p_{st}^f f_{st} - \xi_f^{-1} f_{st} \right\}. \tag{50}$$

The value of a brown energy variety is given by

$$V_t^F = \sum_{s=0}^{\infty} \phi^s \, \mathbb{E}_t \left[\Lambda_{t,t+s} \Pi_{t+s}^F \right]. \tag{51}$$

Innovator's problem on brown energy varieties:

$$\max_{L_{it,M}^S} \quad \varphi_t^F L_{it,M}^S \left(V_t^F - c V_{t,ss}^F \right) - W_t^s L_{it,F}^S \tag{52}$$

where φ_t^F is the innovation productivity of brown innovation:

$$\varphi_t^F = \zeta_F A_t^F \left(L_{t,F}^S\right)^{-(1-\nu)} \tag{53}$$

Green is in the future. The model with brown innovation preserves the green is in the future property, provided that there is green transition underway:

Proposition C.1 (Green Is in the Future). *If the green share of energy G_t/E_t rises over time, then the relative profitability of green varieties increases over time, i.e., $\frac{\Pi_t^G}{\Pi_t^M}$ is increasing in t.*

Proof. See Appendix D. ∎

Proposition C.2 (Cyclicality during the Green Transition). *If the green share of energy G_t/E_t rises over time, $\frac{S_t^G}{S_t^G+S_t^M}$, is countercyclical.*

Proof. See Appendix D. ∎

Proposition C.3 (General Equilibrium Effects). *During the green transition, there exists a threshold $\bar{\epsilon} > 0$ such that green innovation is countercyclical, i.e.,*

$$\frac{\partial \log S_t^G}{\partial \log Y_t} < 0,$$

if and only if the wage elasticity of skilled labor with respect to output, $\frac{\partial \log W_t^s}{\partial \log Y_t}$, exceeds $\bar{\epsilon}$.

Proof. See Appendix D. ∎

C.11. Alternative Formulation of Extraction Cost

In the baseline model, we assume a linear extraction technology for fossil fuel. This assumption facilitates tractability but omits certain empirically relevant features of fossil fuel supply, particularly the presence of increasing marginal extraction costs. In practice, scaling up oil production often entails rising costs due to capacity constraints in drilling equipment, labor availability, and geological limitations such as declining well pressure.

To capture this more realistic aspect of oil production, we follow Bornstein, Krusell, and Rebelo (2023) and introduce a convex cost structure, where the extraction cost depends nonlinearly on the extraction rate. Specifically, we assume that extraction uses final goods to extract oil reserves, and the cost is given by:

$$c^F(\theta_t) = \psi^F (\theta_t)^{\eta^F} R_t, \tag{54}$$

where $\theta_t \equiv \frac{f_t}{R_t}$ denotes the extraction rate.

The representative firm chooses the extraction rate to maximize profits:

$$\max_{\theta_t} P_t^F \theta_t R_t - \psi^F (\theta_t)^{\eta^F} R_t, \tag{55}$$

yielding the first-order condition:

$$P_t^F = \psi^F \eta^F (\theta_t)^{\eta^F - 1}. \tag{56}$$

This convex cost structure introduces an important general equilibrium feedback: as aggregate activity rises and oil demand increases, the marginal cost of extraction rises more than proportionally, leading to procyclical movements in the oil price. This channel tends to amplify the procyclicality of green innovation, which relies on fossil fuel prices as part of its relative cost advantage. In that sense, it can attenuate some of the mechanisms emphasized in our baseline model.

We follow Bornstein, Krusell, and Rebelo (2023) and set $\eta^F = 2$, consistent with micro-level evidence on the cost structure of fracking operations. The scale parameter ψ^F is normalized to 1.

Figure C.6: Alternative fossil extraction technology

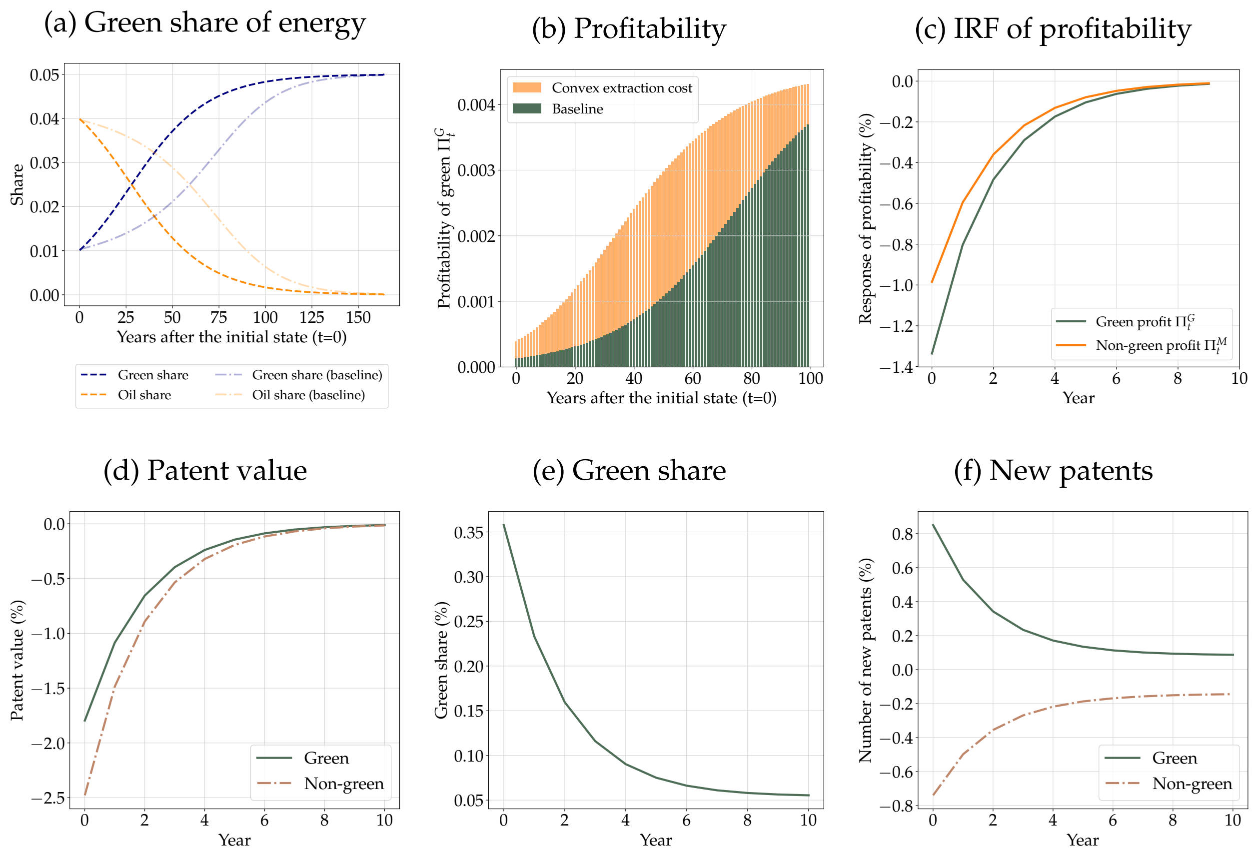

Notes: Model responses under the alternative fossil extraction technology. The convex cost parameter is set to $\eta^F = 2$, while the scale parameter is normalized to $\psi^F = 1$. All other parameters follow the baseline calibration in Section 4.1.

Figure C.6a highlights that under the convex oil production technology, the green transition accelerates significantly, with the green energy share surpassing fossil fuels within 25 years—compared to about 60 years in the baseline. As shown in Panel b, this faster transition is accompanied by a more rapid rise in the profitability of green innovation. Panel c illustrates that, due to the procyclical behavior of oil prices induced by the convex cost structure, the use of green inputs becomes more procyclical as well. Nevertheless, Panel d shows that the value of green patents remains less procyclical than that of non-green patents, although the gap in cyclicality narrows. Panel f confirms that the countercyclicality of new green patenting still holds, and Panel e shows that the green share of innovation remains countercyclical.

C.12. Model with Creative Destruction

In the Appendix, we consider a different model of innovation. Specifically, we endogenize the obsolescence rate to allow for vertical innovation.

Production. There is a representative firm that produces final good by employing unskilled labor L_t, a material composite M_t, and an energy composite E_t:

$$Y_t = (Z_t L_t)^{\alpha_L} M_t^{\alpha_M} E_t^{1-\alpha_L-\alpha_M}, \tag{57}$$

where Z_t is an aggregate labor productivity, evolving as

$$\log Z_t = \rho_z \log Z_{t-1} + \sigma_z \varepsilon_t^z. \tag{58}$$

The final good producer combines fossil fuel f_t and a green energy composite G_t into the energy composite E_t via a CES technology:

$$E_t = \left(f_t^{\frac{\rho-1}{\rho}} + G_t^{\frac{\rho-1}{\rho}} \right)^{\frac{\rho}{\rho-1}}. \tag{59}$$

The parameter ρ governs the elasticity of substitution between fossil fuel and the green energy composite. We assume $\rho > 1$, indicating that f_t and G_t are substitutes.

The green energy composite G_t and the materials composite M_t each aggregate a continuum of differentiated product lines indexed by $j \in [0, 1]$ for green energy and $h \in [0, 1]$ for materials. The aggregation of materials M_t is given by:

$$M_t = \left(\int_0^1 A_{ht}^m m_{ht}^{\frac{1}{\mu_M}} \, dh \right)^{\mu_M}, \tag{60}$$

and the aggregation of green energy G_t is given by:

$$G_t = \left(\int_0^1 A_{jt}^g g_{jt}^{\frac{1}{\mu_G}} \, dj \right)^{\mu_G}. \tag{61}$$

Here, A_{ht}^m and A_{jt}^g represent the qualities of materials and green energy inputs, respectively, while m_{ht} and g_{jt} denote the quantities of each product line.

The final good producer's optimization problem is:

$$\max_{L_t,\{m_{ht}\},f_t,\{g_{jt}\}} P_t\left[(Z_tL_t)^{\alpha} M_t^{\beta} E_t^{1-\alpha-\beta}\right] - \int_0^1 p_{ht}^m\, m_{ht}\, dh - \int_0^1 p_{jt}^g\, g_{jt}\, dj - P_t^f\, f_t. \tag{62}$$

Solving this problem yields the following demand equations:

$$m_{ht} = \left(\frac{p_{ht}^m / A_{ht}^m}{P_t^M}\right)^{\frac{\mu_M}{1-\mu_M}} M_t, \qquad g_{jt} = \left(\frac{p_{jt}^g / A_{jt}^g}{P_t^G}\right)^{\frac{\mu_G}{1-\mu_G}} G_t, \tag{63}$$

where $P_t^M = \left(\int_0^1 (p_{ht}^m/(A_{ht}^m)^{\mu_M})^{\frac{1}{1-\mu_M}}\, dh\right)^{1-\mu_M}$ and $P_t^G = \left(\int_0^1 (p_{jt}^g/(A_{jt}^g)^{\mu_G})^{\frac{1}{1-\mu_G}}\, dj\right)^{1-\mu_G}$ are the corresponding price indices of M_t and G_t.

Intermediate input producers. Intermediate input producers, which include firms that produce both non-green and green energy varieties, m_{ht} and g_{jt}, respectively, maximize profits subject to the demand equations in (63).

Green energy product lines. The green energy product lines are produced by a continuum of firms operating under monopolistic competition.

Each variety j of green energy uses a linear production technology, where the marginal cost of producing one unit is given by ψA_{jt}^g, with ψ representing the constant marginal cost per unit of production, and A_{jt}^g denoting the quantity produced by firm j of the green energy variety. This proportional cost structure reflects the fact that higher-quality products typically require more expensive inputs.

The marginal cost for each variety j can thus be written as:

$$\xi_{jt}^g = \psi A_{jt}^g, \tag{64}$$

The firm's objective is to maximize its profits by choosing the optimal quantity A_{jt} and the corresponding price p_{jt}^g, given the demand for its product and its marginal cost structure.

The profit maximization problem for a firm producing green energy product line j is given by:

$$\Pi_{jt}^G = \max_{p_{jt}^g} \left(p_{jt}^g\, g_{jt} - \xi_{jt}^g g_{jt}\right), \tag{65}$$

Non-green material product lines. Non-green material product lines are produced in a similar fashion to green energy varieties.

Each variety m_{ht} is produced using linear technology, with marginal costs given by ψA^m_{ht}, where A^m_{ht} is the quantity produced by firm h of the non-green material variety. Like green energy products, the cost structure increases with the scale of production, as higher-quality materials demand more expensive inputs.

The marginal cost for each variety h can be written as:

$$\xi^m_{ht} = \psi A^m_{ht}, \tag{66}$$

The firm's objective is to maximize profits by determining the optimal quantity A_{ht} and price p^m_{ht}, taking into account demand and the marginal cost structure.

The profit maximization problem for a firm producing non-green material product line h is given by:

$$\Pi^m_{ht} = \max_{p^m_{ht}} \left(p^m_{ht}\ m_{ht} - \xi^m_{ht} m_{ht} \right). \tag{67}$$

Innovation. In this framework, the engine of economic growth is driven by process innovations that lead to quality improvements. The quality of a product line increases over time as firms introduce innovations. Specifically, the quality of each machine line evolves according to the following "quality ladder" specification:

$$A_{ht} = \lambda^{n_{ht}} A^g_{h0}, \tag{68}$$

$$A_{jt} = \lambda^{n_{jt}} A^m_{j0}, \tag{69}$$

where $\lambda > 1$ is a constant that represents the factor by which the quality increases with each innovation, $A^g_{h0}, A^m_{j0} \in \mathbb{R}^+$ is the initial quality of the product line h, j of either green and non-green at time $t = 0$, and n_{jt}, n_{ht} denotes the number of innovations on this product line between time 0 and t.

Quality improvements are created by R&D. Innovation firms hire skilled labor to conduct R&D. If an innovation firm hires L^S units of skilled labor for research on this product line, then it generates a flow rate:

$$\frac{\zeta_M A_t}{A^m_{ht}} (L^S_{M,t})^\nu, \frac{\zeta_G A_t}{A^g_{jt}} (L^S_{G,t})^\nu. \tag{70}$$

The innovation firm who successfully innovate becomes the leading-edge producer and replaces the previous vintage of the same product. Therefore, the value of a successful innovation can be written as:

$$V^m_{ht}(\lambda A^m_{ht-1}) = \Pi^m_{ht}(\lambda A^m_{ht-1}) + (1-\phi^m_{ht})E_t\Lambda_{t,t+1}V^m_{ht+1}(\lambda A^m_{ht-1}) \tag{71}$$
$$V^g_{jt}(\lambda A^g_{jt-1}) = \Pi^g_{jt}(\lambda A^g_{jt-1}) + (1-\phi^g_{jt})E_t\Lambda_{t,t+1}V^g_{jt+1}(\lambda A^g_{jt-1}) \tag{72}$$

where ϕ^m_{ht}, ϕ^g_{jt} are the rate of new innovations.

The innovation problem implies:

$$\zeta_M A_t V^m_{ht} / A^m_{ht} \nu (L^S_{t,M})^{\nu-1} = W^S_t \tag{73}$$
$$\zeta_G A_t V^g_{ht} / A^g_{ht} \nu (L^S_{t,G})^{\nu-1} = W^S_t \tag{74}$$

where the wage of skilled labor is assumed constant in this partial equilibrium setup. The following two propositions establish that the key mechanism—green profits being more backloaded—holds in the quality-ladder model with creative destruction. We formally prove that this mechanism also implies a countercyclical green share of innovation in a specific case with linear innovation technology and in partial equilibrium.

Proposition C.4 (Green Is in the Future). *During the green transition, the relative profits of green varieties compared to non-green varieties, measured by* $\frac{\Pi^G_t}{\Pi^M_t}$*, increase over time.*

Proposition C.5 (Cyclicality during the Green Transition). *For a linear innovation technology where* $\nu = 1$*, during the green transition, the green share of new varieties,* $\frac{\phi^G_t}{\phi^G_t+\phi^M_t}$*, is countercyclical, where* $\phi^M_t = \int_0^1 \phi^M_{ht}\, dh$ *and* $\phi^G_t = \int_0^1 \phi^G_{jt}\, dj$*.*

To examine whether the countercyclical green (share of) innovation result holds more generally in the quality-ladder model with creative destruction under general equilibrium, we embed the model into the same general equilibrium framework as in Section 4.1 and recalibrate it accordingly. Specifically, we keep the parameters governing the production economy and household preferences unchanged, and calibrate the innovation parameters ζ_M, ζ_L, and λ to match a long-run creative destruction rate of 8% and an output growth rate of 3%.

Figure C.7: Green and non-green patenting responses in creative destruction model

(a) IP value of a new variety (b) Green share (c) Number of new varieties

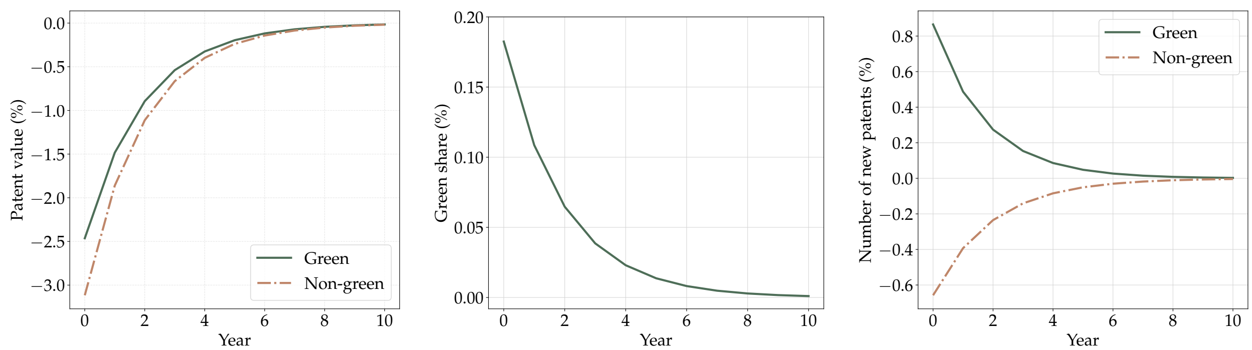

Notes: Impulse responses of the value and number of varieties of green and non-green patents to a 25 basis point monetary policy shock. The calibration of the households and production economy follows Section 4.1, and the innovation parameters ζ_M, ζ_L, and λ to match a long-run creative destruction rate of 8% and an output growth rate of 3%.

To examine whether the countercyclicality of green (share of) innovation extends more generally to a quality-ladder model with creative destruction in general equilibrium, we embed the mechanism into the same general equilibrium framework as in Section 4.1 and recalibrate the model accordingly. Specifically, we keep the production-side and household parameters unchanged, and calibrate the innovation parameters ζ_M, ζ_L, and λ to target a long-run creative destruction rate of 8% and an output growth rate of 3%.

Figure C.7a shows that, as expected, the patent value of green varieties is less procyclical than that of non-green ones. Panel c confirms that the green share of innovation is countercyclical, although the magnitude is somewhat smaller than in Figure 7. Panel b further shows that green innovation is countercyclical, while non-green innovation remains procyclical.

D. Proofs

This appendix contains the corresponding proofs from our analysis.

Proof of Lemma 3.1. The first-order conditions of the final good producer imply:

$$(1-\alpha_L-\alpha_M)\frac{P_tY_t}{E_t}E_t^{\frac{1}{\rho}}f_t^{-\frac{1}{\rho}} = P_t^f, \tag{75}$$

$$(1-\alpha_L-\alpha_M)\frac{P_tY_t}{E_t}E_t^{\frac{1}{\rho}}G_t^{-\frac{1}{\rho}} = P_t^G. \tag{76}$$

It follows that:

$$\frac{f_t}{G_t} = \left(\frac{P_t^G}{P_t^f}\right)^{\rho}. \tag{77}$$

Under monopolistic competition in the green sector, the optimal pricing implies $p_{jt}^g = \mu_G$, which in turn yields $P_t^G = \mu_G (A_t^G)^{1-\mu_G}$.

By the definition of the energy mix:

$$\frac{G_t}{E_t} = \left(1 + \left(\frac{f_t}{G_t}\right)^{\frac{\rho-1}{\rho}}\right)^{-\frac{\rho}{\rho-1}} = \left(1 + \left(\mu_G P_t^f (A_t^G)^{\mu_G - 1}\right)^{-\frac{\rho-1}{\rho}}\right)^{-\frac{\rho}{\rho-1}}. \tag{78}$$

Therefore, $\frac{G_t}{E_t}$ increases overtime if and only if $\frac{P_t^f}{(A_t^G)^{1-\mu_G}}$ increases overtime. ∎

Proof of Proposition 3.1. From equation (26):

$$\begin{aligned} \frac{P_t^G G_t}{P_t Y_t} &= (1 - \alpha_L - \alpha_m) E_t^{\frac{1}{\rho}-1} G_t^{1-\frac{1}{\rho}} \\ &= (1 - \alpha_L - \alpha_m) \left(\left(\frac{f_t}{G_t}\right)^{\frac{\rho-1}{\rho}} + 1\right)^{-1}. \end{aligned} \tag{79}$$

Combining equations (25) and (26), we obtain:

$$\frac{f_t}{G_t} = \left(\frac{P_t^G}{P_t^f}\right)^{\rho}. \tag{80}$$

From the clean energy producer's optimization and the fossil fuel price-setting equation:

$$\frac{f_t}{G_t} = \left(\frac{\theta}{1-\theta} \frac{\left(A_t^G\right)^{1-\mu_G} \mu_G P_t}{\xi_f^{-1} P_t}\right)^{\rho} = \left(\frac{\theta}{1-\theta} \frac{\left(A_t^G\right)^{1-\mu_G} \mu_G}{\xi_f^{-1}}\right)^{\rho}, \tag{81}$$

which is declining over time. Therefore, when $\rho > 1$, it follows that $\frac{P_t^G G_t}{P_t Y_t}$ is increasing over time.

Since the production of varieties of intermediate inputs and clean energy inputs is homogeneous:

$$M_t = \left(A_t^M\right)^{\mu_M} \bar{m}_t, \tag{82}$$

$$G_t = \left(A_t^G\right)^{\mu_G} \bar{g}_t, \tag{83}$$

equations (24) and (79) imply:

$$\frac{P_t^G G_t}{P_t^M M_t} = \frac{A_t^G \mu_G \bar{g}_t}{A_t^M \mu_M \bar{m}_t} = \frac{\alpha_M}{(1-\alpha_L-\alpha_m)} \left(\left(\frac{f_t}{G_t}\right)^{\frac{\rho-1}{\rho}} + 1\right)^{-1}. \tag{84}$$

It follows that:

$$\frac{\bar{g}_t}{\bar{m}_t} = \frac{A_t^M}{A_t^G} \frac{\mu_M \alpha_M}{\mu_G(1-\alpha_L-\alpha_M)} \left(\left(\frac{f_t}{G_t}\right)^{\frac{\rho-1}{\rho}} + 1\right)^{-1}. \tag{85}$$

And because $\frac{A_t^M}{A_t^G}$ is constant in the long run, it implies $\frac{\bar{g}_t}{\bar{m}_t}$ is increasing over time. Finally, by equation (31) and (31),

$$\frac{\Pi_t^G}{\Pi_t^M} = \frac{(\mu_G - 1)\bar{g}_t}{(\mu_M - 1)\bar{m}_t}. \tag{86}$$

Because $\frac{\bar{g}_t}{\bar{m}_t}$ is increasing over time, the proposition follows. ∎

Proof of Proposition 3.2. Define the value of intellectual property holding SDF fixed:

$$\Theta_t^M = \sum_{s=0}^{\tau} (\beta\phi)^s \, \mathbb{E}_t \Pi_{t+s}^m = \sum_{s=0}^{\tau} (\beta\phi)^s \, \mathbb{E}_t (\mu_M - 1) P_{t+s} \bar{m}_{t+s}, \tag{87}$$

$$\Theta_{jt}^G = \sum_{s=0}^{\tau} (\beta\phi)^s \, \mathbb{E}_t \Pi_{t+s}^g = \sum_{s=0}^{\tau} (\beta\phi)^s \, \mathbb{E}_t (\mu_G - 1) P_{t+s} \bar{g}_{t+s}. \tag{88}$$

Now, consider a one-shot shock to Z_t, and the same proof can be applied to persistent shocks and other shocks that affect Y_t. We obtain the following result:

$$\frac{\partial \log \Theta_t^M}{\partial \log Y_t} = \frac{(\mu_M - 1) P_{t,ss} \bar{m}_{t,ss}}{V_{t,ss}^M} \left(\frac{\partial \log \bar{m}_t}{\partial \log Z_t} + \frac{\partial \log P_t}{\partial \log Z_t}\right) \frac{\partial \log Z_t}{\partial \log Y_t}, \tag{89}$$

$$\frac{\partial \log \Theta_t^G}{\partial \log Y_t} = \frac{(\mu_G - 1) P_{t,ss} \bar{g}_{t,ss}}{V_{t,ss}^G} \left(\frac{\partial \log \bar{g}_t}{\partial \log Z_t} + \frac{\partial \log P_t}{\partial \log Z_t}\right) \frac{\partial \log Z_t}{\partial \log Y_t}, \tag{90}$$

where the 'ss' subscript means the variables given no shock. It follows that:

$$\frac{\partial \log \Theta_t^G}{\partial \log Y_t} / \frac{\partial \log \Theta_t^M}{\partial \log Y_t} = \frac{(\mu_G - 1)\bar{g}_{t,ss}}{(\mu_M - 1)\bar{m}_{t,ss}} \frac{V_{t,ss}^M}{V_{t,ss}^G} \frac{\left(\frac{\partial \log \bar{g}_t}{\partial \log Z_t} + \frac{\partial \log P_t}{\partial \log Z_t}\right)}{\left(\frac{\partial \log \bar{m}_t}{\partial \log Z_t} + \frac{\partial \log P_t}{\partial \log Z_t}\right)} \tag{91}$$

From equation (24), we have:

$$P_t^M M_t = A_t^M \mu_M P_t \bar{m}_t = \alpha_M P_t Y_t, \tag{92}$$

which implies that:

$$\bar{m}_t = \frac{\beta}{\mu_G} \frac{Y_t}{A_t^M}. \tag{93}$$

Similarly, by equation (85) and (81):

$$\bar{g}_t = \frac{A_t^M}{A_t^G} \frac{\mu_M \alpha_M}{\mu_G(1 - \alpha_L - \alpha_M)} \left(\left(\frac{\left(A_t^G\right)^{1-\mu_G} \mu_G}{\xi_f^{-1}} \right)^{\rho - 1} + 1 \right)^{-1} \bar{m}_t \tag{94}$$

Therefore, since A_t^M

$$\frac{\partial \log \bar{m}_t}{\partial \log Y_t} = \frac{\partial \log(Y_t / A_t^M)}{\partial \log Y_t} = 1, \tag{95}$$

$$\frac{\partial \log \bar{g}_t}{\partial \log Y_t} = \frac{\partial \log \bar{m}_t}{\partial \log Y_t}. \tag{96}$$

It follows that:

$$\frac{\partial \log \bar{g}_t}{\partial \log Y_t} / \frac{\partial \log \bar{m}_t}{\partial \log Y_t} = 1 \tag{97}$$

Therefore,

$$\frac{\partial \log \Theta_t^G}{\partial \log Y_t} / \frac{\partial \log \Theta_t^M}{\partial \log Y_t} = \frac{(\mu_G - 1)\bar{g}_{t,ss}}{(\mu_M - 1)\bar{m}_{t,ss}} \frac{V_{t,ss}^M}{V_{t,ss}^G}. \tag{98}$$

Because $\bar{g}_t / \bar{m}_t$ is increasing over time, it implies that the value of a green variety is more backloaded than the value of a non-green variety:

$$\frac{(\mu_G - 1)\bar{g}_{t,ss}}{V^G_{t,ss}} < \frac{(\mu_G - 1)\bar{m}_{t,ss}}{V^M_{t,ss}} \tag{99}$$

Therefore,

$$\frac{\partial \log \Theta^G_t}{\partial \log Y_t} / \frac{\partial \log \Theta^M_t}{\partial \log Y_t} < 1, \tag{100}$$

holds.

■

Proof of Lemma C.1. Define

$$\tilde{\Xi}^k_t = \sum_{s=0}^{\infty} \phi^s \, \mathbb{E}_t \left[\Lambda_{t,t+s} \Pi^k_{t+s,ss} \right] \tag{101}$$

for $k \in \{M, G\}$, where $\Xi^k_t = \partial \log \tilde{\Xi}^k_t / \partial \log Y_t$. Note that

$$\begin{aligned} \frac{\partial \tilde{\Xi}^I_t}{\partial Y_t} &= \partial \sum_{s=0}^{\infty} \phi^s \, \mathbb{E}_t \left[\Lambda_{t,t+s} \Pi^I_{t+s,ss} \right] / \partial Y_t && (102) \\ &= \sum_{s=0}^{\infty} \phi^s \, \mathbb{E}_t \left[\frac{\partial \Lambda_{t,t+s}}{\partial Y_t} \Pi^I_{t+s,ss} \right] && (103) \end{aligned}$$

Note that by definition of the SDF:

$$\Lambda_{t,t+s} = \prod_{h=0}^{h=s-1} \Lambda_{t+h,t+h+1}. \tag{104}$$

Consider

$$\frac{\partial \log \Lambda_{t+s,t+s+1}}{\partial \log Y_t} > 0. \tag{105}$$

This implies the procyclicality of SDF is increasing in the time horizon of discounting (i.e., $\frac{\partial \log \Lambda_{t,t+s}}{\partial \log Y_t}$ is increasing in s.)

Because the value of green variety is more backloaded, by equation (103),

$$\frac{\partial \log \tilde{\Xi}^G_t}{\partial \log Y_t} > \frac{\partial \log \tilde{\Xi}^M_t}{\partial \log Y_t}. \tag{106}$$

Conversely, if

$$\frac{\partial \log \Lambda_{t+s,t+s+1}}{\partial \log Y_t} < 0, \tag{107}$$

it holds:

$$\frac{\partial \log \tilde{\Xi}_t^G}{\partial \log Y_t} < \frac{\partial \log \tilde{\Xi}_t^M}{\partial \log Y_t}, \tag{108}$$

which completes the proof. ■

Proof of Corollary C.1. Consider a one-shot shock to Z_t or ϱ_t^D. We can decompose the pratial derivative into the cash flow and discount rate components:

$$\frac{\partial \log \mathcal{V}_t^k}{\partial \log Y_t} = \frac{\Pi_{t,ss}^I}{\mathcal{V}_{t,ss}^I} \frac{\partial \log \Pi_t^I}{\log Y_t} + \sum_{h=1} \frac{(1-c)\Pi_{t+h,ss}^I}{\mathcal{V}_{t,ss}^I} \frac{\partial \log \Lambda_{t,t+h}^I}{\log Y_t}. \tag{109}$$

for $k \in \{M, G\}$. By equation (95) and (96):

$$\frac{\partial \log \bar{g}_t}{\partial \log Y_t} = \frac{\partial \log \bar{m}_t}{\partial \log Y_t} = 1 \tag{110}$$

Combining with the market clearing of final goods:

$$\frac{\partial \log C_t}{\partial \log Y_t} = 1. \tag{111}$$

Note that:

$$\log \Lambda_{t,t+s} = \log \beta + \log C_t - \log C_{t+s} - \log \varrho_t^D + \log \varrho_{t+1}^D. \tag{112}$$

Consider a Z_t shock:

$$\frac{\partial \log \Lambda_{t,t+s}}{\partial \log Y_t} = 1. \tag{113}$$

It follows:

$$\frac{\partial \log \mathcal{V}_t^I}{\partial \log Y_t} = \frac{\Pi_{t,ss}^I}{\mathcal{V}_{t,ss}^I} + \sum_{h=1} \frac{(1-c)\Pi_{t+h,ss}^I}{\mathcal{V}_{t,ss}^I} \tag{114}$$

$$= c\frac{\Pi_{t,ss}^I}{\mathcal{V}_{t,ss}^I} + (1-c). \tag{115}$$

And because the profit of green variety is more backloaded:

$$\frac{\Pi_{t,ss}^G}{\mathcal{V}_{t,ss}^G} < \frac{\Pi_{t,ss}^M}{\mathcal{V}_{t,ss}^M}. \tag{116}$$

It follows:

$$\frac{\partial \log \mathcal{V}_t^G}{\partial \log Y_t} < \frac{\partial \log \mathcal{V}_t^M}{\partial \log Y_t}. \tag{117}$$

If it is the preference shock,

$$\frac{\partial \log \Lambda_{t,t+s}}{\partial \log Y_t} = 1 - \frac{\log \varrho_t^D}{\partial \log Y_t}. \tag{118}$$

Therefore,

$$\frac{\partial \log \mathcal{V}_t^I}{\partial \log Y_t} = \frac{\Pi_{t,ss}^I}{\mathcal{V}_{t,ss}^I} + \sum_{h=1} \frac{(1-c)\Pi_{t+h,ss}^I}{\mathcal{V}_{t,ss}^I}(1 - \frac{\log \varrho_t^D}{\partial \log Y_t}) \tag{119}$$

$$= c\frac{\Pi_{t,ss}^I}{\mathcal{V}_{t,ss}^I} + (1-c) - \sum_{h=1} \frac{(1-c)\Pi_{t+h,ss}^I}{\mathcal{V}_{t,ss}^I} \frac{\log \varrho_t^D}{\partial \log Y_t}. \tag{120}$$

Because the more backloaded profit of green:

$$c\frac{\Pi_{t,ss}^G}{\mathcal{V}_{t,ss}^G} < c\frac{\Pi_{t,ss}^M}{\mathcal{V}_{t,ss}^M}, \qquad \sum_{h=1} \frac{(1-c)\Pi_{t+h,ss}^G}{\mathcal{V}_{t,ss}^G} > \sum_{h=1} \frac{(1-c)\Pi_{t+h,ss}^M}{\mathcal{V}_{t,ss}^M}. \tag{121}$$

As a result,

$$\frac{\partial \log \mathcal{V}_t^G}{\partial \log Y_t} < \frac{\partial \log \mathcal{V}_t^M}{\partial \log Y_t}, \tag{122}$$

which completes the proof. ■

Proof of Proposition 3.3. By the definition of S_t^M and S_t^G:

$$S_t^M = \varphi_{t,M} L_{t,M} = \zeta_M A_t^M (L_{t,M}^S)^\nu, \tag{123}$$
$$S_t^G = \varphi_{t,G} L_{t,G} = \zeta_G A_t^G (L_{t,G}^S)^\nu. \tag{124}$$

And by the innovator's problem given by equation (34) and (34), the proposition is equivalent to show the relative value of green versus non-green innovation is countercyclical. Formally,

$$\frac{\partial \log(\mathcal{V}_t^G / \mathcal{V}_t^M)}{\partial \log Y_t} < 0. \tag{125}$$

Therefore it directly follows from Corollary C.1. ■

Proof of Proposition 3.4. From equation (34) and (35):

$$L_{it,M}^S = \left(\frac{W_t^s}{A_t^M \zeta_M \mathcal{V}_t^m} \right)^{\frac{1}{\nu-1}}, \tag{126}$$
$$L_{it,G}^S = \left(\frac{W_t^s}{A_t^G \zeta_M \mathcal{V}_t^g} \right)^{\frac{1}{\nu-1}}. \tag{127}$$

Therefore, in equilibrium, the new varieties can be solved as:

$$S_t^M = A_t^M \zeta_M \left(L_{t,M}^S \right)^\nu = A_t^M \zeta_M \left(\frac{W_t^s}{A_t^M \zeta_M \mathcal{V}_t^m} \right)^{\frac{\nu}{\nu-1}}, \tag{128}$$
$$S_t^G = A_t^G \zeta_G \left(L_{t,G}^S \right)^\nu = A_t^G \zeta_G \left(\frac{W_t^s}{A_t^G \zeta_G \mathcal{V}_t^g} \right)^{\frac{\nu}{\nu-1}}. \tag{129}$$

It follows that

$$\frac{\partial \log S_t^G}{\partial \log Y_t} = -\frac{\nu}{1-\nu} \left(\frac{\partial \log W_t^s}{\partial \log Y_t} - \frac{\partial \log \mathcal{V}_t^g}{\partial \log Y_t} \right). \tag{130}$$

Therefore, S_t^G is countercyclical if

$$\frac{\partial \log W_t^s}{\partial \log Y_t} > \frac{\partial \log \mathcal{V}_t^g}{\partial \log Y_t}. \tag{131}$$

Next, we show that S_t^M must be procyclical. Combining the skilled labor demand conditions (35) and (34) with the skilled labor market clearing condition:

$$L^S_{it,M} = \left(\frac{C_t\bar{\omega}^s(L^S_{t,M}+L^S_{t,G})^{\psi}}{\varrho^D_t A^M_t \zeta_M \mathcal{V}^m_t}\right)^{\frac{1}{\nu-1}}, \tag{132}$$

$$L^S_{it,G} = \left(\frac{C_t\bar{\omega}^s(L^S_{t,M}+L^S_{t,G})^{\psi}}{\varrho^D_t A^G_t \zeta_G \mathcal{V}^g_t}\right)^{\frac{1}{\nu-1}}. \tag{133}$$

By combining equations (132) and (133) with the skilled labor market clearing condition, we obtain:

$$L^S_t = \left(\frac{C_t\bar{\omega}^s}{\varrho^D_t}\right)^{\frac{1}{\nu-1-\psi}} \left[(A^M_t\zeta_M\mathcal{V}^m_t)^{-\frac{1}{\nu-1}} + (A^G_t\zeta_G\mathcal{V}^g_t)^{-\frac{1}{\nu-1}}\right]^{\frac{\nu-1}{\nu-1-\psi}} \tag{134}$$

$$= \left(\frac{C_t\bar{\omega}^s}{\varrho^D_t}\right)^{\frac{1}{\nu-1-\psi}} (A^M_t\zeta_M\mathcal{V}^m_t)^{\frac{1}{\psi+1-\nu}} \left[1+\left(\frac{A^M_t\zeta_M\mathcal{V}^m_t}{A^G_t\zeta_G\mathcal{V}^g_t}\right)^{\frac{1}{\nu-1}}\right]^{\frac{1-\nu}{\psi+1-\nu}}. \tag{135}$$

Substituting, we obtain:

$$L^S_{it,M} = \left(\frac{C_t\bar{\omega}^s}{\varrho^D_t}\right)^{\frac{1}{\nu-1-\psi}} \left(A^M_t\zeta_M\mathcal{V}^m_t\right)^{\frac{1}{\psi+1-\nu}} \left[1+\left(\frac{A^M_t\zeta_M\mathcal{V}^m_t}{A^G_t\zeta_G\mathcal{V}^g_t}\right)^{\frac{1}{\nu-1}}\right]^{\frac{\psi}{\nu-1-\psi}}, \tag{136}$$

$$L^S_{it,G} = \left(\frac{C_t\bar{\omega}^s}{\varrho^D_t}\right)^{\frac{1}{\nu-1-\psi}} \left[1+\left(\frac{A^M_t\zeta_M\mathcal{V}^m_t}{A^G_t\zeta_G\mathcal{V}^g_t}\right)^{\frac{1}{\nu-1}}\right]^{\frac{\psi}{\nu-1-\psi}} \left(A^M_t\zeta_M\mathcal{V}^m_t\right)^{\frac{1}{\psi+1-\nu}} \left(\frac{A^G_t\zeta_G\mathcal{V}^g_t}{A^M_t\zeta_M\mathcal{V}^m_t}\right)^{\frac{1}{1-\nu}}. \tag{137}$$

Because $\partial \log C_t/\partial \log Y_t = \partial \log \Pi^M_t/\partial \log Y_t$, from the definition of the value of non-green varieties:

$$\frac{\partial \log C_t}{\partial \log Y_t} < \frac{\partial \log \mathcal{V}^M_t}{\partial \log Y_t}. \tag{138}$$

And because $\mathcal{V}^M_t$ is more procyclical than $\mathcal{V}^G_t$ from Proposition 3.3, it follows that $L^S_{t,M}$

must be procyclical, or equivalently

$$\frac{\partial \log S_t^M}{\partial \log Y_t} > 0. \tag{139}$$

■

Proof of Corollary 3.1. Recall, in equilibrium:

$$L_{t,M}^S = \left(\frac{C_t \bar{\omega}^s}{\varrho_t^D}\right)^{\frac{1}{\nu-1-\psi}} \left(A_t^M \zeta_M \mathcal{V}_t^m\right)^{\frac{1}{\psi+1-\nu}} \left[1 + \left(\frac{A_t^M \zeta_M \mathcal{V}_t^m}{A_t^G \zeta_G \mathcal{V}_t^g}\right)^{\frac{1}{\nu-1}}\right]^{\frac{\psi}{\nu-1-\psi}}, \tag{140}$$

$$L_{t,G}^S = \left(\frac{C_t \bar{\omega}^s}{\varrho_t^D}\right)^{\frac{1}{\nu-1-\psi}} \left[1 + \left(\frac{A_t^M \zeta_M \mathcal{V}_t^m}{A_t^G \zeta_G \mathcal{V}_t^g}\right)^{\frac{1}{\nu-1}}\right]^{\frac{\psi}{\nu-1-\psi}} \left(A_t^M \zeta_M \mathcal{V}_t^m\right)^{\frac{1}{\psi+1-\nu}} \left(\frac{A_t^G \zeta_G \mathcal{V}_t^g}{A_t^M \zeta_M \mathcal{V}_t^m}\right)^{\frac{1}{1-\nu}}. \tag{141}$$

If ψ goes to infinity:

$$L_{t,M}^S = \left[1 + \left(\frac{A_t^M \zeta_M \mathcal{V}_t^m}{A_t^G \zeta_G \mathcal{V}_t^g}\right)^{\frac{1}{\nu-1}}\right]^{-1}, \tag{142}$$

$$L_{t,G}^S = \left[1 + \left(\frac{A_t^G \zeta_G \mathcal{V}_t^g}{A_t^M \zeta_M \mathcal{V}_t^m}\right)^{\frac{1}{\nu-1}}\right]^{-1}, \tag{143}$$

where $L_{t,G}^S$ is countercyclical. And for $\psi = 0$, $L_{t,G}^S$ must be procyclical. Therefore, by the intermediate value theorem, the proposition holds. ■

Proof of Corollary 3.2. The same proof of Proposition 3.4 applies. Because the moneatry shock affects the value of innovations only through affecting Y_t. ■

Proof of Proposition C.1 - C.3. When there is brown innovation, the relationship of brown and green energy in equilibrium becomes:

$$\frac{F_t}{G_t} = \left(\frac{P_t^G}{P_t^F}\right) = \left(\frac{(A_t^G)^{1-\mu_G}\mu_G}{(A_t^F)^{1-\mu_F}\mu_F \zeta_f^{-1}}\right). \tag{144}$$

The green transition happens if:

$$\frac{(A_t^G)^{\mu_G - 1}\mu_G}{(A_t^F)^{\mu_F - 1}\mu_F\xi_f^{-1}} \tag{145}$$

is increasing over time. This condition requires the green innovation outpaces the brown innovation. However, given the existence of green transition, other conditions for Lemma 3.1, Proposition 3.3 and 3.4 are exactly the same for the model with or without brown innovation. Therefore the same proof applies. ■

Proof of Proposition C.4. By the profit maximization problem for firms producing green and non-green product lines in equation (65) and (67), and the demand function of green and non-green product lines implied by equation (63), the optimal price of green and non-green is:

$$p_{ht}^m = \mu_M \psi A_{ht}^m, \qquad p_{jt}^g = \mu_G \psi A_{jt}^g. \tag{146}$$

Therefore, the production of green and non-green products across product lines are homogeneous, which we denote as $\bar{m}_t, \bar{g}_t$. Therefore:

$$P_t^M = (A_t^M)^{1-\mu_M}\mu_M\psi, \qquad P_t^G = (A_t^G)^{1-\mu_G}\mu_G\psi, \tag{147}$$

$$M_t = (A_t^M)^{\mu_M}\bar{m}_t, \qquad G_t = (A_t^G)^{\mu_G}\bar{g}_t, \tag{148}$$

where

$$A_t^M = \int_0^1 A_{ht}^m \, dh, \qquad A_t^G = \int_0^1 A_{jt}^g \, dj. \tag{149}$$

Recall from the baseline model, we derive:

$$\frac{P_t^G G_t}{P_t^M M_t} = \frac{\alpha_M}{(1-\alpha_L-\alpha_m)}\left(\left(\frac{f_t}{G_t}\right)^{\frac{\rho-1}{\rho}} + 1\right)^{-1}. \tag{150}$$

Therefore, the same condition as equation (85) holds

$$\frac{\bar{g}_t}{\bar{m}_t} = \frac{A_t^M}{A_t^G}\frac{\mu_M\alpha_M}{\mu_G(1-\alpha_L-\alpha_M)}\left(\left(\frac{f_t}{G_t}\right)^{\frac{\rho-1}{\rho}} + 1\right)^{-1}. \tag{151}$$

Henceforth $\frac{\bar{g}_t}{\bar{m}_t}$ is increasing given the green transition, which completes the proof.

■

Proof of Proposition C.5. Recall the optimization condition of the innovator's problem:

$$\zeta_M \tilde{V}^m_{ht} = w^s, \tag{152}$$

$$\zeta_G \tilde{V}^g_{jt} = w^s, \tag{153}$$

where w^s denotes the normalized wage of skilled labor, which is assumed constant in this partial equilibrium setting. $\tilde{V}^m_{ht}$ and $\tilde{V}^g_{jt}$ represent the normalized value of innovation:

$$\tilde{V}^m_{ht} = \pi^m_{ht} + (1-\phi^m_{ht})E_t[\Lambda_{t,t+1}\tilde{V}^m_{ht+1}], \tag{154}$$

$$\tilde{V}^g_{jt} = \pi^g_{jt} + (1-\phi^g_{jt})E_t[\Lambda_{t,t+1}\tilde{V}^g_{jt+1}]. \tag{155}$$

Thus, the optimality condition can be rewritten as:

$$\phi^m_{ht} = \frac{\pi^m_{ht} + E_t[\Lambda_{t,t+1}\tilde{V}^m_{ht+1}] - \zeta_M^{-1}w^s}{E_t[\Lambda_{t,t+1}\tilde{V}^m_{ht+1}]}, \tag{156}$$

$$\phi^g_{jt} = \frac{\pi^g_{jt} + E_t[\Lambda_{t,t+1}\tilde{V}^g_{jt+1}] - \zeta_G^{-1}w^s}{E_t[\Lambda_{t,t+1}\tilde{V}^g_{jt+1}]}. \tag{157}$$

By symmetry, we drop the subscripts j and h in the following expressions. The ratio of green to non-green innovation intensities can be expressed as:

$$\frac{\phi^g_t}{\phi^m_t} = \frac{\pi^g_t + E_t[\Lambda_{t,t+1}\tilde{V}^g_{t+1}] - \zeta_G^{-1}w^s}{\pi^m_t + E_t[\Lambda_{t,t+1}\tilde{V}^m_{t+1}] - \zeta_M^{-1}w^s} \times \frac{E_t[\Lambda_{t,t+1}\tilde{V}^m_{t+1}]}{E_t[\Lambda_{t,t+1}\tilde{V}^g_{t+1}]}. \tag{158}$$

Now consider a one-shot shock to Z_t. Regarding the second term $\frac{E_t[\Lambda_{t,t+1}\tilde{V}^m_{t+1}]}{E_t[\Lambda_{t,t+1}\tilde{V}^g_{t+1}]}$, since the shock does not affect $\tilde{V}^m_{t+1}$, and the effect of the shock on $\Lambda_{t,t+1}$ cancels out between numerator and denominator, this term remains unaffected by the one-shot shock.

For the first term, Proposition C.4 has established that the relative profit of green innovation grows compared to that of non-green innovation. Therefore, the logic of the proof of Proposition 3.3 applies here as well.

■

References Appendix

Acemoglu, Daron, Philippe Aghion, Lint Barrage, and David Hémous (2023). *Climate change, directed innovation, and energy transition: The long-run consequences of the shale gas revolution*. Tech. rep. National Bureau of Economic Research.

Aghion, Philippe, Antoine Dechezleprêtre, David Hémous, Ralf Martin, and John Van Reenen (2016). "Carbon taxes, path dependency, and directed technical change: Evidence from the auto industry". *Journal of Political Economy* 124.1, pp. 1–51.

Arora, Ashish, Sharon Belenzon, Larisa Cioaca, Lia Sheer, Hyun Moh Shin, and Dror Shvadron (2024). "DISCERN: Duke Innovation & Scientific Enterprises Research Network". *Zenodo. https://doi.org/10.5281/zenodo.3594642* 3594642.

Arora, Ashish, Sharon Belenzon, and Lia Sheer (2021). "Knowledge spillovers and corporate investment in scientific research". *American Economic Review* 111.3, pp. 871–898.

Bauer, Michael D. and Eric T. Swanson (2023). "A reassessment of monetary policy surprises and high-frequency identification". *NBER Macroeconomics Annual* 37.1, pp. 87–155.

Baumeister, Christiane and James D. Hamilton (2019). "Structural interpretation of vector autoregressions with incomplete identification: Revisiting the role of oil supply and demand shocks". *American Economic Review* 109.5, pp. 1873–1910.

Bornstein, Gideon, Per Krusell, and Sergio Rebelo (2023). "A world equilibrium model of the oil market". *The Review of Economic Studies* 90.1, pp. 132–164.

Calel, Raphael and Antoine Dechezleprêtre (2016). "Environmental policy and directed technological change: evidence from the European carbon market". *Review of Economics and Statistics* 98.1, pp. 173–191.

Cloyne, James, Clodomiro Ferreira, Maren Froemel, and Paolo Surico (Mar. 2023). "Monetary Policy, Corporate Finance, and Investment". *Journal of the European Economic Association*, jvad009. ISSN: 1542-4766.

Engle, Robert F., Stefano Giglio, Bryan Kelly, Heebum Lee, and Johannes Stroebel (2020). "Hedging climate change news". *The Review of Financial Studies* 33.3, pp. 1184–1216.

Fernald, John G. (2014). "A quarterly, utilization-adjusted series on total factor productivity". Federal Reserve Bank of San Francisco.

Gavriilidis, Costas, Diego R. Kaenzig, Ramya Raghavan, and James H. Stock (2025). "The Macroeconomic Effects of Climate Policy Uncertainty".

Gilchrist, Simon and Egon Zakrajšek (2012). "Credit spreads and business cycle fluctuations". *American Economic Review* 102.4, pp. 1692–1720.

Hall, Bronwyn H., Adam B. Jaffe, and Manuel Trajtenberg (2001). *The NBER patent citation data file: Lessons, insights and methodological tools*.

Hémous, David, Morten Olsen, Carlo Zanella, and Antoine Dechezleprêtre (2025). "Induced Automation Innovation: Evidence from Firm-level Patent Data".

Jarociński, Marek and Peter Karadi (2020). "Deconstructing monetary policy surprises—the role of information shocks". *American Economic Journal: Macroeconomics* 12.2, pp. 1–43.

Kahle, Kathleen M. and René M. Stulz (2017). "Is the US public corporation in trouble?" *Journal of Economic Perspectives* 31.3, pp. 67–88.

Känzig, Diego R. (2021). "The macroeconomic effects of oil supply news: Evidence from OPEC announcements". *American Economic Review* 111.4, pp. 1092–1125.

Kogan, Leonid, Dimitris Papanikolaou, Amit Seru, and Noah Stoffman (2017). "Technological innovation, resource allocation, and growth". *The Quarterly Journal of Economics* 132.2, pp. 665–712.

Migotto, Mauro and Ivan Haščič (2015). "Measuring environmental innovation using patent data". *OECD Environment Working Papers* 89.89, pp. 1–59.

Porter, Alan L., Mark Markley, Richard Snead, and Nils C. Newman (2023). "Twenty years of US nanopatenting: Maintenance renewal scoring as an indicator of patent value". *World Patent Information* 73, p. 102178.